

UC Santa Cruz

UC Santa Cruz Electronic Theses and Dissertations

Title

Movement, Habitat, and Foraging Behavior of Weddell Seals (*Leptonychotes Weddellii*) in the Western Ross Sea, Antarctica

Permalink

<https://escholarship.org/uc/item/0jx2107r>

Author

Goetz, Kimberly Thea

Publication Date

2015

Peer reviewed|Thesis/dissertation

UNIVERSITY OF CALIFORNIA
SANTA CRUZ

**MOVEMENT, HABITAT, AND FORAGING BEHAVIOR OF WEDDELL
SEALS (*LEPTONYCHOTES WEDDELLII*) IN THE WESTERN ROSS SEA,
ANTARCTICA**

A dissertation submitted in partial satisfaction
of the requirements for the degree of

DOCTOR OF PHILOSOPHY

in

ECOLOGY AND EVOLUTIONARY BIOLOGY

by

Kimberly Thea Goetz

June 2015

The Dissertation of Kimberly T. Goetz
is approved:

Professor Daniel P. Costa, Chair

Dr. Sharon Stammerjohn

Professor Pete Raimondi

Associate Professor, Patrick Halpin

Tyrus Miller
Vice Provost and Dean of Graduate Studies

Copyright © by
Kimberly Thea Goetz
2015

Table of Contents

List of Tables	vi
List of Figures	ix
Abstract	xiii
Acknowledgments	xvi
1. Introduction	1
2. Assessing the accuracy of animal-borne CTD tags under laboratory and <i>in situ</i> conditions	6
Abstract.....	6
Introduction.....	7
Methods.....	9
Independent laboratory calibration.....	9
Comparison of manufacturer and independent calibrations.....	12
<i>Laboratory</i>	12
<i>In situ</i>	13
Results	16
Comparison of manufacturer and independent calibrations.....	16
<i>Laboratory – Newly purchased tags</i>	16
<i>Laboratory – Impact of deployment and battery replacement</i>	17
<i>In situ - SRDL tags as received by manufacturer</i>	22
<i>In situ - Impact of SRDL attachment</i>	24
Discussion	25
Tables.....	34
Figures.....	38
3. Seasonal habitat preference and foraging behavior of Weddell seals in the western Ross Sea, Antarctica	47
Abstract.....	47
Introduction.....	49

Methods	55
Animal capture and handling	55
Environmental data.....	55
Tracking and diving data.....	57
Weddell seal habitat and foraging models	60
<i>Habitat models</i>	60
<i>Horizontal foraging models</i>	62
<i>Vertical foraging models</i>	63
Results	64
Habitat models	65
Horizontal foraging models.....	67
Vertical foraging models	69
Discussion	69
Conclusion.....	74
Tables.....	77
Figures.....	83
4. Using stable isotopes and tracking data to reveal the foraging ecology of Weddell seals in the western Ross Sea, Antarctica.....	89
Abstract.....	89
Introduction.....	91
Methods.....	94
Animal capture and sample collection.....	94
Stable isotope analysis.....	95
Statistical analysis.....	98
<i>Isotopic variation</i>	98
<i>Diet and foraging ecology</i>	99
Results	101
Isotopic variation	101
Diet and foraging ecology	103
Discussion	106

Isotopic variation	106
Diet and foraging ecology	109
Caveats of isotopic interpretation	114
Conclusions	115
Tables.....	117
Figures	121
5. Synthesis	125
Recommended improvements to CTD-SRDL tags	125
Habitat preference, foraging behavior and diet.....	126
Response to anthropogenic disturbance	128
Future directions	129
Appendix.....	131
Bibliography.....	135

List of Tables

Table 2.1: Laboratory calibration results from 44 newly-purchased SRDL tags. Mean (ME) and mean absolute error (MAE) with standard deviations (SD) for temperature and conductivity values produced from the manufacturer and our independent calibration are provided for each of four bins. ME and MAE are relative to temperature and conductivity values measured by laboratory equipment (Sea-bird Electronics, model 3F thermistor and Guildline, model 8400B salinometer).....34

Table 2.2: Laboratory calibration results from eight SRDL tags before and after deployment, and after battery replacement. Mean and mean absolute error (ME and MAE) with standard deviations (SD) for temperature and conductivity produced from the manufacturer and our independent calibration are provided for each of four bins. All error values are relative to temperature and conductivity values measured by laboratory equipment (Sea-bird Electronics, model 3F thermistor and Guildline, model 8400B salinometer).....35

Table 2.3: *In situ* results from 16 newly-purchased SRDL tags. Mean and mean absolute error (ME and MAE) with standard deviations (SD) for temperature and conductivity produced from the manufacturer and our independent calibration are provided for each of four depth bins. ME and MAE values are relative to temperature and conductivity values measured by a CTD profiler (Sea-bird Electronics, model 19-03).36

Table 2.4: *In situ* results from nine newly-purchased SRDL tags deployed on nine Weddell seals in the Ross Sea, Antarctica. Mean and mean absolute error (ME and MAE) with standard deviations (SD) for temperature and conductivity values produced from the manufacturer and our independent calibration are provided for each of three depth bins. ME and MAE values are relative to temperature and conductivity values measured by a CTD profiler (Sea-bird Electronics, model 19-03). Data collected during seal deployment are compared to results collected before deployment for the same nine tags (right column).....37

Table 3.1: Covariates utilized in the general additive models examining Weddell seal occurrence and foraging behavior in the western Ross Sea, Antarctica.....77

Table 3.2: Mean and standard deviation of eight environmental variables: ice concentration (ICECON, %), distance from the 10% ice concentration contour (DICE10, km), bathymetric depth (BATH, m), bathymetric slope (SLOPE, degree), modified circumpolar deep water index at 150 m (MCDW), mixed layer depth (MLD, m), distance from the coast (DCOAST, km), and distance to the continental shelf, or 1000 m isobath (DSHELF, km). Results are shown for both Weddell seal (present) and Correlated Random Walk (CRW, absent) locations. Data were analyzed separately for each season and mean values represent population means obtained by

averaging individual means. Asterisks indicate a significant difference between present and absent values at the $p \leq 0.05$ level for a given environmental value, within a season, obtained from Wilcoxon signed rank tests..... 78

Table 3.3: Wilcoxon signed rank test results comparing seasonal values for eight environmental variables: ice concentration (ICECON, %), distance from the 10% ice concentration contour (DICE10, km), bathymetric depth (BATH, m), bathymetric slope (SLOPE, degree), modified circumpolar deep water index at 150 m (MCDW), mixed layer depth (MLD, m), distance from the coast (DCOAST, km), and distance to the continental shelf, or 1000 m isobath (DSHELF, km). Only Weddell seals with associated environmental data for all four seasons were included in this statistical analysis (n=25). Bolded p -values are significant at the $p = 0.05$ level..... 79

Table 3.4: Mean and standard deviation of five Weddell seal dive metrics: dive duration (DDUR, min), bottom duration (BDUR, min), descent rate (DRATE, ms^{-1}), maximum dive depth (m), and percent water column depth (PWC, %). Data were analyzed separately for each season and mean values represent population means obtained by averaging individual means..... 80

Table 3.5: Wilcoxon signed rank test results comparing seasonal values for five dive metrics: dive duration (DDUR, min), bottom time (BOTDUR, min), descent rate (DRATE, ms^{-1}), maximum dive depth (MXDEP, m), and percent water column depth (PWC, %). Only Weddell seals with associated dive data for all four seasons were included in this statistical analysis (n=30). Bolded p -values are significant at the $p = 0.05$ level..... 81

Table 3.6: Covariates included in the final habitat preference and foraging behavior models by season. Models preceded by ‘H’ indicate habitat preference models and those preceded by ‘F’ indicate foraging behavior models. The percent deviance explained, R^2 adjusted value, number of locations, number of individuals, estimated degrees of freedom, and AIC values for each model are also provided..... 82

Table 4.1: Weddell seal tissue samples (RBC: red blood cells, and vibrissae) per variable (mass, sex, location, year, season, and age) used in generalized linear mixed models and Student’s t -test for age..... 117

Table 4.2: Predictors of $\delta^{13}\text{C}$ and $\delta^{15}\text{N}$ from two Weddell seal tissues (RBC: red blood cells, and vibrissae) obtained from generalized linear mixed models..... 118

Table 4.3: Species identification, assigned prey group, number of individuals, standard length, mass and isotopic values ($\delta^{13}\text{C}$ and $\delta^{15}\text{N}$) of Weddell seal prey species collected from the Ross Sea 2010-2012. Isotope values are presented as mean \pm standard deviation. Due to indistinguishable isotopic differences, species belonging to the same prey group were combined before using in mixing models to estimate Weddell seal diet..... 119

Table 4.4: Results from hierarchical cluster analysis to examine Weddell seal foraging strategies. Variables are defined as: P100M: proportion of dives > 100 m; AMAXDEP: average maximum dive depth (m); ADESCENT: average descent rate during a dive; ABOTDUR: average time spent within 80% of maximum dive depth (min); ADIVEDUR: average dive duration (min), P20MIN: proportion of dives over 20 minutes; APERDEP: average proportion of the water column used by diving Weddell seals 120

List of Figures

Figure 2.1: Percent data by direction of error (left column) and cumulative probability distribution across absolute temperature errors (right column) for four temperature bins (-2-0, 0-4, 4-6, >6 °C). Error values are the differences between values measured by the SRDL temperature sensor and those measured by the SB thermistor in the laboratory for the manufacturer calibration (top row) and our independent calibration (bottom row). Dotted lines indicate the manufacturer’s stated accuracy of $\pm 0.005^\circ\text{C}$ for temperature..... 38

Figure 2.2: Percent data by direction of error (left column) and cumulative probability distribution across absolute conductivity errors (right column) for four conductivity bins (25-29, 29-34, 34-47, 47-55 mScm^{-1}). Error values are the differences between values measured by the SRDL conductivity sensor and those measured in the laboratory for the manufacturer calibration (top row) and our independent calibration (bottom row). Dotted lines indicate the manufacturer’s stated accuracy of $\pm 0.01 \text{ mScm}^{-1}$ for conductivity..... 39

Figure 2.3: Percent data by direction of error (first and third columns) and cumulative probability distribution across absolute temperature errors (second and fourth columns) for four temperature bins (-2-0, 0-4, 4-6, >6 °C). Error values are the differences between values measured by the SRDL temperature sensor and those measured by the SB thermistor in the laboratory for the manufacturer calibration (left two columns) and our independent calibration (right two columns) for tags of varying condition (before deployment – top row; after deployment – middle row; after re-battery – bottom row). Dotted lines indicate the manufacturer’s stated accuracy of $\pm 0.005^\circ\text{C}$ for temperature..... 40

Figure 2.4: Percent data by direction of error (first and third columns) and cumulative probability distribution across absolute conductivity errors (second and fourth columns) for four conductivity bins (25-29, 29-34, 34-47, 47-55 mScm^{-1}). Error values are the differences between values measured by the SRDL conductivity sensor and those measured in the laboratory for the manufacturer calibration (left two columns) and our independent calibration (right two columns) for tags of varying condition (before deployment – top row; after deployment – middle row; after re-battery – bottom row). Dotted lines indicate the manufacturer’s stated accuracy of $\pm 0.01 \text{ mScm}^{-1}$ for conductivity..... 41

Figure 2.5: Percent data by direction of error (left column) and cumulative probability distribution across absolute temperature errors (right column). Data were collected from the Ross Sea, Antarctica, and error values are the differences in temperature values measured by the SRDL sensor and those measured by a CTD profiler (Sea-bird Electronics, model 19-03) for the manufacturer calibration (top) and our independent calibration (bottom) for four depth bins (5-50, 50-100, 100-150,

and 150-200 m). *In situ* temperature values ranged from -1.8 to -1.3 °C. Dotted lines indicate the manufacturer's stated accuracy of $\pm 0.005^\circ\text{C}$ for temperature. 42

Figure 2.6: Percent data by direction of error (left column) and cumulative probability distribution across absolute conductivity errors (right column). Data were collected from the Ross Sea, Antarctica, and error values are the differences in conductivity values measured by the SRDL sensor and those measured by a CTD profiler (Sea-bird Electronics, model 19-03) for the manufacturer calibration (top) and our independent calibration (bottom) for four depth bins (5-50, 50-100, 100-150, and 150-200 m). *In situ* conductivity values ranged from 26.5 to 27.5 mScm^{-1} . Dotted lines indicate the manufacturer's stated accuracy of $\pm 0.01 \text{ mScm}^{-1}$ for conductivity. 43

Figure 2.7: Locations of CTD casts collected by deployed SRDL tags (red circles) that are within five kilometers (white buffers) and two days of CTD casts collected by a CTD profiler (Sea-bird Electronics, model 19-03) (black asterisks). Only CTD casts collected by the CTD profiler within the buffer of the SRDL tags were included in the analysis. 44

Figure 2.8: Percent data by direction of error (left column) and cumulative probability distribution across absolute temperature errors (right column). Data were collected from the Ross Sea, Antarctica, and error values are the differences in temperature values measured by the SRDL sensor while deployed on the head of a seal and those measured by a CTD profiler (Sea-bird Electronics, model 19-03) for the manufacturer calibration (top) and our independent calibration (bottom) for three depth bins (5-50, 50-100, and 100-150 m). *In situ* temperature values ranged from -1.8 to -1.3 °C. Dotted lines indicate the manufacturer stated accuracy of $\pm 0.005^\circ\text{C}$ for temperature. 45

Figure 2.9: Percent data by direction of error (left column) and cumulative probability distribution across absolute conductivity errors (right column). Data were collected from the Ross Sea, Antarctica, and error values are the differences in conductivity values measured by the SRDL sensor while deployed on the head of a seal and those measured by a CTD profiler (Sea-bird Electronics, model 19-03) for the manufacturer calibration (top) and our independent calibration (bottom) for three depth bins (5-50, 50-100, and 100-150 m). *In situ* conductivity values ranged from 26.5 to 27.5 mScm^{-1} . Dotted lines indicate the manufacturer stated accuracy of $\pm 0.005^\circ\text{C}$ for temperature. 46

Figure 3.1: Weddell seal tracklines in the western Ross Sea during 2010 (blue), 2011 (red), and 2012 (black). Animals were tagged around Ross Island (n=22) and along the Victoria Land coast (n=41) with deployment locations denoted by stars. The dotted line represents the shelf break, or 1000 m bathymetric contour. 83

Figure 3.2: Results from the final predictive generalized additive model for each season. Plots show the relationship between Weddell seal occurrence in the western Ross Sea and eight environmental variables: ice concentration (ICECON, %), distance from the 10% ice concentration contour (ICEDIST10, km), bathymetric depth (BATH, m), bathymetric slope (SLOPE, degree), modified circumpolar deep water index (MCDW), mixed layer depth (MLD, m), distance from the coast (DCOAST, km), and distance to the continental shelf, or 1000 m isobath (DSHELF, km). The shaded areas represent the 95% confidence interval. The effect of the explanatory variable on the response is on the logit scale where zero (solid black line) or negative numbers show no effect. 84

Figure 3.3: Panels A-D show the probability of Weddell seal presence in the western Ross Sea by season with warmer colors indicating a higher probability of seal occurrence and hatched areas representing preferred habitat. Predicted Weddell seal foraging, as measured by First Passage Time (FPT), is shown on panels E-H and predicted Weddell seal foraging within preferred habitat is shown on panels I-L. The analysis area was determined by the extent of tracking data for each season. 85

Figure 3.4: Results from the final generalized additive model for each season. Plots show the relationship between First Passage Time (FPT) for Weddell seals in the western Ross Sea and eight environmental variables: ice concentration (ICECON, %), distance from the 10% ice concentration contour (ICEDIST10, km), bathymetric depth (BATH, m), bathymetric slope (SLOPE, degree), modified circumpolar deep water index (MCDW), mixed layer depth (MLD, m), distance from the coast (DCOAST, km), and distance to the continental shelf, or 1000 m isobath (DSHELF, km). The shaded areas represent the 95% confidence interval. The effect of the explanatory variable on the response is on the log scale where zero (solid black line) or negative numbers show no effect. 86

Figure 3.5: Smoothed function for day of year (DOY) in predicting log First Passage Time (FPT), shaded and non-shaded areas represent seasons, from summer to spring, respectively. The shaded areas represent the 95% confidence interval. The effect of the explanatory variable on the response is on the log scale where zero (solid black line) or negative numbers show no effect. 87

Figure 3.6: Results from the final generalized additive model used to predict First Passage Time (FPT) for each season. Plots show the relationship between FPT for Weddell seals in the western Ross Sea and three dive metrics: dive duration (DDUR, min), percent water column depth (PWC, %), and descent rate (DRATE ms^{-1}). The shaded areas represent the 95% confidence interval. The effect of the explanatory variable on the response is on the log scale where zero (solid black line) or negative numbers show no effect. 88

Figure 4.1: Weddell seal capture and sample (red blood cells and vibrissae) locations near Ross Island and along the Victoria Land coast. 121

- Figure 4.2:** Isotopic values ($\delta^{13}\text{C}$ and $\delta^{15}\text{N}$) for red blood cells (RBC) and vibrissae segments. Ellipses indicate the 95% confidence interval and density plots show less variation in $\delta^{15}\text{C}$ and $\delta^{15}\text{N}$ values for RBC than vibrissae. 122
- Figure 4.3:** Vibrissae $\delta^{13}\text{C}$ and $\delta^{15}\text{N}$ values from the base of the vibrissa to the furthest extent for six individual Weddell seals. Values for $\delta^{13}\text{C}$ are shown on the left axis (black) and $\delta^{15}\text{N}$ values are shown on the right (red). Dotted lines represent the mean vibrissae $\delta^{13}\text{C}$ and $\delta^{15}\text{N}$ values for all Weddell seals (n=45). 122
- Figure 4.4:** Stable isotope values ($\delta^{13}\text{C}$ and $\delta^{15}\text{N}$) for nine fish species or species groups. Points and lines represent means and standard deviations, respectively, of $\delta^{13}\text{C}$ and $\delta^{15}\text{N}$ values. Red blood cell and vibrissae isotopic values for Weddell seals are shown as a black triangle and square, respectively 123
- Figure 4.5:** The proportional contribution of nine fish species or species groups to the diet of Weddell seals in the western Ross Sea, Antarctica, as determined by (A) red blood cells (RBC) and (B) mean vibrissae $\delta^{13}\text{C}$ and $\delta^{15}\text{N}$ values. Points and lines show median and interquartile range, respectively 123
- Figure 4.6:** The proportional contribution of nine fish species or species groups to the diet of four individual Weddell seals, as determined by vibrissae $\delta^{13}\text{C}$ and $\delta^{15}\text{N}$ values. Points and lines show median and interquartile range, respectively 124
- Figure 4.7:** Complete tracks (January-October) for 13 Weddell seals in the western Ross Sea and the proportional contribution of nine fish species or species groups to the diet of seals clustered into four different foraging strategies, as determined by vibrissae $\delta^{13}\text{C}$ and $\delta^{15}\text{N}$. Points and lines show median and interquartile range, respectively 124

Abstract

Movement, habitat, and foraging behavior of Weddell seals (*Leptonychotes Weddellii*) in the western Ross Sea, Antarctica

by

Kimberly Thea Goetz

Weddell seals (*Leptonychotes weddellii*) are one of Antarctica's top predators, yet surprisingly little information exists about their year-round movement, habitat, and foraging behavior. Previous attempts to determine the overwinter behavior of Weddell seals were met with limited success due to early tag failure. Conductivity Temperature and Depth – Satellite Relay Data Loggers (CTD-SRDL tags) now make it possible to collect animal movement and oceanographic data on the same scale. These tags are deployed on marine vertebrates with the assumption that oceanographic data collected by miniaturized sensors are on par with standard oceanographic equipment. Movement data collected by the tags, in combination with oceanographic data can be used to study the seasonal habitat preference and foraging behavior of Weddell seals. Tracking data can also be linked to diet to provide a complete picture of the seasonal ecology of the southernmost mammal on Earth. Unlike previous studies which were biased towards prey with indigestible hard parts, stable isotopes can be used to provide a more complete picture of both digestible and indigestible components of prey species.

In the first data chapter (**chapter 2**), I assess the accuracy of the temperature and conductivity sensors on the CTD-SRDL tags to determine their performance relative to standard oceanographic equipment. I found that CTD tags were not comparable to high-precision oceanographic equipment, but still provided invaluable oceanographic data and were fully capable of identifying water mass characteristics and seasonal changes in otherwise inaccessible areas. This study provides the first independent assessment of CTD tag performance in laboratory (pre- and post-deployment, and after battery replacement) and under *in situ* conditions (before and during deployment). In the second data chapter (**chapter 3**), I explain and predict Weddell seal habitat and foraging behavior from a suite of environmental variables as well as examine the relationship between foraging behavior and dive metrics. I found that seasonal sea-ice extent, open water polynyas, and the diverse topography of the Ross Sea were important in determining the habitat preference and foraging behavior of Weddell seals in the western Ross Sea. This work provides insight into how Weddell seals might adjust their habitat preferences and foraging behavior in light of increased climate change. Finally, in the last data chapter (**chapter 4**), I used stable isotopes ($\delta^{13}\text{C}$ and $\delta^{15}\text{N}$) to examine the diet of Weddell seals over two time scales. I found that Antarctic silverfish (*Pleurogramma antarcticum*), Antarctic icefish (*Neopagetopsis ionah*) and several *Trematomus* species were important prey items, but their proportional contribution to Weddell seal diet varied among individuals and across time scales. Overall, this dissertation provides critical insight into the

movement, habitat, and feeding ecology of this important top predator of the Ross Sea ecosystem.

Acknowledgments

I cannot begin to express how grateful I am to the many people who gave their love and support throughout my graduate career. I was truly fortunate to have had Dr. Dan Costa as my adviser. Thank you so much for the amazing once-in-a-lifetime experiences you gave me. I feel privileged and honored to have shared so many field seasons with you and will forever cherish our many experiences on the ice. You are an incredible mentor and scientist with a heart of gold, always doing what you can to see your graduate students succeed. You have an uncanny ability to always see the ‘big picture’ and have helped me become a better scientist, for which I am eternally grateful.

Dr. Pete Raimondi provided statistical advice on numerous occasions. Pete, thank you so much for always being responsive no matter how many panicky emails I managed to send you in a single day (and I’m pretty sure I hold the record). You are truly one of the most intelligent people I know and you are so incredibly generous with your time despite your overwhelming responsibilities. Dr. Sharon Stammerjohn and Dr. Patrick Halpin composed the remainder of my committee and were instrumental in giving me advice on how to improve my dissertation and subsequent publications. Thank you both for your encouraging words and support. I would also like to thank Dr. Rita Mehta who was not on my committee but always offered words of encouragement. I am also grateful to Dr. Jerry Kooyman and Dr. Paul Ponganis for giving me the opportunity to work for them and believing in me every step of the way.

I was fortunate to work with an amazing team of scientists in Antarctica. Dr. Jennifer Burns, Linnea Pearson, and Michelle Shero – we will forever be ‘teamtype-A’. Thank you for teaching me to appreciate physiology even though I will continue to deny it. Dr. Michelle Larue, Brad Herried, Spencer Niebuhr, Clair Porter, and Paul Morin from the Polar Geospatial Center were always eager and ready to help our project despite their busy schedule. I would like to specifically thank Michelle Larue for her contribution, especially for filling in for me in the field when I managed to contract the ‘Antarctic crud’ every season. Michelle, you are truly a joy and an inspiration to be around.

Dr. Brad Buckley, Dr. Sean Place, Dr. Art Devries, Dr. Paul Cziko, and Dr. Alex Bochdansky provided essential prey species for isotopic analysis. Their generous contributions allowed me to quantify Weddell seal diet. I would like to thank Mike Dinniman who generously allowed me to use data from his Regional Oceanographic Model of the Ross Sea. I am also thankful to Jim Stockel for always allowing me to use the calibration facilities at the Naval Postgraduate School, often on short notice, and helping troubleshoot problems along the way. Many thanks to Dr. Luis Hückstädt and Dr. Patrick Robinson for teaching and assisting me with CTD tag calibrations, possibly the most tedious task on the planet. Finally, I would like to thank ‘teamtype-A’ again for assisting me with CTD casts in the field.

I am grateful to my colleagues at the National Marine Mammal Lab. From the day I decided to leave and pursue my PhD, Phil Clapham, Kim Shelden, and Dave Rugh have offered nothing but support and encouragement. Thank you so much for

your understanding and for always believing in me. Dave you have been such an amazing mentor and friend and I will always cherish the years we worked together.

I am grateful to the National Science Foundation (NSF) for providing the funding and logistical support for this project. I received additional funding from Achievement Rewards for College Students (ARCS) that allowed me to analyze additional samples that will better explain Weddell seal foraging. I am honored that the ARCS foundation recognized my work as an ‘outstanding academic achievement’ and allowed me to further pursue my academic interests. Finally, I would like to thank the Ecology and Evolutionary Biology Department and the University of California, Santa Cruz, for believing in me and awarding me the President’s dissertation year fellowship. Also, thank you to the administrative staff in our department, Susan Thuringer, Debbie Inferrera, Kathy Durcan, and Maria Choy, who were always there to answer questions and help along the way.

I am deeply indebted to the wonderful people in my lab. Thank you for being my friends, mentors, and colleagues throughout this journey called grad school. You were always there through the bad times, offering a shoulder to cry on, and always there to drag me out to celebrate the good times. Patrick Robinson, thank you for being a great friend and teaching me so much in my first years as a graduate student. I never would have thought that I would learn to love MATLAB and I am grateful we never bet on it. Thank you to all my officemates throughout the years that put up with all my creative pets. Liz McHuron and Sarah Peterson, I miss our brain-storming sessions and learned so much from both of you. Luis (aka pumpkin) and Mel

Connors, you guys truly kept me sane. Watching Walking Dead without you is just not the same.

Thank you Chandra Goetsch, Sarah Kienle, Lisa Shwartz, Stella Villegas, and Rachael Orben for all your help over the years. Chandra, you have been so supportive from the day I met you and thank you for believing in me. Rachael, thank you so much for editing many drafts of my work. Sarah Kienle, you always manage to make me laugh even if you did add Disney music to my Pandora station. Finally, I would like to thank the many undergraduate volunteers that helped me process my data. Specifically, I am grateful to Xochitl Rojas-Rocha and Roxanne Beltran for the many hours they spent in the lab processing whisker samples. Xochitl, you are a truly exceptional student and I have no doubt that you will be successful no matter where life takes you.

Léa Georges, Gitte McDonald, Sam Simmons, Melinda Connors, Sarah Maxwell, and Melinda Fowler, thank you for being the people you are. Each of you has added so much to my life. No matter how stressed I was, you always managed to be there for me and offer support. Thank you for your unwavering friendship. Sheri Lindeman, Barbara Hagerman, Jen Maresh, you are family to me and I love you all so much. Sheri, it seems like only yesterday we met in second grade. While we have taken different roads in life, we are still as close as we were 29 years ago and I have no doubt we will be just as close for the rest of our lives. Barbara, I cannot possibly express how much your love and support has meant to me. Thank you for guiding me along the journey called 'life'. I truly can't imagine my life without you. Jen, we have

been through so much over the last 12 years and I can't thank you enough for your support, love, help, and encouragement. I'm excited to see where the next 12 years will take us.

I would like to thank my mom and brother for understanding why I am always busy with this thing called a 'dissertation.' I know I have missed many holidays and visits over the years and I am truly sorry. While our family is far from perfect and we have been through a lot together, the past has made me the strong person I am today for which I am eternally grateful. Finally, I would like to thank Stefan Jendersie who unexpectedly came into my life and made the last few months of dissertation writing bearable. Thank you for your love and understanding during one of the most stressful times of my life; I am grateful to have found a partner-in-crime and I cannot wait to build a future with you

Introduction

Weddell seals (*Leptonychotes weddellii*) play an important role in the Antarctic ecosystem as one of the only resident top predators, yet very little data exist on their year-round movement and foraging behavior. In addition, oceanographic data are severely lacking in the Southern Ocean and the highly productive waters of the Ross Sea, particularly in the winter (Arrigo et al., 1998). As a result, abiotic-biotic mechanisms that link oceanographic features with Weddell seal behavior are unknown. Consequently, outfitting Weddell seals with Conductivity, Temperature, and Depth – Satellite Relay Data Loggers (CTD-SRDL or CTD tags) has great potential for providing valuable biological and oceanographic data. During the eight months Weddell seals spend foraging at-sea, they sample conditions under the pack-ice, dive deep enough to collect data from the whole water column, and cover a large geographic area.

While data collected by CTD tags are paramount to understanding the movement and foraging behavior of a seal, one must first consider the limitations of their on-board oceanographic sensors to ensure the data are used appropriately by both the biological and oceanographic communities. CTD tags have been deployed on marine animals around the world with the implicit trust that tags are performing according to the accuracy and precision specified by the manufacturer. These specifications are on par with highly accurate and precise oceanographic equipment used for decades to measure physical properties of the ocean. However, sensor limitation, such as measurement drift or noise, can not only lead to incorrect linkages

between animals and their environment but also to the distribution of erroneous oceanographic data.

Once corrected for device error, data from CTD tags allow us to extend the scope of our study beyond coarse linkages of prey and predator distributions to correlate the foraging behavior of marine animals with their physical and oceanographic environment (Block et al., 2002; Lydersen et al., 2002; Biuw et al., 2007; Simmons et al., 2007). Data collected by these tags can be used to characterize habitat and identify foraging areas for Weddell seals in the Ross Sea, a process that is particularly challenging due to the 3-dimensional and highly dynamic nature of the marine environment. Understanding how Weddell seals respond behaviorally to both abiotic and biotic features is fundamental for forecasting how climate change may impact these top predators.

Logistical challenges limit the collection of dietary information on marine predators, especially those that overwinter in Antarctic ecosystems. Therefore, we lack a comprehensive understanding of trophic linkages between Weddell seals and their prey. While scat and stomach content analyses have provided some data on Weddell seal diet, these analyses were limited to non-assimilated prey parts, such as indigestible fish otoliths, and so can be highly biased towards particular prey species while completely missing others (Bodey et al., 2011). Some prey species, such as the Antarctic toothfish (*Dissostichus mawsoni*) cannot be detected using traditional methods because hard parts are not consumed. Stable isotope analysis is a powerful biochemical tool for studying foraging ecology that bypasses the limitations of

traditional methods by quantifying the ratios of carbon and nitrogen isotopes present in seal tissues; these isotopes indicate the trophic level at which a predator is feeding as well as broad-scale habitat characteristics. Stable isotope analyses can be further extended by using statistically robust mixing models to determine the proportional contribution of prey species to the overall diet, provided $\delta^{13}\text{C}$ and $\delta^{15}\text{N}$ values for potential prey species are available. This method is especially valuable since it can estimate the proportion of toothfish in the diet of Weddell seals, which may provide insight on the impact that the proposed 50% reduction in toothfish due to commercial long-lining (Pinkerton et al., 2007) may have on this seal population.

In **chapter 2**, I assessed the accuracy of CTD tag sensors relative to the manufacturer stated accuracy in both laboratory and *in-situ* conditions. I quantified the error in temperature and conductivity measurements at various stages of the tag's condition and showed that, despite not performing within the manufactured-stated accuracy, results were useful at the level of animal behavior. In addition, I provided recommendations for the re-deployment of tags, and offered suggestions that are likely to improve the performance of tag sensors.

In **chapter 3**, I used data collected by CTD tags to describe and predict habitat preferences and foraging behaviors of Weddell seals in the western Ross Sea. These models showed that the diverse bathymetry, seasonal ice concentration, and oceanographic features were important in determining seasonal habitat preferences and foraging behaviors. In addition, I showed that foraging was highest when seals were either less than 30% to the bottom (pelagic) or were near or at the bottom

(benthopelagic). Overall, Weddell seal foraging behavior was relatively low in the summer compared to the rest of the year which may be attributed to energetic limitations imposed by reproduction and molt life history stages.

In **chapter 4**, I 1) examined carbon and nitrogen isotopic variation in relation to Weddell seal mass, sex, season, year, tagging location, body condition, and age, 2) quantified the contribution of prey species to overall diet, and 3) linked diet to animal distribution and foraging patterns. My analysis showed that mass was a significant predictor of $\delta^{13}\text{C}$ and $\delta^{15}\text{N}$ in both red blood cells (RBC) and vibrissae, though the strength and direction of the relationship varied by year. In addition, I found that older individuals (> 10 years) had significantly enriched RBC $\delta^{13}\text{C}$ and $\delta^{15}\text{N}$, suggesting they were feeding at a higher trophic level than younger seals. The prey group consisting of Antarctic silverfish (*Pleurogramma antarcticum*) and *Trematomus newnesi* was the dominant prey of Weddell seals from the Ross Sea, although their relative importance varied among tissue types, suggesting temporal variation in diet. The Antarctic icefish (*Neopagetopsis ionah*) contributed between 39% and 57% to the diet of Weddell seals over a shorter time scale, while the Antarctic toothfish contributed < 10% to overall diet. However, given the high energetic density of toothfish, I suggest that this species may be an important prey item for Weddell seals, especially during the post-molt recuperation period when animals are at their leanest. Year-round movement and diving data revealed that foraging patterns were associated with different diets.

Together, chapters 2, 3 and 4 identify the limitations of CTD tags and show how movement data collected from these tags can be used to model the seasonal movement, habitat preference, foraging behavior, and diet of Weddell seals. Finally, in **chapter 5**, I synthesis the data presented in these three chapters and discuss the findings in relation to anthropogenic threats and future directions.

CHAPTER 2

Assessing the accuracy of animal-borne CTD tags under laboratory and *in situ* conditions

ABSTRACT

Electronic animal-borne tags capable of collecting oceanographic data are at the forefront of bio-logging technology. Conductivity Temperature and Depth – Satellite Relay Data Loggers (CTD-SRDL tags), manufactured by the Sea Mammal Research Unit (SMRU), are deployed on marine vertebrates with the assumption that oceanographic data are within the manufacturer stated accuracy of ± 0.005 °C for temperature and ± 0.01 mScm⁻¹ for conductivity. We tested this assumption by comparing mean error (ME) and mean absolute error (MAE) in temperature and conductivity produced by the manufacturer calibration and our independent calibration in both laboratory and *in situ* conditions. Furthermore, we tested the impact of deployment, battery replacement, and tag attachment on the accuracy of temperature and conductivity for both calibrations. Our results show that MAE in temperature and conductivity under laboratory and *in situ* conditions was higher than the manufacturer's stated accuracy. In the laboratory, ME of the manufacturer calibration was within the stated accuracy of ± 0.005 °C for temperatures > 0 °C. MAE across all temperatures was greater than the stated accuracy of ± 0.005 °C. For conductivity, ME values produced from the manufacturer calibration were higher than the stated accuracy of ± 0.01 mScm⁻¹, ranging from 0.011 mScm⁻¹ (SD=0.031) to 0.046 mScm⁻¹ (SD=0.058). Post-deployment, ME values for the manufacturer

calibration were higher than before deployment for temperatures > 0 °C. Overall, MAE was 0.017 °C (SD=0.019) post-deployment compared to 0.013 °C (SD=0.017) pre-deployment and 0.028 (SD=0.022) post-battery replacement. This study provides the first independent assessment of CTD tag performance in laboratory (pre- and post-deployment and after battery replacement) and under *in situ* conditions (before and during deployment). Ultimately, this analysis will help researchers assess the accuracy of oceanographic data collected by marine vertebrates and provide the information necessary to determine when an independent calibration is warranted.

INTRODUCTION

Bio-logging technology has long been used to study the behavior of wide-ranging marine vertebrates (Fedak, MA, 2004; Naito, 2004; Ropert-Coudert and Wilson, 2005; Ropert-Coudert et al., 2009; Rutz and Hays, 2009; Bograd et al., 2010). Until recently, relating the movement and dive behavior of marine animals to habitat features was limited to remotely-sensed data (Hooker et al., 1999; Hamazaki, 2002; Goetz et al., 2007; Torres et al., 2008) or shipboard measurements of oceanographic features (Joiris, 1991; Ribic et al., 1991; Chapman et al., 2004; Tynan et al., 2005). While these studies continue to provide important insights into species' behavior, such environmental data are too coarse in space and time to assess individual fine scale behavior in a multidimensional oceanographic environment.

The miniaturization of oceanographic sensors and recent advancements in bio-logging technology have facilitated the creation of electronic tags capable of collecting oceanographic data on the same temporal and spatial scale as animal

behavior (Costa, 1993; Costa and Crocker, 1996; Campagna et al., 2000; Charrassin and Bost, 2001; Block et al., 2002; Biuw et al., 2007; Simmons et al., 2007; Robinson et al., 2012). In addition, environmental data collected by animal-borne sensors can increase our understanding of physical oceanography, especially in areas where high ice density prevents ship and Argo float operation, or where high cloud coverage impedes data collection from remote sensing platforms. Oceanographic data collected by marine animals have increased our understanding of ocean variability and heat flux, deep water turnover, frontal structure, bathymetry, and currents (Wilson et al., 1994; Lydersen et al., 2002; Simmons et al., 2006; Boehme et al., 2008; Charrassin et al., 2008; Costa et al., 2008; Roquet et al., 2009; 2009; Padman et al., 2010; Grist et al., 2011; Robinson et al., 2012).

Due to the increasing popularity of using marine animals as oceanographic samplers, voids where little or no data exist are being filled with oceanographic data collected by free-ranging animals. For example, over 1.4 million oceanographic casts collected by marine mammals are available for download in the World Ocean Database (WOD), which seeks to make quality oceanographic data available without restriction. If calibrated and attached properly, animal-borne sensors have great potential to increase our oceanographic understanding in remote or inaccessible areas. However, tag performance is rarely validated under laboratory or *in situ* conditions (Hooker and Boyd, 2003; Simmons et al., 2009; Roquet et al., 2011; Nordstrom et al., 2013). Because data derived from animal-borne sensors are likely to increase in the

future, it is critical to assess whether the accuracy of oceanographic sensors attached to free ranging animals is comparable to other oceanographic platforms.

Conductivity Temperature and Depth – Satellite Relay Data Loggers (CTD-SRD L tags, referred to ‘SRDL tags’ hereafter) were developed by the Sea Mammal Research Unit (SMRU, Scotland) and contain an inductive conductivity sensor and a fast response Platinum Resistance Temperature Detector (PRT) manufactured by Valeport Ltd (UK). The sensors are calibrated by Valeport, sent to SMRU where they are integrated with the SRDL platform, and returned to Valeport for an additional calibration. According to the manufacturer, these sensors collect temperature and conductivity profiles with an accuracy of $\pm 0.005^{\circ}\text{C}$ and $\pm 0.01\text{mScm}^{-1}$, respectively. However, an independent assessment of the accuracy of these tags under laboratory and *in situ* conditions has not been performed. In addition, there are no data on the sensor drift associated with these tags after deployment, and after battery replacement. Therefore, the objectives of this study were to assess the performance of SRDL tag sensors relative to the manufacturer’s stated accuracy 1) in the laboratory: before and after deployment, and after battery replacement, and (2) under *in situ* conditions while attached to a CTD profiler and while deployed on a seal.

METHODS

Independent laboratory calibration

A total of 44 2009-2012 generation CTD-SRD L tags were independently calibrated at the Naval Postgraduate School (NPS, Monterey Bay, California) prior to deployment. We also re-calibrated the tags post-deployment on Weddell seals to

examine the effect of a nine month deployment in Antarctic waters on tag performance. Finally, each tag was calibrated again after battery replacement.

Temperature and conductivity calibrations were conducted sequentially. During the temperature calibration, all tags were placed in a temperature bath and allowed to equilibrate to each of five sequential temperatures between -2 and 25 °C. Temperatures below 0°C were achieved by the addition of ethanol. The temperature bath was equipped with both a mixer and a computer-controlled heating/cooling element to maintain temperature stability. In addition, a high precision thermistor (Sea-bird Electronics, model 3F, accuracy ± 0.001 between -5 and 35°C) interfaced with a computer was used to record temperature readings at least once per second. These temperatures were considered ‘truth’ when calibrating the temperature sensors of the tags.

The conductivity calibrations were conducted using five seawater baths ranging in salinity from 16 to 37. All seawater baths were thoroughly mixed during the calibrations. Tags were hung by their antennae and positioned such that they were at least 15 cm away from the bath walls, the mixer, and other tags to eliminate near-field effects. All tags were allowed to equilibrate for a minimum of 5 minutes. Water samples were collected from each bath at the beginning, middle, and end of the calibration period. Each collection bottle and cap was rinsed before the sample was taken from the middle (distance and depth) of the bath. We used seasoned glass seawater bottles with a plastic stopper and cap to store samples until processing using a salinometer (Guildline, model 8400B, accuracy < 0.002 between 2 and 42 PSU)

within 24 hours. The salinometer was calibrated using standard seawater before and after processing the water samples.

To determine the new temperature calibration string, first we plotted time against temperature as recorded by the tag sensor and the thermistor in the temperature bath. For each temperature equilibration period (five distinct temperatures), we selected the most stable two-minute period, measured by the lowest standard deviation in temperature collected by the SRDL tag. For each of five, two-minute stable temperature periods per tag, we calculated the mean raw (uncalibrated) temperature recorded by both the tag (observed) and the thermistor (actual). Like the manufacturer, we fit a quadratic function to the actual and observed values and the resulting coefficients were used to construct a temperature calibration string for each tag.

A similar approach was used to compare mean raw (uncalibrated) conductivity values collected by the tag (observed) to the conductivity measured in the lab (actual). For each of five conductivity baths, we identified the most stable two-minute period as measured by the lowest standard deviation in conductivity. Next, we calculated conductivity (actual) for each water sample from the following variables: conductivity ratio measured by the salinometer, bath temperature, salinometer temperature, and pressure. Salinometer temperature and pressure remained constant at 24°C and 1 dbar, respectively. The conductivity ratio of the bath at the time each water sample was collected was determined by applying a linear fit to the time and conductivity ratio measured by the salinometer during three periods

(beginning, middle, and end) in which the tags were submerged in the baths. Using the midpoint of the selected two-minute stable period and the coefficients from this fit, we calculated the conductivity ratio of each bath for every tag. Because the conductivity measurement is dependent on the accuracy of the temperature sensor, we applied a tag-specific linear regression to the temperature data collected in the salinity baths and the temperature calibration data collected earlier the same day. The mean raw temperature (observed) collected by the tag during the selected two-minute stable period in each conductivity bath was used in the function to determine the actual temperature of the bath. Finally, like the manufacturer, we used a cubic function to fit the actual and observed conductivity values and the resulting coefficients were used to construct the conductivity calibration string for each tag.

Comparison of manufacturer and independent calibrations

Laboratory

Once tags were programmed with the new calibration strings, we examined the performance of these calibrations to reproduce the water temperature and conductivity of the water baths. The mean raw temperature and conductivity values (observed) collected by SRDL tags during each selected two-minute stable period were input into the calibration strings (manufacturer and independent) to calculate actual temperature and conductivity measured by the tag. We assessed the accuracy and precision of the manufacturer and our independent calibration by taking the mean and standard deviation of the differences between temperature and conductivity values measured by the manufacturer calibration and those measured by highly

accurate oceanographic equipment (mean error, referred to as ME hereafter). The mean of the absolute error (mean absolute error, referred to as MAE hereafter) and standard deviation were also calculated in order to assess the magnitude of temperature and conductivity error. ME and MAE were also examined relative to the accuracy stated by the manufacturer (± 0.005 °C for temperature and ± 0.01 mScm⁻¹ for conductivity). Data were placed in one of four bins based on quantiles to ensure roughly equal sample size in each bin.

This same procedure was used to assess whether deployment or battery replacement impacts the accuracy and precision of SRDL tag sensors. We examined the performance of both the manufacturer and our independent calibration relative to the stated accuracy of the SRDL sensors through time and condition (eight tags before and after deployment and five after battery replacement). Differences between SRDL tag temperature and conductivity values and those collected by highly accurate laboratory equipment were used to calculate ME, MAE, and standard deviations.

In situ

Of the 44 SRDL tags that were independently calibrated in the lab, 16 were further tested in the field near McMurdo Station, Antarctica to determine the accuracy and precision of temperature and conductivity measured by the sensors in a non-laboratory setting. Temperature and conductivity values obtained from newly purchased SRDL tags were compared to those collected from a CTD profiler ('truth') (Sea-bird Electronics, model 19-03, hereafter referred to as 'SB profiler') before and during deployment on a seal. Data collected from the SB profiler (measurement

accuracy of ± 0.01 °C and ± 0.01 mScm⁻¹ for temperature and conductivity, respectively) were corrected for conductivity and temperature drift based on pre and post instrument calibrations.

Before deployment, tags were attached to the SB profiler and lowered into the water column up to two times to a maximum of 180 m or until reaching the seafloor. CTD casts were conducted in waters ranging in temperature from -1.8 to -1.3 °C and conductivity from 26.5 to 27.5 mScm⁻¹.

Pressure recorded by SRDL tags was corrected to account for the initial 10 decibar offset automatically applied to the pressure data while in calibration mode. Raw values collected by each tag were processed using the manufacturer and our independent calibration string to calculate real temperature and conductivity values. Finally, we calculated mean temperature and conductivity for each one-meter depth bin for all CTD casts collected by both the SRDL tags and the SB profiler.

We examined ME, MAE, and standard deviations in temperature and conductivity of SRDL tags (calculated from the differences between SRDL tags and the SB profiler) for both the manufacturer calibration and our independent calibration. Due to memory limitations, SRDL tags only record CTD profiles after an animal reaches a specified depth. Therefore, only data for the upcast was used for comparison. To eliminate noise associated with equipment exiting the water, we also limited our analysis to data below five meters.

In addition to assessing *in situ* SRDL tag performance before deployment, we compared temperature and conductivity of CTD casts collected by the tag sensors to

those collected by the SB profiler while deployed on a seal. During January -February 2012, we used the SB profiler to collect 20 CTD casts at ice holes proximate to the locations where Weddell seals with SRDL tags were collecting data. We calculated distances between each SB cast and the casts collected by the 16 SRDL tags deployed on seals. Because we found that the water column appeared stable over five km (sometimes as much as 50 km depending on location) and over a five day period we chose casts collected from SRDL tags within two days and five kilometers of casts collected by the SB profiler for comparison. Because SRDL tags only transmit salinity via satellite, for this subset of casts, we used a custom built MATLAB function developed by James Stockel (2008) to convert salinity to conductivity for comparison purposes. These values were used to back-solve the polynomial calibration equations for raw temperature and conductivity values which were then processed through the original manufacturer and our independent calibration equations. We calculated ME, MAE, and standard deviation of the differences between the temperature and conductivity values recorded by the SRDL tags (for both the manufacturer and our independent calibration) and the SB profiler across three depth bins. Because very few seals dove below 150 m, we did not include depth data below 150 m.

RESULTS

Comparison of manufacturer and independent calibrations

Laboratory – Newly purchased tags

With the exception of temperatures below 0 °C, ME of the manufacturer calibrations was within the stated accuracy of ± 0.005 °C (Table 2.1, Fig. 2.1). However, standard deviation ranging from 0.008 to 0.188 °C across temperatures suggests low precision. The overall ME and MAE produced by the manufacturer calibration was 0.005 (SD=0.015) and 0.009 (SD=0.012), respectively. MAE across all temperatures was greater than the stated accuracy of ± 0.005 °C (Table 2.1). Depending on temperature bin, 34-61% of the data were within ± 0.005 °C (Fig. 2.1).

For our independent calibrations, ME and MAE were less than the manufacturer stated accuracy of ± 0.005 °C for all temperature bins, including those below 0 °C (Table 2.1). The standard deviations around ME and MAE for our independent calibration were smaller than those produced by the manufacturer calibration, indicating higher precision (Table 2.1). Over 90% of the data were within than the stated accuracy of the tag (Fig. 2.1).

For conductivity, ME values produced from the manufacturer calibration were higher than the stated accuracy of ± 0.01 mScm⁻¹, ranging from 0.011 mScm⁻¹ (SD=0.031) to 0.046 mScm⁻¹ (SD=0.058) across conductivity bins (Table 2.1). Similarly, MAE values were less accurate with increasing conductivity (Table 2.1). The standard deviation around ME and MAE values increased with increasing conductivity values. Overall, ME and MAE values produced by the manufacturer

calibration were 0.026 (SD=0.042) and 0.040 mScm⁻¹ (SD=0.030). The majority of the errors were positive, indicating that the tag sensor tended to overestimate conductivity values (Fig. 2.1). Approximately 15% of the conductivity errors within the 25-29 mScm⁻¹ bin were within the stated accuracy of the sensor, while 3-8% of the error values from the three remaining bins were within 0.01 mScm⁻¹ (Fig. 2.2).

For our independent calibration, conductivity ME and MAE values were all within the stated accuracy. However, ME and MAE were highest for conductivity values between 29 and 34 mScm⁻¹ (ME=0.004, SD=0.010; MAE=0.007, SD=0.009) (Table 2.1). Overall, the conductivity ME and MAE produced by our independent calibration was 0.000 (SD=0.007) and 0.004 mScm⁻¹ (SD=0.005), respectively. Standard deviations around MA and MAE values for our independent calibration were lower than those produced from the manufacturer calibration (Table 2.1). After our independent calibration, 84-100% of the data were within the stated accuracy of 0.01 mScm⁻¹ (Fig. 2.2).

Laboratory – Impact of deployment and battery replacement

After a 9-10 month deployment on eight individual Weddell seals, eight SRDL tags were recovered and recalibrated in the lab. For this subset of tags, we compared ME and MAE before and after deployment and after battery replacement (Table 2.2). Similar to results from the 44 tags combined, before deployment, ME and MAE values from the manufacturer calibration were highest for temperatures below 0 °C (ME=0.029, SD=0.026; MAE=0.029, SD=0.026) and lowest for temperatures > 6 °C (ME=-0.001, SD=0.008; MAE=0.005, SD=0.006) (Table 2.2). The manufacturer

calibration produced temperature ME and MAE within the stated accuracy of ± 0.005 °C only for temperatures > 6 °C (Table 2.2). Before deployment, the overall ME produced by the manufacturer calibration was 0.010 °C (SD=0.019) (Table 2.2). The percentage of data within the manufacturer specified accuracy for temperature increased with increasing temperature, ranging from 4 to 76% (Fig. 2.3).

With our independent calibration, before deployment, temperature ME and MAE values were within the manufacturer stated accuracy of ± 0.005 °C for all temperature bins (Table 2.2). The overall accuracy for our independent calibration was 0.000 °C (SD=0.004) compared to 0.010 °C (SD=0.019) for the manufacturer calibration. In addition, the standard deviations around ME and MAE values produced by our independent calibration were smaller than those produced by the manufacturer calibration (Table 2.2). With our independent calibration, 62-100% of the temperature values were within the specified accuracy of the tag prior to deployment (Fig. 2.3).

Post-deployment, ME values for the manufacturer calibration were higher than before deployment for all temperatures greater than 0 °C (Table 2.2). For these temperatures, ME values post-deployment were negative with 24-41% of the data within the stated ± 0.005 °C accuracy (Table 2.2, Fig. 2.3). Before deployment, most of the temperature errors were positive or within ± 0.005 °C. However, after deployment, negative temperature errors increased. Because temperature errors between -2 and 0 °C were primarily positive before deployment, this downward shift upon deployment increased the accuracy of the temperature values (Table 2.2, Fig.

2.3). The standard deviation in the manufacturer ME values for each temperature bin was greater after tag deployment than before (Table 2.2). Overall, MAE was 0.017 °C (SD=0.019) post-deployment compared to 0.013 °C (SD=0.017) pre-deployment.

While our independent calibration improved the accuracy of the temperature sensors pre-deployment, like the manufacturer calibration, accuracy was reduced post-deployment; ME after deployment was -0.019 °C (SD=0.020) compared to 0.000 (SD=0.004) before deployment (Table 2.2). MAE for our independent calibration was 0.020 °C (SD=0.019) compared to 0.017 °C (SD=0.019) for the manufacturer calibration. The standard deviation in temperature errors was similar for both the manufacturer and our independent calibration (Table 2.2). Temperature errors for our independent calibration shifted from values that were within the stated accuracy before deployment to negative values after deployment (Fig. 2.3). Across the four temperature bins, 17%, 20%, 43% and 0% of the data were within the ± 0.005 °C accuracy (Fig. 2.3).

After battery replacement in five of the eight recovered SRDL tags, the manufacturer calibration produced temperatures that were less accurate and precise (ME=-0.008, SD=0.035) than those produced during both pre- (ME=0.010, SD=0.019) and post-deployment (ME=-0.005, SD=0.025) calibrations (Table 2.2). For all temperatures greater than 0 °C, the manufacturer calibration produced ME values that were higher than both pre- and post-deployment ME values. MAE values produced by the manufacturer calibration followed the same trend (Table 2.2). Across all temperatures, the percentage of negative errors increased from pre-deployment to

post-deployment and again after battery replacement (Fig. 2.3). After battery replacement, 0-18% of the temperature errors was within the specified accuracy of the sensor (Fig. 2.3).

While our independent calibration was more accurate than the manufacturer calibration overall, temperature accuracy decreased from before deployment (ME=0.000, SD=0.004) to after deployment (ME=-0.019, SD=0.020), and further decreased after battery replacement (ME=-0.022, SD=0.024), following the same trend as the manufacturer calibration (Table 2.2). A higher percentage of errors were negative after battery replacement than either pre- or post- deployments (Fig. 2.3). The percentage of data within the 0.005 °C stated accuracy of the temperature sensor was 0, 2, 6 and 0 across increasing temperature bins (Fig. 2.3).

Before deployment, the manufacturer calibration produced conductivity values that followed the same pattern as those from the larger dataset of 44 tags examined previously; MAE increased from 0.042 mScm⁻¹ (SD=0.034) to 0.095 mScm⁻¹ (SD=0.065) with increasing conductivity (Table 2.2). Overall, ME was 0.004 (SD=0.076) and MAE was 0.059 (SD=0.048). The percentage of data within the 0.01 mScm⁻¹ stated accuracy for the tags ranged between 0 and 10, with the majority of the conductivity values overestimated by the manufacturer calibration (Fig. 2.4).

Our independent calibration produced ME and MAE values that were within the stated accuracy of ± 0.01 mScm⁻¹ for all conductivity bins (Table 2.2). The standard deviation in conductivity errors produced by our independent calibration was smaller than those produced by the manufacturer calibration. Pre-deployment, MAE

for our independent calibration was 0.005 (SD=0.007) for all conductivities measured in the lab, compared to 0.059 (SD=0.048) for the manufacturer calibration. For our independent calibration, data within the specified accuracy of the conductivity sensor ranged from 76-100% (Fig. 2.4).

After deployment, ME and MAE produced by the manufacturer calibration were higher than the manufacturer stated accuracy of $\pm 0.01 \text{ mScm}^{-1}$ for newly purchased tags (Table 2.2). MAE was higher post-deployment (MAE=0.091, SD=0.034) than pre-deployment (MAE=0.059, SD=0.048) (Table 2.2). A larger proportion of errors was positive compared to post-deployment errors for all conductivity bins (Fig. 2.4). With the exception of 1% of the 25-29 mScm^{-1} data, all conductivity errors were higher than the $\pm 0.01 \text{ mScm}^{-1}$ manufacturer accuracy (Fig. 2.4).

Post-deployment, MAE for our independent calibration ranged from 0.052 mScm^{-1} (SD=0.044) to 0.117 mScm^{-1} (SD=0.127), increasing across increasing conductivity bins. Overall, MAE for our independent calibration (MAE=0.074 SD=0.081) was lower than the MAE for the manufacturer calibration (MAE=0.091, SD=0.034). After deployment, the majority of the conductivity errors were positive and 0-14% of the errors within the different conductivity bins were within the $\pm 0.01 \text{ mScm}^{-1}$ stated accuracy (Fig. 2.4).

After battery replacement, conductivity ME values produced by the manufacturer calibration were shifted below both pre- and post-deployment values (Table 2.2). The standard deviation in error values was higher after battery

replacement than before. MAE across all conductivity bins for the manufacturer calibration was 0.081 mScm^{-1} ($SD=0.088$) (Table 2.2). After battery replacement, the percentage of positive conductivity errors decreased from pre- and post- deployment values and a higher percentage of data (0-17%) was within the manufacturer stated accuracy of $\pm 0.01 \text{ mScm}^{-1}$ (Fig. 2.4).

For our independent calibration, MAE after battery replacement ($MAE=0.076$, $SD=0.082$) was higher than the post- ($MAE=0.074$, $SD=0.081$) and pre-deployment ($MAE=0.005$, $SD=0.007$) (Table 2.2). ME values for our independent calibration followed a similar pattern to those produced by the manufacturer calibration; after deployment, ME values were shifted above pre-deployment ME values. However, following battery replacement, ME values were shifted below pre-deployment ME values (Table 2.2). Similar to data produced by the manufacturer calibration, the percentage of positive errors produced by our independent calibration post-deployment, decreased after battery replacement (Fig. 2.4). However, the percentage of data within the manufacturer stated accuracy for conductivity ranged from 3-16%, an increase from post-deployment values produced by our independent calibration (Fig. 2.4).

In situ - SRDL tags as received by manufacturer

The overall ME for *in situ* temperature produced by the manufacturer calibration were $0.021 \text{ }^{\circ}\text{C}$ ($SD=0.016$) (Table 2.3). The majority of the temperature errors for all depth bins were positive, indicating that the manufacturer calibration overestimated temperature in the field (Fig. 2.5). Six percent of the data in the 5-50 m

bin were within the manufacturer's ± 0.005 °C stated accuracy. However, SRDL temperature accuracy decreased with increasing depth such that 0% of the data in the 150-200 m depth bin were within ± 0.005 °C (Fig. 2.5).

Across depths, ME produced by our independent calibration was 0.018 °C (SD=0.015) (Table 2.3). Similar to results produced by the manufacturer calibration, temperature errors produced by our independent calibration increased with increasing depth (Table 2.3). Our independent calibration also produced positive errors similar to the manufacturer calibration (Fig. 2.5).

For conductivity, ME and MAE produced by the manufacturer calibration was 0.043 (SD=0.018) and 0.044 (SD=0.016) mScm^{-1} , both of which were higher than the manufacturer stated accuracy of ± 0.01 mScm^{-1} for newly purchased tags (Table 2.3). Similar to the *in situ* temperature errors, the majority of conductivity errors produced by the manufacturer calibration were positive (Fig. 2.6). In addition, over 90% of the data in each depth bin were higher than the ± 0.01 mScm^{-1} accuracy.

Although ME and MAE produced by our independent calibration (ME=0.031, MAE=0.032 mScm^{-1}) were less than ME and MAE from the manufacturer calibration, the standard deviation in conductivity errors was higher for our independent calibration (Table 2.3). While the majority of the data in each depth bin was positively skewed, a larger percentage of the data produced by our independent calibration (18-26%) was within the stated ± 0.01 mScm^{-1} accuracy than the data produced by the manufacturer calibration (2-4%) (Fig. 2.6).

In situ - Impact of SRDL attachment

In total, there were 18 CTD-SRDL casts collected by nine seals that were within five kilometers and two days of eight SB CTD casts (Fig. 2.7). Temperature ME and MAE produced by the manufacturer calibration during deployment (ME=0.040, SD=0.0126; MAE=0.094, SD=0.093) were higher than those produced when the nine SRDL tags were attached to the SB profiler (ME=0.021, SD=0.015; MAE=0.023, SD=0.012) (Table 2.4). During deployment, temperature ME and MAE were higher than the stated accuracy of ± 0.005 °C across all depths (Table 2.4). For depths between 5 and 100 m, temperatures measured by the manufacturer calibration were less precise than temperatures measured at depths between 100 and 150 m (Table 2.4). The majority of the data in each depth bin was positively skewed and less than six percent of the data were within the manufactured stated accuracy of ± 0.005 °C (Fig. 2.8).

During deployment, our independent calibration produced MAE values between 0.068 °C (SD=0.060) and 0.104 °C (SD=0.095) across depth bins (Table 2.5). While Temperature ME produced by our independent calibration (ME=0.033, SD=0.127) was less than ME for the manufacturer calibration (ME=0.040, SD=0.126), overall MAE values were the same for the two calibrations (Table 2.4). MAE values for the SRDL tags before deployment were less than MAE values during deployment on a Weddell seal. Similar to results produced by the manufacturer calibration, the majority of the errors produced by our independent calibration were

positively skewed with less than eight percent of the data within the stated accuracy for the temperature sensor (Fig. 2.8).

Like temperature, conductivity ME and MAE produced by the manufacturer calibration during deployment (ME=0.277, SD=0.239; MAE=0.331, SD=0.155) were higher than pre-deployment values (ME=0.044, SD=0.019; MAE=0.044, SD=0.018) (Table 2.4). Similar to the trend for temperature, standard deviation of conductivity ME and MAE decreased with increasing depth for both the manufacturer and our independent calibration (Table 2.4). Over 80% of the error values produced by the manufacturer calibration were positively skewed with only two, zero, and three percent of the data within the stated $\pm 0.01 \text{ mScm}^{-1}$ accuracy of the tag across the three depth bins (Fig. 2.9).

Our independent calibration produced slightly lower conductivity ME and MAE values (ME=0.265, SD=0.239; MAE=0.319, SD=0.149) than the manufacturer calibration (Table 2.4). However, these ME and MAE values produced while SRDL tags were attached to a seal were higher than those produced when tags were attached to the SB profiler (Table 2.4). The majority of the conductivity errors produced by our independent calibration were positively skewed and less than seven percent of the data were within the $\pm 0.01 \text{ mScm}^{-1}$ accuracy (Fig. 2.9).

DISCUSSION

Our understanding of animal behavior and our ability to collect oceanographic data in remote areas has been revolutionized by the miniaturization of oceanographic sensors that can be incorporated into electronic tags and deployed on marine animals.

SRDL tags provide the perfect solution for merging biologists' interest in animal behavior and habitat utilization with oceanographers' interest in the physical properties of seawater. To further enhance this synergy, we need to understand the intricacies and limitations of using SRDL tags deployed on marine animals to collect oceanographic data. While SRDL tag sensors are accurate enough to detect water masses, in order to detect changes within a water mass, defining ME and MAE is essential. A clear understanding of the errors and limitations inherent in temperature and conductivity measurements obtained from animal-borne CTD tags is critical when integrating these data with those collected from other oceanographic platforms.

In the laboratory, the manufacturer calibration performed within the stated accuracy of ± 0.005 °C for all temperatures except those below 0 °C. Therefore, independent calibration may be necessary when SRDL tags are deployed on animals that frequent waters less than 0 °C. Our *in situ* calibration test in the Ross Sea, Antarctica, where temperatures were below freezing, confirmed this finding. Temperature ME and MAE were higher than the stated accuracy of the sensor for all temperatures below 0 °C, regardless of depth. While our independent calibrations produced temperature errors that were slightly less than the manufacturer calibration under *in situ* conditions, these errors were also higher than the manufacturer's stated accuracy. The difference in the temperature errors produced by our independent calibration in the lab and in the field may be due to sensor delay; in the laboratory, tags were allowed to equilibrate, at a constant depth, to a range of temperatures and

the most stable period was selected for analysis whereas under *in situ* conditions, SRDL tags actively sampled the water column.

The manufacturer calibration overestimated conductivity in the laboratory beyond the expected $\pm 0.01 \text{ mScm}^{-1}$, while our independent calibration produced highly accurate values across all measured conductivities. While both calibrations overestimated conductivity under *in situ* conditions, $\sim 20\%$ of the data in each depth bin produced from our independent calibration were within the $\pm 0.01 \text{ mScm}^{-1}$ accuracy. Less accurate conductivity values in the field than in the lab for both calibrations may be a byproduct of our calibration methods in which depth was held constant and only the most stable two minute duration in conductivity was used to create the new calibration strings.

Our independent calibration performed better under laboratory conditions than the manufacturer calibration, which was expected since the manufacturer calibrated tag sensors under different environmental conditions. The large spread in temperature and conductivity errors for both the manufacturer and our independent calibrations in Ross Sea waters less than 100 m, also suggest that SRDL tag sensors may be slow to respond in a dynamic environment typical of surface waters. A previous study found that rapid changes in temperature induced larger errors in both temperature and derived salinity likely resulting from a thermal mass effect in which the core temperature of the tag leads to slower response times (Roquet et al., 2011). Also, pressure effects on the sensors themselves may lead to differences in accuracies between lab and field conditions.

Boehme et al. (2009) concluded that the conductivity sensor is highly sensitive to obstructions in the external field. The higher than expected conductivity errors created by the manufacturer calibration in the lab may have been related to the addition of an epoxy base plate to the bottom of the SRDL tag for attachment in the field. However, contact between the bottom of the tag and the wall of the conductivity bath in a previous study produced deviations in salinity that were less than when interference was introduced to other parts of the tag (Boehme et al., 2009) suggesting that any conductivity error due to the addition of a base plate to the bottom of a SRDL tag should be negligible. Even after our independent calibration, which corrected any possible error created by the addition of a base plate, conductivity MAE in the field was higher than the stated accuracy of the sensor.

Researchers must consider how sensor characteristics change over the period of deployment. Further, in some cases, SRDL tags are recovered and re-deployed and thus knowledge of sensor durability becomes important. Our results show that temperature and conductivity MAE for both calibrations were higher after a 9-10 month deployment on a Weddell seal. Based on typical Weddell seal behavior of reaming ice to maintain breathing holes and feeding immediately below the ice surface, these high errors were not surprising; SRDL tags were subject to rough conditions and recovered damaged and often with broken antennae. The proximity of ice and damaged antennae to the sensor, in combination with the sensitivity of the conductivity cell, may have created higher than expected drift in conductivity and probably represent a worst case scenario that may not be representative for other

marine animals like elephant seals that exist in less hostile oceanic environments. In fact, tags recovered from elephant seals are often in considerably better condition than tags recovered from Weddell seals (Costa, unpublished data).

In addition to deployment, battery replacement also impacted the accuracy of temperature and conductivity measurements produced by the manufacturer and our independent calibration. While overall temperature MAE was higher than pre- or post-deployment values, conductivity MAE was lower after battery replacement than post-deployment. However, the higher standard deviation in conductivity ME and MAE for both calibrations indicates lower precision after battery replacement. The improved accuracy is likely due to the power-intensive nature of the conductivity cell. The accuracy of the SRDL temperature sensor appeared to degrade over time. Before deployment, the majority of the temperatures produced from the manufacturer calibration was either within the expected ± 0.005 °C accuracy or was higher than the temperatures measured in the laboratory. After deployment, a higher percentage of the temperature data were lower than those measured in the laboratory. This pattern continued after battery replacement at which time most temperature values were underestimated by the manufacturer calibration. Our independent calibration produced results that also showed a downward shift from positive to negative temperature errors. However, because the majority of the temperature data were within the expected accuracy before deployment, a higher percentage of the data in each temperature range was underestimated after deployment and battery replacement than data produced by the manufacturer calibration.

Based on observations of thermal response time, sensitivity of the conductivity sensor to objects proximate to its external magnetic field, and the unique insulative and conductive properties of Weddell seals, we suspected that tag deployment would impact the accuracy of temperature and conductivity measurements. In fact, we found that temperature and conductivity MAE was higher during deployment than before deployment. Because we used CTD casts from SRDL tags collected within days of SRDL tag deployment, it is unlikely that low battery power or a damaged antenna influenced the results. However, casts collected by SRDL tags were compressed into 16 representative values for depth, temperature and conductivity for transmission via ARGOS satellite. Due to limitations in bandwidth when SRDL tags communicate with ARGOS, precision in depth values decreases with increasing depth. For example, precision is ± 1 m at 20 m and ± 5 m at 200 m depth. This decrease in precision may introduce error when seals dive to deeper depths. Similarly, Weddell seal behavior (three-dimensional dynamic movement, reaming ice holes, and feeding proximate to the ice) cannot be controlled and undoubtedly influences the accuracy of the SRDL sensors. Therefore, temperature and conductivity ME and MAE reported during deployment on a seal should be considered the maximum error due to the additive effect of tag attachment and other possible influences.

Although ME and MAE values between the manufacturer and our independent calibration under *in situ* conditions were not as disparate as those produced by the two calibrations under laboratory conditions, our calibration

produced more accurate results overall. However, ME and MAE temperature and conductivity values for both calibrations were higher than the stated accuracy of the sensors under *in situ* conditions. These results suggest that the accuracy of oceanographic data can be increased by performing independent calibrations on the SRDL sensors, especially when *in situ* conditions are expected to be outside the manufacturer calibration range for temperature and conductivity. Due to the substantial loss in accuracy after deployment, we strongly recommend re-calibrating tags before re-deployment. Similarly, if SRDL tags are recovered after a 6-9 month deployment, we advise replacing the battery (due to the power requirements of the conductivity sensor) and re-calibrating the tag sensors.

Even after performing independent calibrations, researchers using SRDL tags should be aware that temperature and conductivity shifts associated with *in situ* conditions are likely to be higher than 1) offsets produced in the lab and 2) the manufacturer stated accuracy of the sensors. In addition, under *in situ* conditions, the quality of data collected by SRDL sensors may also be impacted by measurement drift, sensor fouling, and interference of the magnetic field around the conductivity sensor (McCafferty et al., 1999; Hooker and Boyd, 2003; Fedak, Mike, 2004; Boehme et al., 2009; Roquet et al., 2011). Based on the results of this study, we believe that in order to improve the quality of data collected by SRDL tags, attention should be directed towards 1) improving the stability of the conductivity sensor when exposed to external objects, 2) calibrating the temperature sensor to a minimum of -2 °C, and 3) decreasing the response time of the tag.

As long as researchers are aware of and able to correct for temperature and conductivity errors, data collected by SRDL tags deployed on marine animals are a powerful complement to data collected by traditional oceanographic equipment. Even without independent calibrations, corrections can be made post-deployment using methods presented in Roquet et al (2014). In this approach, the SMRU tag is calibrated against a known CTD measurement that is obtained during some time when the tag is in the vicinity of a deep stable water mass. The SMRU-CTD data are then post-processed according to that known profile. SRDL tags provide a cost effective method for collecting large quantities of oceanographic data in remote areas and during times when other technologies are limited or cannot be used. For example, Weddell seals outfitted with SRDL tags were able to collect the most extensive oceanographic dataset ever recorded for the Ross Sea during the winter when 24-hours of darkness and heavy sea ice prevail. The miniaturization of oceanographic sensors and the development of SRDL technology enable tags to be attached to marine animals evolved to thrive in some of the most extreme environmental conditions on earth. As a result, CTD-SRDL tags are able to record both behavior data and oceanographic data in areas that might otherwise go unstudied. While temperature and conductivity collected by SMRU CTD tags may not be comparable to high-precision oceanographic equipment, they provide invaluable oceanographic data. SRDL tag sensors are as or more accurate than expendable bathythermographs (XBT; Temperature ± 0.15 °C) and expendable CTDs (XCTD; Temperature ± 0.01 °C; Conductivity ± 0.03 mScm⁻¹) (Sy and Wright, 2000), and fully capable of

identifying water mass characteristics and seasonal changes in otherwise inaccessible areas.

TABLES

Table 2.1: Laboratory calibration results from 44 newly-purchased SRDL tags. Mean (ME) and mean absolute error (MAE) with standard deviations (SD) for temperature and conductivity values produced from the manufacturer and our independent calibration are provided for each of four bins. ME and MAE are relative to temperature and conductivity values measured by laboratory equipment (Sea-bird Electronics, model 3F thermistor and Guildline, model 8400B salinometer).

Temperature (°C)		-2 - 0	0 - 4	4 - 6	>6	Overall
Manufacturer	ME ± SD	0.013 ± 0.188	0.004 ± 0.014	0.000 ± 0.014	0.002 ± 0.008	0.005 ± 0.015
	MAE ± SD	0.014 ± 0.018	0.011 ± 0.11	0.009 ± 0.011	0.006 ± 0.006	0.009 ± 0.012
Independent	ME ± SD	0.000 ± 0.003	0.000 ± 0.002	-0.001 ± 0.002	0.000 ± 0.001	0.000 ± 0.002
	MAE ± SD	0.002 ± 0.002	0.001 ± 0.002	0.001 ± 0.002	0.001 ± 0.001	0.001 ± 0.002
Conductivity (mScm⁻¹)		25 - 29	29 - 34	34 - 47	47 - 55	Overall
Manufacturer	ME ± SD	0.011 ± 0.031	0.028 ± 0.032	0.029 ± 0.041	0.046 ± 0.058	0.026 ± 0.042
	MAE ± SD	0.027 ± 0.019	0.038 ± 0.020	0.042 ± 0.027	0.061 ± 0.042	0.040 ± 0.030
Independent	ME ± SD	-0.001 ± 0.007	0.004 ± 0.010	-0.001 ± 0.004	0.000 ± 0.001	0.000 ± 0.007
	MAE ± SD	0.005 ± 0.005	0.007 ± 0.009	0.002 ± 0.003	0.001 ± 0.001	0.004 ± 0.005

Table 2.2: Laboratory calibration results from eight SRDL tags before and after deployment, and after battery replacement. Mean and mean absolute error (ME and MAE) with standard deviations (SD) for temperature and conductivity produced from the manufacturer and our independent calibration are provided for each of four bins. All error values are relative to temperature and conductivity values measured by laboratory equipment (Sea-bird Electronics, model 3F thermistor and Guildline, model 8400B salinometer).

		Temperature (°C)	-2 - 0	0 - 4	4 - 6	>6	Overall
Manufacturer	Before deployment	ME ± SD	0.029 ± 0.026	0.006 ± 0.011	0.007 ± 0.017	-0.001 ± 0.008	0.010 ± 0.019
		MAE ± SD	0.029 ± 0.026	0.008 ± 0.010	0.010 ± 0.015	0.005 ± 0.006	0.013 ± 0.017
	After deployment	ME ± SD	0.008 ± 0.022	-0.009 ± 0.026	-0.009 ± 0.024	-0.010 ± 0.028	-0.005 ± 0.025
		MAE ± SD	0.018 ± 0.014	0.017 ± 0.021	0.015 ± 0.020	0.021 ± 0.020	0.017 ± 0.019
	After re-battery	ME ± SD	0.023 ± 0.038	-0.015 ± 0.031	-0.017 ± 0.028	-0.012 ± 0.043	-0.008 ± 0.035
		MAE ± SD	0.034 ± 0.026	0.025 ± 0.022	0.025 ± 0.021	0.030 ± 0.026	0.028 ± 0.022
Independent	Before deployment	ME ± SD	0.001 ± 0.005	-0.001 ± 0.004	0.001 ± 0.005	-0.001 ± 0.002	0.000 ± 0.004
		MAE ± SD	0.003 ± 0.003	0.003 ± 0.003	0.003 ± 0.003	0.001 ± 0.001	0.003 ± 0.003
	After deployment	ME ± SD	0.000 ± 0.003	0.000 ± 0.003	0.001 ± 0.002	-0.001 ± 0.001	0.000 ± 0.002
		MAE ± SD	0.002 ± 0.002	0.002 ± 0.002	0.002 ± 0.001	0.001 ± 0.001	0.002 ± 0.001
	After re-battery	ME ± SD	0.004 ± 0.001	-0.003 ± 0.006	0.003 ± 0.005	-0.003 ± 0.000	0.000 ± 0.006
		MAE ± SD	0.004 ± 0.001	0.006 ± 0.004	0.006 ± 0.002	0.003 ± 0.000	0.005 ± 0.003
		Conductivity (mScm-1)	25 - 29	29 - 34	34 - 47	47 - 56	Overall
Manufacturer	Before deployment	ME ± SD	-0.015 ± 0.054	0.006 ± 0.064	-0.002 ± 0.077	0.039 ± 0.113	0.004 ± 0.076
		MAE ± SD	0.042 ± 0.034	0.051 ± 0.034	0.057 ± 0.049	0.095 ± 0.065	0.059 ± 0.048
	After deployment	ME ± SD	0.020 ± 0.069	0.059 ± 0.053	0.049 ± 0.097	0.113 ± 0.036	0.066 ± 0.072
		MAE ± SD	0.062 ± 0.027	0.075 ± 0.020	0.101 ± 0.027	0.113 ± 0.036	0.091 ± 0.034
	After re-battery	ME ± SD	-0.049 ± 0.092	-0.028 ± 0.107	-0.082 ± 0.158	0.038 ± 0.072	-0.033 ± 0.116
		MAE ± SD	0.069 ± 0.075	0.066 ± 0.083	0.111 ± 0.136	0.072 ± 0.028	0.081 ± 0.088
Independent	Before deployment	ME ± SD	-0.003 ± 0.008	0.007 ± 0.014	-0.002 ± 0.005	0.001 ± 0.002	0.000 ± 0.009
		MAE ± SD	0.005 ± 0.006	0.009 ± 0.013	0.003 ± 0.005	0.001 ± 0.001	0.005 ± 0.007
	After deployment	ME ± SD	0.008 ± 0.028	0.000 ± 0.038	0.004 ± 0.056	-0.024 ± 0.056	-0.005 ± 0.048
		MAE ± SD	0.013 ± 0.025	0.022 ± 0.030	0.030 ± 0.046	0.024 ± 0.056	0.023 ± 0.042
	After re-battery	ME ± SD	-0.001 ± 0.002	0.002 ± 0.004	-0.001 ± 0.002	0.000 ± 0.000	0.000 ± 0.002
		MAE ± SD	0.002 ± 0.001	0.003 ± 0.003	0.001 ± 0.001	0.000 ± 0.000	0.002 ± 0.002

Table 2.3: *In situ* results from 16 newly-purchased SRDL tags. Mean and mean absolute error (ME and MAE) with standard deviations (SD) for temperature and conductivity produced from the manufacturer and our independent calibration are provided for each of four depth bins. ME and MAE values are relative to temperature and conductivity values measured by a CTD profiler (Sea-bird Electronics, model 19-03).

Temperature (°C)		5 – 50 m	50 – 100 m	100 – 150 m	150 – 200 m	Overall
Manufacturer	ME ± SD	0.015 ± 0.025	0.018 ± 0.011	0.024 ± 0.007	0.029 ± 0.008	0.021 ± 0.016
	MAE ± SD	0.022 ± 0.018	0.020 ± 0.008	0.024 ± 0.007	0.029 ± 0.008	0.023 ± 0.012
Independent	ME ± SD	0.012 ± 0.024	0.016 ± 0.010	0.021 ± 0.006	0.026 ± 0.008	0.018 ± 0.015
	MAE ± SD	0.021 ± 0.018	0.017 ± 0.007	0.021 ± 0.006	0.026 ± 0.008	0.021 ± 0.011
Conductivity (mScm⁻¹)		5 – 50 m	50 – 100 m	100 – 150 m	150 – 200 m	Overall
Manufacturer	ME ± SD	0.042 ± 0.026	0.042 ± 0.015	0.044 ± 0.013	0.045 ± 0.013	0.043 ± 0.018
	MAE ± SD	0.044 ± 0.022	0.042 ± 0.014	0.044 ± 0.013	0.045 ± 0.013	0.044 ± 0.016
Independent	ME ± SD	0.031 ± 0.031	0.030 ± 0.024	0.032 ± 0.022	0.024 ± 0.022	0.031 ± 0.025
	MAE ± SD	0.035 ± 0.027	0.031 ± 0.023	0.032 ± 0.022	0.034 ± 0.022	0.032 ± 0.024

Table 2.4: *In situ* results from nine newly-purchased SRDL tags deployed on nine Weddell seals in the Ross Sea, Antarctica. Mean and mean absolute error (ME and MAE) with standard deviations (SD) for temperature and conductivity values produced from the manufacturer and our independent calibration are provided for each of three depth bins. ME and MAE values are relative to temperature and conductivity values measured by a CTD profiler (Sea-bird Electronics, model 19-03). Data collected during seal deployment are compared to results collected before deployment for the same nine tags (right column).

		Seal				CTD Profiler
Temperature (°C)		5 - 50	50 - 100	100 - 150	Overall	Overall
Manufacturer	ME ± SD	0.035 ± 0.136	0.067 ± 0.125	0.006 ± 0.090	0.040 ± 0.126	0.021 ± 0.015
	MAE ± SD	0.097 ± 0.100	0.105 ± 0.096	0.064 ± 0.057	0.094 ± 0.093	0.023 ± 0.012
Independent	ME ± SD	0.032 ± 0.136	0.065 ± 0.125	0.004 ± 0.091	0.033 ± 0.127	0.019 ± 0.014
	MAE ± SD	0.097 ± 0.100	0.104 ± 0.095	0.068 ± 0.060	0.094 ± 0.091	0.021 ± 0.011
Conductivity (mScm ⁻¹)		5 - 50	50 - 100	100 - 150	Overall	Overall
Manufacturer	ME ± SD	0.274 ± 0.248	0.316 ± 0.228	0.217 ± 0.227	0.277 ± 0.239	0.044 ± 0.019
	MAE ± SD	0.328 ± 0.168	0.361 ± 0.145	0.287 ± 0.124	0.331 ± 0.155	0.044 ± 0.018
Independent	ME ± SD	0.026 ± 0.248	0.306 ± 0.230	0.202 ± 0.224	0.265 ± 0.239	0.037 ± 0.024
	MAE ± SD	0.318 ± 0.167	0.353 ± 0.147	0.275 ± 0.120	0.319 ± 0.149	0.038 ± 0.022

FIGURES

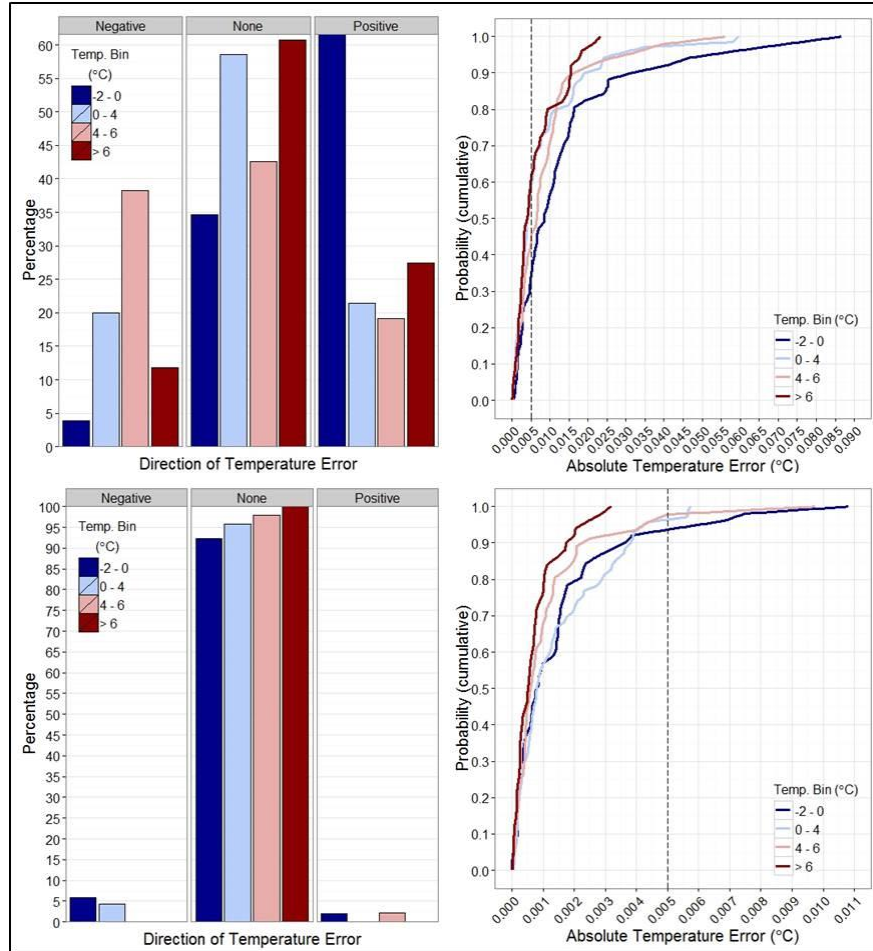


Figure 2.1: Percent data by direction of error (left column) and cumulative probability distribution across absolute temperature errors (right column) for four temperature bins (-2-0, 0-4, 4-6, >6 °C). Error values are the differences between values measured by the SRDL temperature sensor and those measured by the SB thermistor in the laboratory for the manufacturer calibration (top row) and our independent calibration (bottom row). Dotted lines indicate the manufacturer's stated accuracy of $\pm 0.005^{\circ}\text{C}$ for temperature.

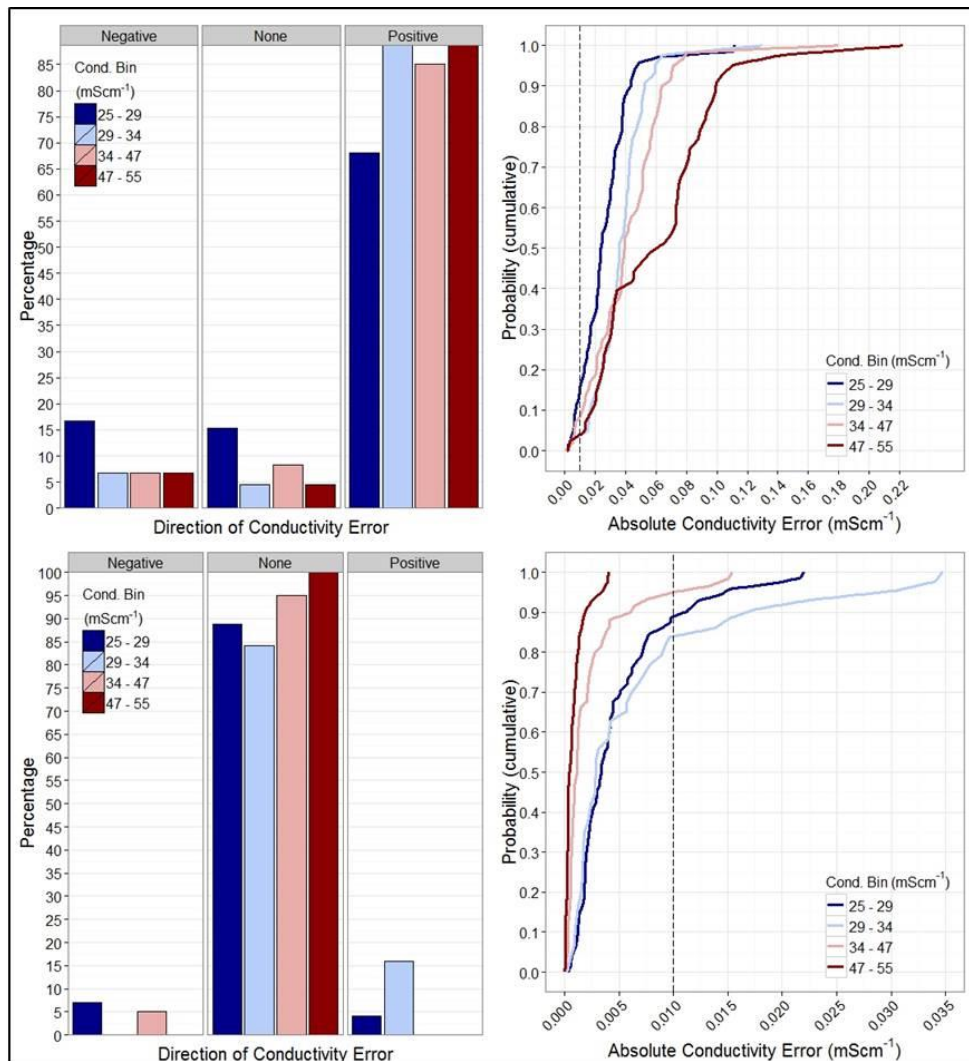


Figure 2.2: Percent data by direction of error (left column) and cumulative probability distribution across absolute conductivity errors (right column) for four conductivity bins (25-29, 29-34, 34-47, 47-55 mScm⁻¹). Error values are the differences between values measured by the SRDL conductivity sensor and those measured in the laboratory for the manufacturer calibration (top row) and our independent calibration (bottom row). Dotted lines indicate the manufacturer's stated accuracy of ± 0.01 mScm⁻¹ for conductivity.

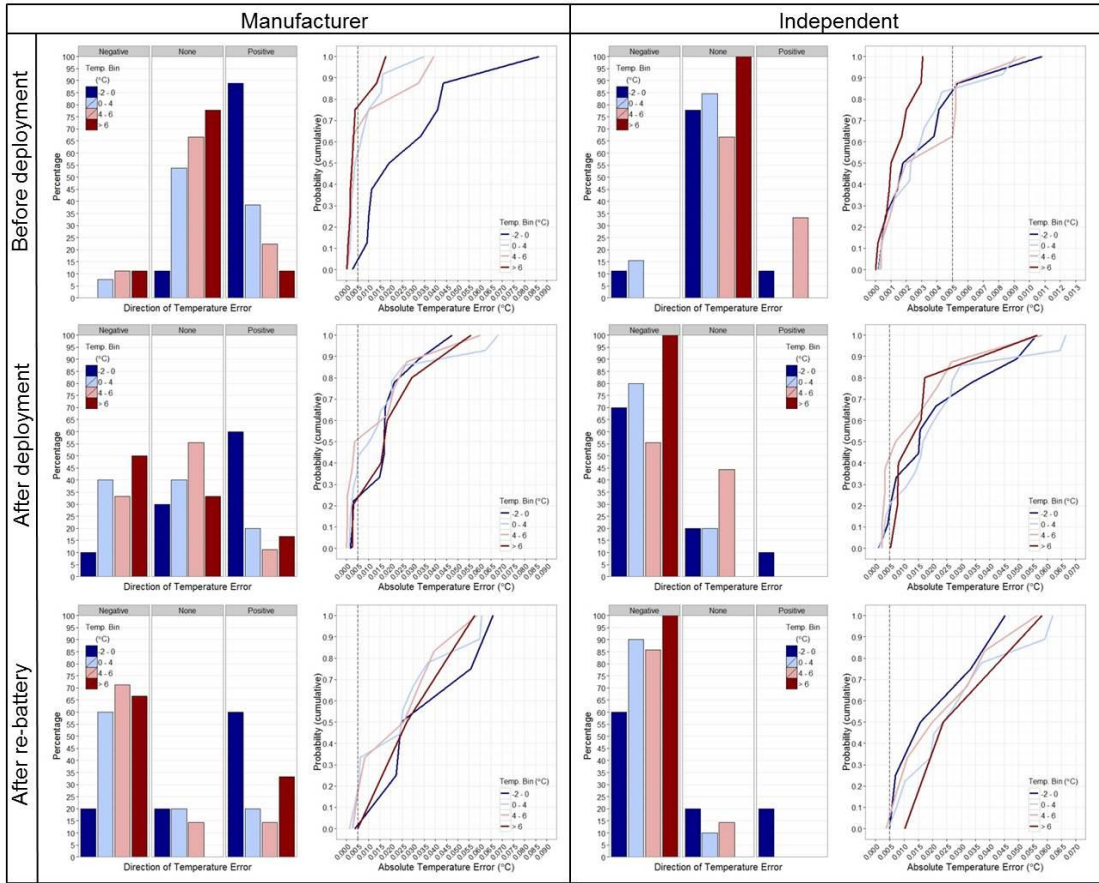


Figure 2.3: Percent data by direction of error (first and third columns) and cumulative probability distribution across absolute temperature errors (second and fourth columns) for four temperature bins ($-2-0, 0-4, 4-6, >6$ °C). Error values are the differences between values measured by the SRDL temperature sensor and those measured by the SB thermistor in the laboratory for the manufacturer calibration (left two columns) and our independent calibration (right two columns) for tags of varying condition (before deployment – top row; after deployment – middle row; after re-battery – bottom row). Dotted lines indicate the manufacturer’s stated accuracy of $\pm 0.005^{\circ}\text{C}$ for temperature.

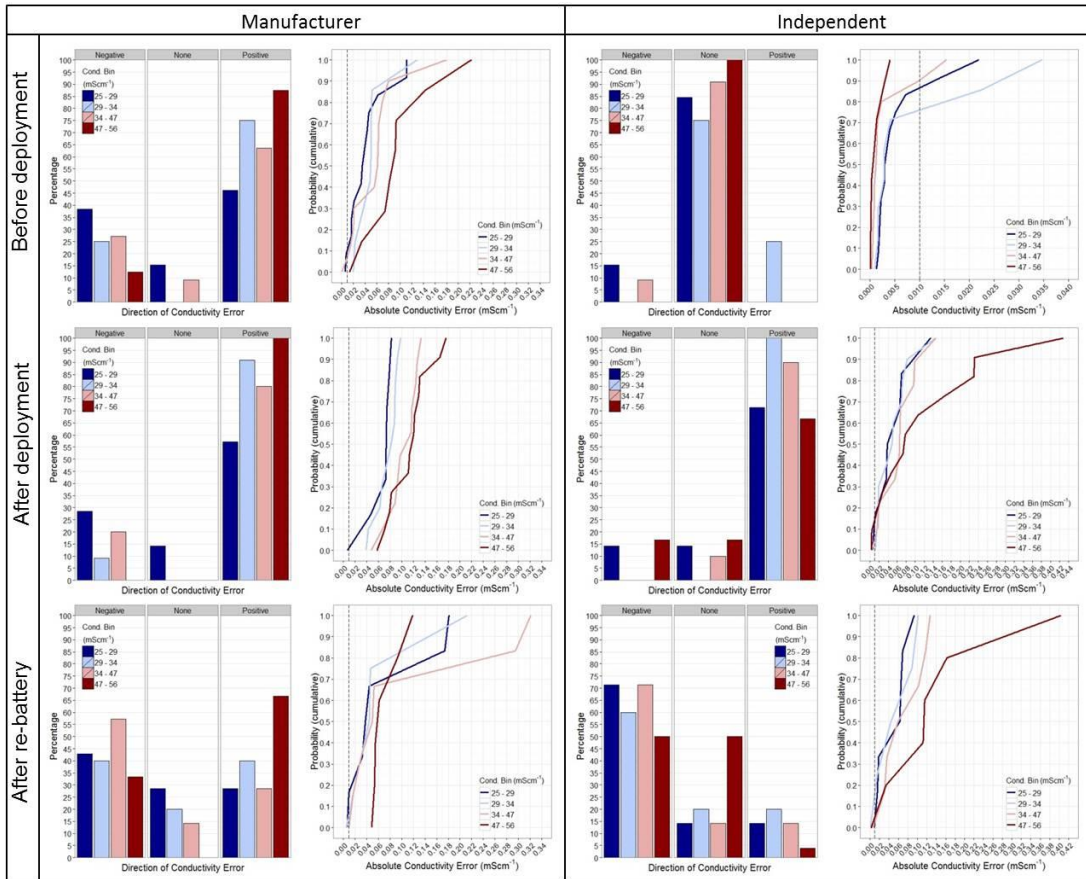


Figure 2.4: Percent data by direction of error (first and third columns) and cumulative probability distribution across absolute conductivity errors (second and fourth columns) for four conductivity bins (25-29, 29-34, 34-47, 47-55 mScm⁻¹). Error values are the differences between values measured by the SRDL conductivity sensor and those measured in the laboratory for the manufacturer calibration (left two columns) and our independent calibration (right two columns) for tags of varying condition (before deployment – top row; after deployment – middle row; after re-battery – bottom row). Dotted lines indicate the manufacturer’s stated accuracy of $\pm 0.01 \text{ mScm}^{-1}$ for conductivity.

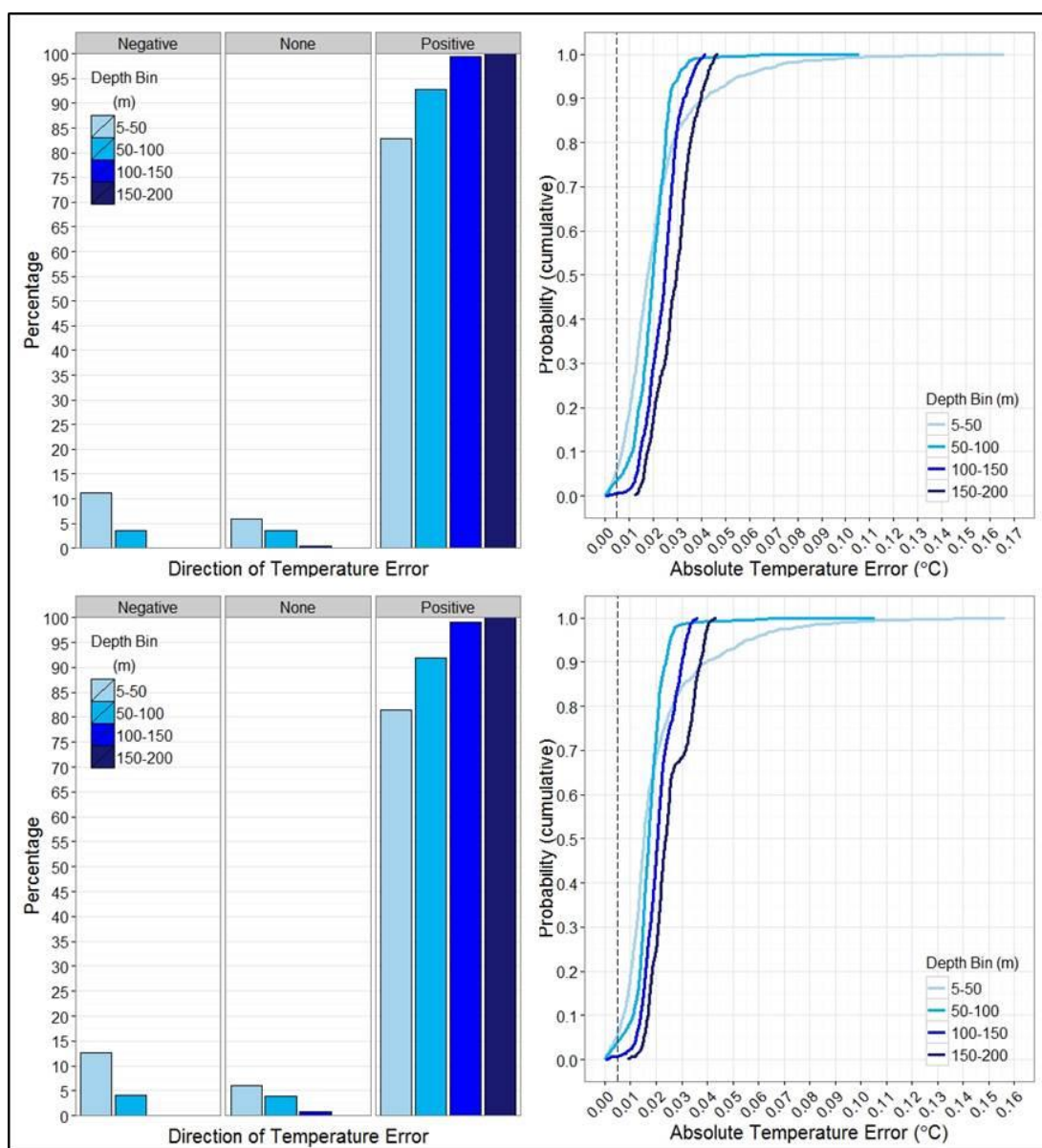


Figure 2.5: Percent data by direction of error (left column) and cumulative probability distribution across absolute temperature errors (right column). Data were collected from the Ross Sea, Antarctica, and error values are the differences in temperature values measured by the SRDL sensor and those measured by a CTD profiler (Sea-bird Electronics, model 19-03) for the manufacturer calibration (top) and our independent calibration (bottom) for four depth bins (5-50, 50-100, 100-150, and 150-200 m). *In situ* temperature values ranged from -1.8 to -1.3 °C. Dotted lines indicate the manufacturer’s stated accuracy of $\pm 0.005^{\circ}\text{C}$ for temperature.

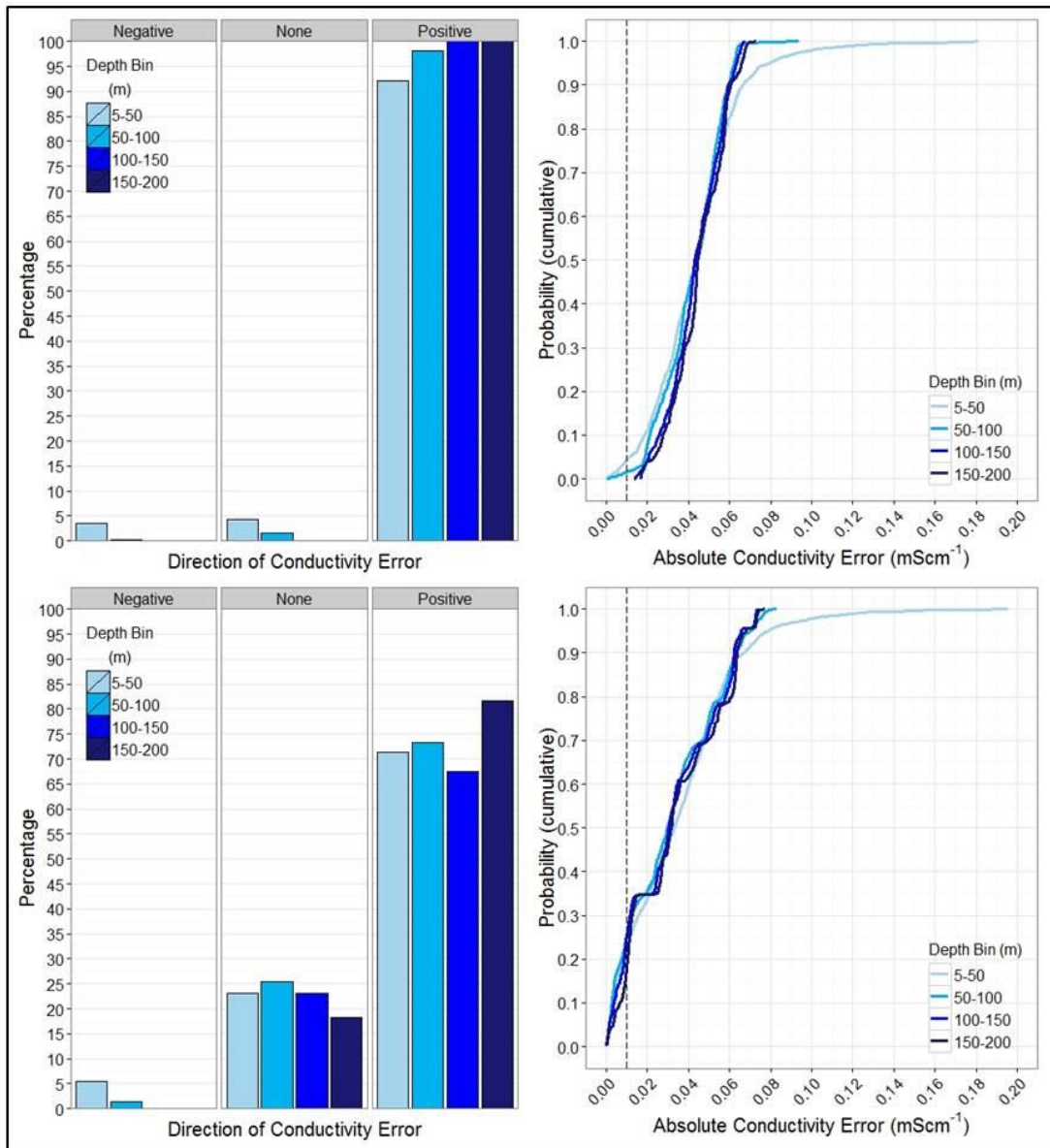


Figure 2.6: Percent data by direction of error (left column) and cumulative probability distribution across absolute conductivity errors (right column). Data were collected from the Ross Sea, Antarctica, and error values are the differences in conductivity values measured by the SRDL sensor and those measured by a CTD profiler (Sea-bird Electronics, model 19-03) for the manufacturer calibration (top) and our independent calibration (bottom) for four depth bins (5-50, 50-100, 100-150, and 150-200 m). *In situ* conductivity values ranged from 26.5 to 27.5 mScm⁻¹. Dotted lines indicate the manufacturer's stated accuracy of ± 0.01 mScm⁻¹ for conductivity.

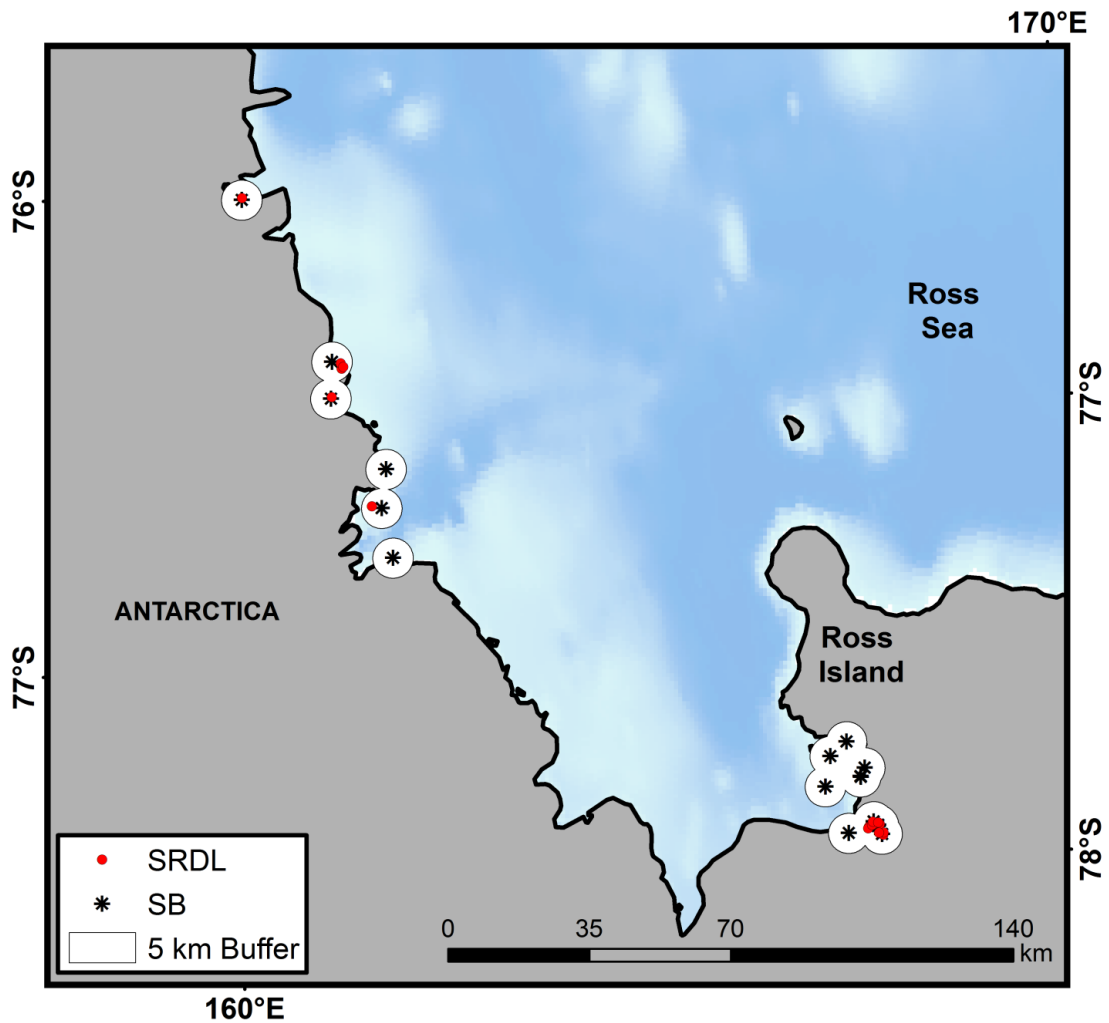


Figure 2.7: Locations of CTD casts collected by deployed SRDL tags (red circles) that are within five kilometers (white buffers) and two days of CTD casts collected by a CTD profiler (Sea-bird Electronics, model 19-03) (black asterisks). Only CTD casts collected by the CTD profiler within the buffer of the SRDL tags were included in the analysis.

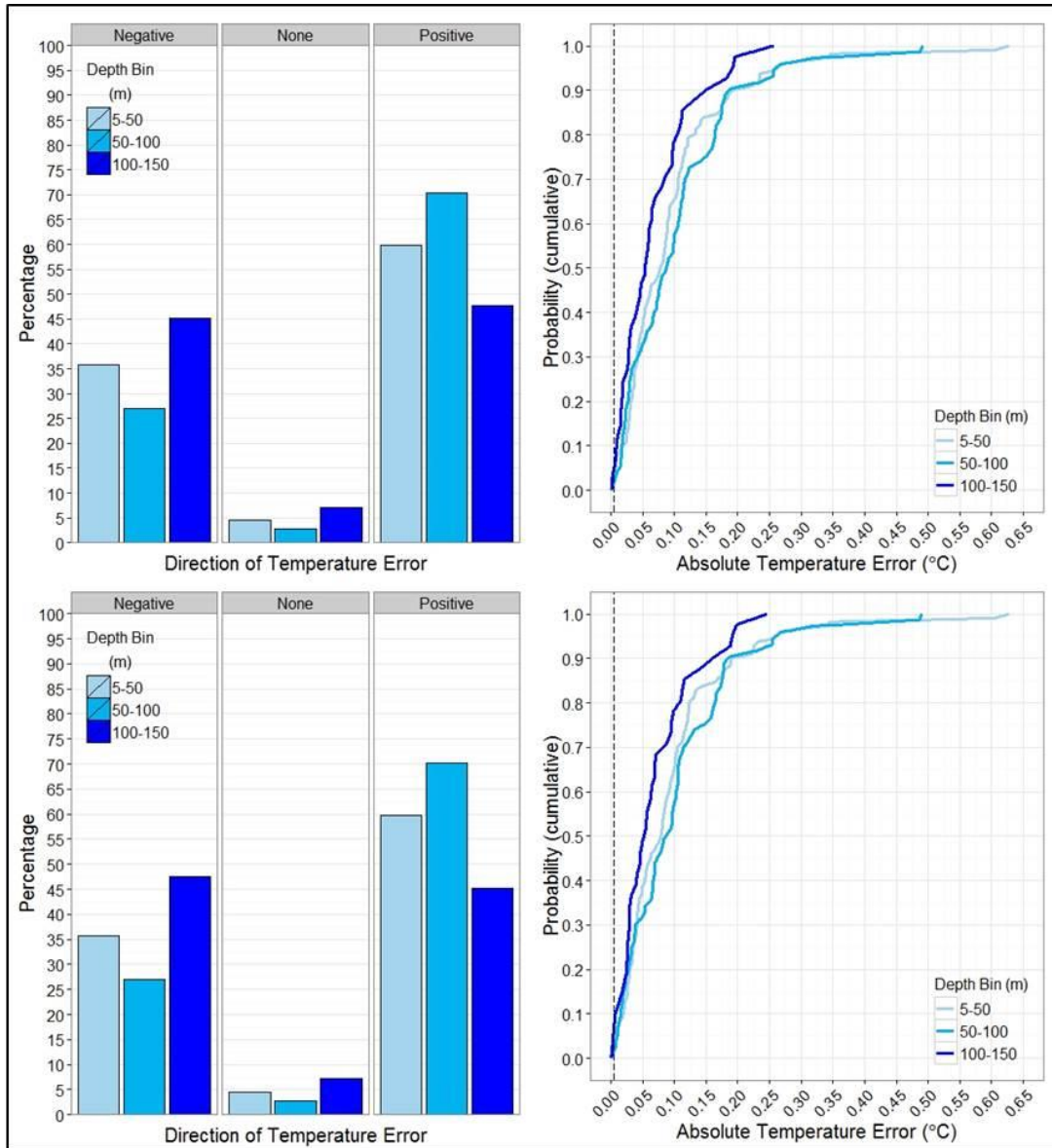


Figure 2.8: Percent data by direction of error (left column) and cumulative probability distribution across absolute temperature errors (right column). Data were collected from the Ross Sea, Antarctica, and error values are the differences in temperature values measured by the SRDL sensor while deployed on the head of a seal and those measured by a CTD profiler (Sea-bird Electronics, model 19-03) for the manufacturer calibration (top) and our independent calibration (bottom) for three depth bins (5-50, 50-100, and 100-150 m). *In situ* temperature values ranged from -1.8 to -1.3 °C. Dotted lines indicate the manufacturer stated accuracy of $\pm 0.005^\circ\text{C}$ for temperature.

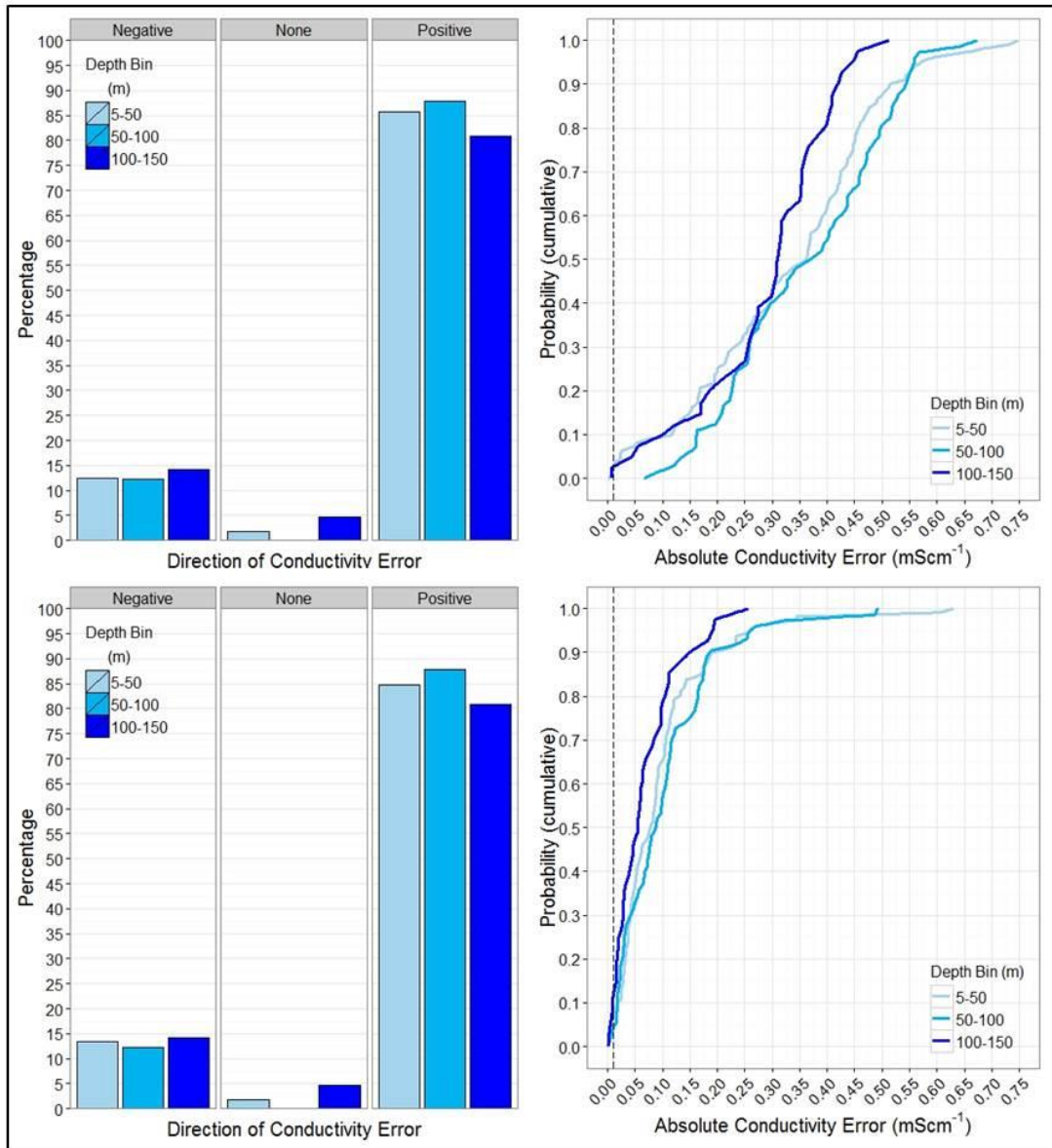


Figure 2.9: Percent data by direction of error (left column) and cumulative probability distribution across absolute conductivity errors (right column). Data were collected from the Ross Sea, Antarctica, and error values are the differences in conductivity values measured by the SRDL sensor while deployed on the head of a seal and those measured by a CTD profiler (Sea-bird Electronics, model 19-03) for the manufacturer calibration (top) and our independent calibration (bottom) for three depth bins (5-50, 50-100, and 100-150 m). *In situ* conductivity values ranged from 26.5 to 27.5 mScm⁻¹. Dotted lines indicate the manufacturer stated accuracy of $\pm 0.005^{\circ}\text{C}$ for temperature.

CHAPTER 3

Seasonal habitat preference and foraging behavior of Weddell seals in the western Ross Sea, Antarctica

ABSTRACT

Weddell seals (*Leptonychotes weddellii*) are top predators in the Southern Ocean and have the southernmost distribution of any mammal on Earth. While the McMurdo Sound population of seals has been extensively studied in the summer, over 20 years have passed since attempts were made to understand their overwinter behavior. Between January and February 2010-2012, we tagged 60 Weddell seals in McMurdo Sound and north along the Victoria Land coast using bio-logging technology. We used general additive models to explain and predict the probability of Weddell seal presence and foraging behavior from eight environmental variables: ice concentration, distance from the 10% ice concentration contour, bathymetry, bathymetric slope, mixed layer depth, modified circumpolar deep water index, distance from the coast, and distance from the continental shelf break. Furthermore, we examined the relationship between foraging behavior and three dive metrics: dive duration, descent rate, and dive depth relative to bathymetric depth. The environmental variables that were significant in explaining Weddell seal presence showed different relationships from those explaining foraging behavior and changed seasonally. Overall, we found that Weddell seal foraging behavior was relatively low in the summer compared to the rest of the year, which may be attributed to the limited

foraging that occurs during reproduction and molting. Habitat and foraging models showed the importance of the seasonal sea-ice extent, open water polynyas, and the diverse topography in explaining the habitat preference and foraging behavior of Weddell seals in the western Ross Sea. In addition, using dive parameters to predict foraging behavior, we found that foraging was higher when seals were either less than 30% to the bottom (pelagic) or were near or at the bottom (benthopelagic). Across seasons, Weddell seals preferentially exploited the diverse topography of the Ross Sea, which is composed of a series of shallow banks (<400 m) and deeper troughs (>500 m) that provides pathways for productive circumpolar deep water (CDW) to flow onto the shelf. This study highlights the importance of overwinter foraging, specifically in recouping body mass lost during the previous summer due to the energetic demands associated with breeding and molting. Knowing how seals respond to seasonal shifts in their natural environment may provide clues as to how Weddell seals will modify their habitat preferences and foraging behavior in response to climate change.

INTRODUCTION

Accurately describing and understanding animal movement is a fundamental challenge in ecology and is necessary for determining habitat use and foraging behavior. The advent of bio-logging technology and the increased accessibility of remotely-sensed data have revolutionized our understanding of ecology and the interplay between an animal's behavior and its environment (Costa et al., 2010; Costa et al., 2012). Furthermore, the integration of Global Positioning System (GPS) and Advanced Research and Global Observation Satellite (ARGOS) technologies into animal attachment devices, have allowed us to extend our knowledge of species behavior from coarse observations to a continuous temporal record. These continuous movement datasets, in combination with real-time and remotely-sensed environmental features, make it possible to predict the geographic distribution and habitat use of species (Guisan and Zimmermann, 2000; Pearce and Ferrier, 2000; Thuiller et al., 2009).

Animals respond to environmental features either because they have direct preferences for a given habitat (perhaps due to physiology), or indirect preferences for certain environmental features that are associated with prey aggregations. When the latter is true, optimal foraging theory predicts that organisms maximize fitness by behaving in ways that increase their ability to capture and consume prey (MacArthur and Pianka, 1966). Therefore, predators should adjust their movement to reflect prey density and availability. For example, organisms are likely to spend more time in areas where prey are abundant, resulting in noticeable changes in behavior such as

increased turn angles and decreased travel speeds. These behavioral changes are referred to as Area Restricted Searches (ARS) and are likely to occur when prey are aggregately distributed, thus, resulting in increased search activity in a given area (Fauchald and Tveraa, 2003).

Quantifying the movement and preferred habitat characteristics of marine mammals is challenging because their underwater behavior cannot be easily observed and their movement is four-dimensional, varying over space and time. Apex marine predators are known to target areas where oceanographic features such as currents, frontal systems, thermal layers, water masses, seamounts and continental shelf breaks increase primary productivity and the availability of prey (Tynan et al., 2005; Etnoyer et al., 2006; Bluhm et al., 2007). These oceanographic features aggregate prey and, therefore, allow predators to forage more efficiently (Keiper et al., 2005; Bailleul et al., 2007; Hyrenbach et al., 2007). For many marine predators, persistent regions of localized productivity appear to be essential for reproduction and survival (Crocker et al., 2006), however, many of the oceanographic features aggregating prey create a heterogeneous environment that can change from day to day and across seasons.

The Southern Ocean is home to six species of pinnipeds: Antarctic fur seals, (*Arctocephalus gazelle*), crabeater seals, (*Lobodon carcinophagus*), Weddell seals, (*Leptonychotes weddellii*), Ross seals, (*Ommatophoca rossii*), leopard seals, (*Hydrurga leptonyx*), and southern elephant seals, (*Mirounga leonine*) (Laws, 1977). These pinnipeds are high-level predators and play an important role in the predator-prey dynamics of the ecosystem. Sea-ice provides a platform for Antarctic seals to

rest, breed, and/or give birth and is therefore essential for survival. However, the climate around Antarctica is changing and sea-ice is predicted to decrease by 7% per decade along the west Antarctic peninsula and increase by at least 5% per decade in the Ross Sea (Smith et al., 2007). In order to predict the impact of climate change on top predators, it is important to understand existing predator-prey dynamics.

Weddell seals are the southern-most mammal to reside year-round in Antarctic waters. They are the second deepest diving phocid after the southern elephant seal, with recorded dives greater than 600 m (Kooyman, 1966). Weddell seals are thought to feed primarily on Antarctic silverfish (*Pleuragramma antarcticum*), although other recorded prey species include Antarctic toothfish (*Disssostichus mawsoni*), *Trematomus* species, cephalopods, and invertebrates (Dearborn, 1965; Plötz et al., 1991; Burns et al., 1998). During the austral spring (October-November), Weddell seals return from foraging to established colonies on the fast-ice where they give birth, and later breed and molt in austral summer (January-February). Although Weddell seals are considered capital breeders, research has shown that these animals forage sporadically during the reproductive season (Wheatley et al., 2008). In other words, Weddell seals adjust their behavior to balance physiological demands with locally available prey resources. These four months on-ice are energetically costly, with females losing approximately 38% of their body mass during lactation alone (Wheatley et al., 2006). Therefore, the overwinter foraging trip (February-September) is critical for Weddell seals to recoup body mass

and increase body condition while spending most of their time within the Ross Sea pack-ice.

Due to their accessibility and relatively docile nature, Weddell seals have been studied extensively since the 1960s (DeVries and Wohlschlag, 1964; Dearborn, 1965; Kooyman, 1966; Stirling, 1968; Stirling, 1969) with research being conducted as far back as the early 1900's (Wilson, 1907). In addition, because of their circumpolar distribution, several populations have been studied around Antarctica (Atka: McIntyre et al., 2013; Weddell Sea: Plötz et al. 2001 & 1991, Bornemann et al., 1998; Dumont D'Urville: Heerah et al. 2013; Prydz Bay: Lake et al., 2003, 2006 & 1997).

The most intensely studied population of Weddell seals is that of McMurdo Sound, where research has focused on both physiology and ecology during the austral spring and summer. To date, studies have focused on broad-scale movement and dive behavior (Castellini et al., 1992; Burns and Castellini, 1998; Burns et al., 1999), fine-scale three-dimensional tracking using acoustics devices or accelerometers (Harcourt et al., 2000; Hindell et al., 2002; Mitani et al., 2003; Davis et al., 2004; Davis et al., 2013), population dynamics (Stirling, 1968; Stirling, 1969; Cameron et al., 2007; LaRue et al., 2011; Rotella et al., 2012), physiology (Kooyman et al., 1980a; Burns et al., 1997; Wheatley et al., 2006; Wheatley et al., 2007; Hindle et al., 2009; Hindle and Horning, 2010), and foraging (Davis et al., 1999; Fuiman et al., 2002; Ponganis and Stockard, 2007). In contrast, very little is known about Weddell seal habitat use or foraging behavior during the eight months of the year when they are foraging within the Ross Sea pack-ice. Previous to this work, Testa (1994) was the only study to show

that some Weddell seals from the western Ross Sea (WRS) travel north during the fall and into the winter. However, tag failure and the lack of remotely-sensed satellite data limited the interpretation of behavior.

The Ross Sea ecosystem is particularly unique due to its vast shallow regions, significant polynyas, diverse topography, and extensive ice shelf (Smith et al., 2007). Unlike most places in Antarctica, the Ross Sea is entirely ice free during the austral summer (except embayments) and 100% ice covered during austral winter. In addition, sea-ice concentration on the shelf is routinely lower than off-shelf, deeper waters (Jacobs and Comiso, 1989). In early autumn (late February and March) ice growth advances southward from off-shelf waters where it eventually meets sea-ice advancing northward from the Ross sea ice shelf and Victoria Land coast. This polynya drives much of the Ross Sea's physical oceanography and the later ice formation in the western central shelf waters in autumn, resulting in lower ice concentration and destratification of the water column throughout the winter (Jacobs and Comiso, 1989; Smith et al., 2007; Petty et al., 2014). Sea-ice extent continues to increase until late September, after which the fast-ice retreats southward until mid-February (Jacobs and Comiso, 1989).

The combination of fast-ice retreating southwards and pack-ice advecting northwards due to persistent katabatic winds off the continent, exposes the Ross Sea polynya in the austral spring (Smith and Gordon, 1997). During this time, increases in nutrients and phytoplankton biomass cause increased phytoplankton growth rates. This increase is facilitated by the transport of warm, nutrient-rich Circumpolar Deep

Water (CDW) onto the Ross Sea continental shelf through a series of north-south deep troughs separated by shallow banks. Once on the shelf, this water mass becomes modified (MCDW) and creates warm subsurface waters in both spring and winter (Dinniman et al., 2003). By December or January, the maximum phytoplankton growth rate is reached within the polynya and, at this point, the Ross Sea is the most productive region in the Southern Ocean (Smith and Gordon, 1997; Arrigo et al., 1998).

While a tremendous amount of information exists about Weddell seals in the WRS as well as about the hydrography and ocean circulation of the Ross Sea shelf, no information exists on how these animals interact with environmental features across seasons. Our study examines seasonal habitat preferences and foraging behavior of Weddell seals in the WRS using bio-logging technology and remotely-sensed data that were not previously available. Specifically, our goals were to model Weddell seal seasonal habitat and foraging behavior in relation to environmental variables as well as to model seasonal foraging behavior in relation to various dive parameters. Our models provide the first year-round description of Weddell seal habitat preference and foraging behavior in the WRS. Our findings also provide insight on how a top-predator, such as the Weddell seal, may adjust its behavior in response to climate change.

METHODS

Animal capture and handling

Between January and February (2010-2012), we deployed 60 Satellite Relay Data Loggers (SRDL), developed by the Sea Mammal Research Unit (SMRU Ltd, Scotland), on Weddell seals (9 males, 51 females). Field work was conducted from McMurdo Station, Antarctica, and tag deployment occurred around Ross Island (n=20) and along the Victoria Land coast north to the Drygalski Ice Tongue (n=40) (Fig. 3.1).

Weddell seals were chemically immobilized with an intramuscular injection of a tiletamine HCL/zolazepam HCL mixture (0.5 mg kg^{-1}). Twelve minutes post-injection, animals were captured using a hoop net. Subsequent intravenous injections containing a combination of ketamine hydrochloride and diazepam were administered intravenously, when necessary, to maintain immobilization. Tags were attached to the head of each seal with five-minute epoxy (Devcon or Loctite brand). All handling techniques and tagging methods conform to standard protocols and were approved by National Marine Fisheries Service permit #87-1851, the Antarctic Conservation Act, and the Institutional Animal Care and Use Committee at the University of California, Santa Cruz and the University of Alaska, Anchorage.

Environmental data

Parameters used in this analysis include: ice concentration (ICECON), distance from the 10% ice contour (DICE10), bathymetric depth (BATH), bathymetric slope (SLOPE), mixed layer depth (MLD), the modified circumpolar

deep water index value at 150 m (MCDW), distance from the continental shelf break (DSHELF), and distance from the coast (DCOAST) (Table 3.1).

We used daily Advanced Microwave Scanning Radiometer (AMSR-E or AMSR2) sea ice concentration data with a 6.25 km resolution from the University of Bremen (<http://www.iup.uni-bremen.de/seaice/amsr/>, accessed Jan 2010-Jan 2014). Because daily sea ice concentration values were stored in byte format (0 to 200), we used the raster calculator tool in ArcGIS 10.1 (Environmental Systems Research Institute) to convert ice concentration data to percent ice cover. We also calculated distance to 10% ice concentration contours using the 'Spatial Analyst' extension in ArcGIS.

To examine ocean depth, we used ETOPO-1, a one arc-minute global relief model of the earth's surface (Amante and Eakins, 2009) (<http://www.ngdc.noaa.gov/mgg/global/>, accessed April 2013). From bathymetric depth, we calculated bathymetric slope, the degree change from one depth value to the next. The 1000 m bathymetric contour was used to denote the continental shelf break (Knox, 2007) and the 'Spatial Analyst' extension in ArcGIS 10.1 was employed to create a distance surface representing distance from the Antarctic shelf break. In addition, we obtained a high resolution coastline, Global Self-consistent Hierarchical High-resolution Shorelines (GSHHS) (Wessel and Smith, 1996) (<http://www.ngdc.noaa.gov/mgg/shorelines/gshhs.html>, accessed January 2012) and calculated distance to the continental coastline.

A meso-scale regional oceanographic model system (ROMS) developed by Dinniman et al. (2007) was used to obtain daily estimated oceanographic data from 2010 through 2012 (temperature and modified circumpolar deep water). This model had five-kilometer horizontal grid spacing and 24 vertical layers whose thickness varied with water column depth but was focused towards the top and bottom surfaces (e.g. for a typical Ross Sea depth of 500 m, the maximum thickness was 40.47 m while the top and bottom layers were 4.97 m and 6.32 m thick, respectively) (Dinniman et al., 2007). Using model parameters, we calculated the depth, pressure, salinity, and temperature for each vertical layer and then interpolated to a one-meter vertical resolution. We used the seawater toolbox (http://www.cmar.csiro.au/datacentre/ext_docs/seawater.htm, accessed March, 2010), to calculate seawater density (Millero et al., 1980; Fofonoff, 1983). Density was used to calculate MLD, defined as a 0.01 kg m^{-3} difference in density from the stable surface value (Smith Jr et al., 2000). Finally, we obtained MCDW at 150 m, the average dive depth for all tagged seals.

Tracking and diving data

Position estimates obtained from ARGOS were filtered using a basic speed filter to remove unrealistic locations (i.e., locations resulting in a maximum horizontal speed $> 15 \text{ km h}^{-1}$ were removed). Weddell seal positions were interpolated every two hours using a forward looking particle filtering model (Tremblay et al., 2009), which accounts for the errors associated with each ARGOS location class. Dive locations were determined by linking dive time with time along the trackline, and linearly

interpolated to the nearest minute. Finally, tracklines were truncated based on the time of the first and last transmitted dive times. One tag was eliminated from all dive analysis since partial tag failure resulted in animal location data with no associated dive data.

Using the Geospatial Modelling Environment (MGGET, Version 07.2.1), we created 50 correlated random walks (CRW) for each animal by making random draws from the distribution of angles and step lengths between subsequent points along each track (Beyer, 2004). Each CRW had the same number of steps as the corresponding seal track for comparison purposes. We randomly selected six of the 50 CRW to represent the possible behavior of each animal, unbiased by environmental drivers, to create > 2:1 ratio for the number of CRW to seal locations each season. Previous work suggests that a 2:1 ratio leads to stable model coefficients (Aarts et al., 2008). For this analysis, points along an animal's track were categorized as 'present' (where an animal was tracked) while those along each CRW were categorized as 'absent' (where an animal could have been based on movement parameters but was not observed in our tracking data).

To determine probable foraging areas along each track, we identified area restricted searches by calculating first passage time (FPT), a measure of search effort. FPT, or the time required for an animal to cross a circle of a given radius (Fauchald and Tveraa, 2003), was calculated for each track after removing all haul-out periods and data gaps longer than a week. We used a modification of the Fauchald and Tveraa (2003) method in which the circle radius associated with the peak log variance was

determined separately for each animal to account for individual variability (Robinson et al., 2007). After examining the average log variance in FPT for every one kilometer increase in radii values ranging from one to fifty kilometers, we were able to identify the scale of operation for Weddell seals as three kilometers. Using this scale, we calculated FPT for every location along the track for each animal.

Using the 'Spatial Analyst' extension in ArcGIS 10.1, we extracted values for each point (presence and absence) to represent the following covariates: ICECON, DICE10, BATH, SLOPE, DCOAST, DSHELF, MLD, and MCDW. Because ICECON, DICE10, MLD, and MCDW were available daily, these values were extracted for each unique date along the tracks. Locations that had null values for any of the eight environmental variables were eliminated from the dataset.

Each track and dive location was categorized into one of four seasons, delineated using the equinox and solstice dates. Note that the number of days and individuals in each season is a function of tag deployment duration. Finally, we calculated the following metrics for each dive: maximum dive depth (MXDEP), dive duration (DDUR), time spent in the bottom phase of a dive (within 80% of the maximum dive depth) (BOTDUR), descent rate (DRATE), and maximum dive depth relative to bathymetric depth, or percent within the water column (PWC) with 0% = surface and 100% = seafloor (Table 3.1).

We calculated population means (average of individual means) and standard deviations for the eight environmental variables and five dive parameters per season. In addition, we used the 'coin' package in R 3.0.2 to run Wilcoxon signed rank tests,

a non-parametric version of the paired t-test, to compare: (1) mean values of each environmental variable for seal presence and absence, (2) mean values of each environmental variable for each season using the 25 individuals with data across all seasons, and (3) mean values of each dive variable per season using the 30 individuals with data spanning all seasons.

Weddell seal habitat and foraging models

Habitat models

We ran correlation matrices to test the level of dependency between environmental variables and found no evidence of correlation ($r > 0.70$). Using both tracking and CRW data, we modeled the presence/absence of Weddell seals relative to environmental variables for each season using a generalized additive model (GAM) with a logistic link (Wood, 2011; R Development Core Team, 2013). We used GAMs because they are non-parametric and can model non-linear relationships that are typical of complex environments. Animal ID was included in each model as a random effect in order to account for individual behavior. In these models, the effect of the predictor variables are additive (Redfern et al., 2006) and follow the form:

$$P_{ij} = \frac{\exp[\beta_0 + \sum_i f_i(x_i)]}{1 + \exp[\beta_0 + \sum_i f_i(x_i)]} \quad (1)$$

where P_i is the probability of presence for each individual seal j , β_0 is the intercept to be estimated by the model and x_i is the value of the i th explanatory variable whose function f_i is to be estimated.

A GAM with a cubic regression spline, allowing for shrinkage, was fit to the data. By shrinking the degrees of freedom to zero for each variable judged to be unimportant to the model, the shrinkage term provides an effective way of removing variables (Durussel et al., 2009). All models within three AIC units of the model with the lowest AIC were considered equivalent, and the most parsimonious was selected as the final model. We used the geoR package in R (Ribeiro Jr and Diggle, 2001; Diggle and Ribeiro Jr, 2007) to check for spatial autocorrelation within the model. Due to presence of spatial autocorrelation, we selected only points along each track (both real and CRW) that were at least 6.5 km apart (the lowest cell resolution of the included environmental variables). Spatial autocorrelation was no longer present and we re-ran the models using this reduced dataset.

For each of the four final models (one per season), we used a ‘receiver operating characteristic’ (ROC) curve to assess the diagnostic accuracy of the model (Goetz et al., 2007; Goetz et al., 2011). ROC analysis measures how well a receiver is able to detect a signal in the presence of noise. In this case, a Weddell seal is either present or absent in a particular habitat unit and the ROC curve predicts a threshold at which the seal is present (Legendre and Legendre, 2012). This optimal threshold optimizes errors of omission versus errors of commission. The ‘area under the curve’ (AUC) measures the discrimination ability of the model to correctly classify a Weddell seal as present or absent (Thuiller et al., 2009). AUC values range from 0.5 (no discrimination ability) to 1 (perfect discrimination ability) (Pearce and Ferrier, 2000). We used the ROC library (Atkinson and Mahoney, 2004) for ROC and AUC

analysis of the model. Based on the threshold value, we classified habitat suitability as Weddell seal habitat or non-habitat.

In order to predict habitat in areas where animal behavior was unknown, we ran each of the final four models without the random effect term. The ‘predict GAM from rasters’ tool in the Marine Geospatial Ecology Toolbox (MGET, Version 0.8a54) (Roberts et al., 2010) was used to create daily habitat probability grids for each respective season. Within each season, daily habitat probability grids were averaged to create a single probability surface. The ROC value was then used to determine habitat preference for summer, fall, winter, and spring. The predictive probability models were limited to the data extent for each season and mapped into geographic space using ArcGIS 10.1.

Horizontal foraging models

To examine foraging behavior, we used the same location data as in the habitat preference models except haul-out periods and CRW data were removed. We predicted foraging intensity by fitting a GAM with a cubic regression spline, with shrinkage, to the data. The response variable, FPT, was log-transformed and the GAM model was fit to equation (2) using an identity link:

$$\log(FPT)_{ij} = \beta_0 + \sum_i f_i(x_i) \quad (2)$$

where FPT_i is the predicted FPT of an individual Weddell seal j , β_0 is the intercept to be estimated by the model and x is the value of the i th explanatory variable whose function f_i is to be estimated.

Animal ID was included as a random effect in all models to account for individual animal behavior, though this term was removed when predicting foraging areas in places where animals did not visit. Using the same methods described for the habitat model, we removed spatial autocorrelation and reran models using a reduced dataset.

The MGET toolbox was used to create daily foraging prediction surfaces that were averaged per season to create overall foraging predictions for summer, fall, winter, and spring. The analysis extent was limited to the data boundary created from the kernel density analysis and mapped into geographic space. Finally, we mapped the product of each predictive foraging surface with its corresponding predictive habitat preference surface to create an overall grid depicting areas with high foraging within preferred habitat for each season.

Because we wanted to understand how foraging behavior changes throughout the year, we fit an additional GAM model using log FPT as the response variable and day of year (DOY) as the explanatory variable. GAM models and the removal of spatial autocorrelation follow the methods described above.

Vertical foraging models

To understand the links between horizontal searching and dive behavior, we used GAM models to examine the relationship between FPT and dive parameters

(DDUR, BOTDUR, MXDEP, DRATE, PWC) for each season. Each dive was assigned a FPT value based on the encompassing three kilometer FPT search radius. Only dives within this search radius were used in this analysis. Because MXDEP and PWC as well as BOTDUR and DDUR were highly correlated ($r > 0.70$), MAXDEP and BOTDUR were not included in the models. Spatial autocorrelation was accounted for and seasonal GAMs were run using methods described above.

RESULTS

Weddell seals tagged near Ross Island and along the Victoria Land coast dispersed and traveled throughout the entire WRS but remained entirely on the continental shelf (Fig. 3.1). The mean values for the majority of the eight environmental variables for absence data were significantly different ($p < 0.05$) from the presence data in each of the four seasons (Table 3.2). In addition, nearly all environmental variables in the summer were significantly different from those in the other three seasons – fall, winter, and spring (Table 3.3).

While bottom and dive duration were similar in summer and fall, durations increased in winter and spring (Table 3.4). A similar trend was seen in maximum dive depth in which Weddell seals dived deeper as the seasons progressed. In fact, maximum dive depth in spring was nearly twice that of summer despite diving to similar locations within the water column (PWC). The majority of the five dive parameters were significantly different ($p < 0.05$) between seasons (Table 3.5). Interestingly, values for all dive parameters in summer were significantly different from winter.

Habitat models

In the summer, all environmental variables were significant and accounted for 42% of the deviation in Weddell seal occurrence (Table 3.6). The probability of Weddell seal presence increased with increasing ice concentration up to ~40%, after which probability of occurrence decreased (Fig. 3.2). Seal presence also increased with increasing MCDW index values and with increasing distance from the 10% ice concentration contour (preferring open water), but decreased with increasing distance from the coast and the continental shelf break. Weddell seals were least likely to occupy waters 500-600 m deep in the summer and preferred either shallower or deep waters (Fig. 3.2). During this time of year, Weddell seals also occupied areas with steep bathymetric slope.

During the fall, all environmental variables were significant except ICECON and they explained 48% of the deviation in Weddell seal occurrence (Table 3.2). Weddell seals were more likely to be present further than 200 km from the coast and within 200 km of the of the continental shelf break (Fig 3.2). In the fall, the probability of Weddell seal presence decreased with increasing depth and bathymetric slope. During this season, the probability of seal presence was highest when MLD was less than 50 m and when MCDW index was greater than 45 (Fig. 3.2). In general, seals tended to prefer areas within 200 km of the 10% ice contour.

All environmental variables were significant in explaining Weddell seal presence during the winter, explaining 41% of the variation in seal occurrence. The relationship between seal presence and ice concentration was negative and, in

general, seals preferred ice concentrations $< 60\%$. Seal presence increased < 200 km and > 1200 km from the 10% ice concentration contour (Fig. 3.2). In addition, the probability of Weddell seal presence was highest at intermediate depths and increased with increasing bathymetric slope (Fig. 3.2). The relationship between Weddell seal occurrence and distance from the coast was negative while the opposite was true for seal presence and distance from the shelf break. In general, Weddell seal presence increased with increasing MCDW index values and MLD (Fig. 3.2).

In the spring, the only environmental variables significant in explaining Weddell seal occurrence were BATH, MCDW, DCOAST, and DSHELF. Together, these variables explained 32% of the deviation in Weddell seal presence. Seals showed a preference for water depths ~ 400 m as well as intermediate MCDW index values (Fig. 3.2). The probability of Weddell seal occurrence increased with decreasing distance from the shelf break.

The ROC value for each habitat preference model was 0.36, 0.42, 0.28, and 0.31 for summer, fall, winter, and spring, respectively. Values above these thresholds were considered 'habitat' for the corresponding season and values below the thresholds were classified as 'non-habitat' (Fig. 3.3A-D). The AUC value for the seasonal models ranged from 0.90 to 0.92, meaning that each model correctly distinguished between Weddell seal presence and absence at least 90% of the time after accounting for model variables. Preferred habitat across all seasons was located in the central WRS towards the continental shelf break (Fig. 3.3A-D). From summer

through spring, only 9%, 10%, 15%, and 14% of the seasonal extent for Weddell seals was non-preferred habitat.

Horizontal foraging models

At the three-kilometer scale, all environmental variables, except SLOPE, were significant predictors of FPT during summer (Table 3.6). FPT, a metric for foraging, increased with increasing ice concentration and decreased with increasing distance from the 10% ice concentration (Fig. 3.4). In addition, FPT increased with depth up to 200 m. Finally, FPT was highest when MLD was between ~20 and 70 m and when the MCDW index was < 20 . In the summer, FPT increased > 150 km from the coast and when animals were closest and furthest from the continental shelf break (Fig. 3.4).

Like summer, all environmental variables except SLOPE were significant in predicting FPT in fall. FPT increased with ice concentrations greater than 90% and water depths < 500 m (Fig. 3.4). However, FPT was lowest closest to and furthest from the 10% ice concentration contour. In fall, the relationship between FPT and distance to the shelf break was positive while the relationship between FPT and distance to the coast was negative. Finally, FPT decreased at extreme high and low MCDW values but increased with increasing MLD (Fig. 3.4).

In winter, Weddell seals exhibited highest FPT when ice concentration was greater than 90% (Fig. 3.4). FPT was also highest when water depths were less than 320 m or greater than 800 m and where bathymetric slope was greater than ~ 0.8

degrees. In winter, FPT for Weddell seals increased with increasing distance from the shelf break.

The relationship between FPT and bathymetric slope in spring was the same as winter, with a positive relationship between FPT and slope (Fig. 3.4). FPT was highest when water depth was less than 500 m and distance from the 10% ice concentration contour was < 800 km. In spring, the relationship between FPT and distance from the shelf break showed a decrease to ~ 320 km, followed by a peak, and a subsequent increase after 500 m. In addition, FPT generally increased with the MCDW index (Fig. 3.4).

In all four seasons, foraging models predicted highest FPT in the coastal vicinity of Ross Island and dispersed throughout the central WRS. In addition, summer, fall, and winter models predict high FPT values from Ross Island, north along the Victoria Land coast up to the Drygalski ice tongue (Fig. 3.3E-H). Seasonal predictions of Weddell seal occurrence (Fig. 3.3A-D) were combined with seasonal predictions of FPT (Fig. 3.3E-H) to provide information on important foraging areas within preferred habitat (Fig. 3.3I-L). Highest predicted FPT within preferred Weddell seal habitat occurred around Ross Island (though difficult to see) and extended from the central WRS to the furthest extent of Weddell seal travel in each season (Fig. 3.3I-L). FPT varied markedly throughout the year; lowest values were found in summer followed by a slight peak in fall, a continued increase until reaching an overall peak in winter, and a gradual decline in spring (Fig. 3.6). DOY explained 35% of the deviation in FPT.

Vertical foraging models

Using GAM models to understand the relationship between FPT and four vertical foraging parameters, we found that DDUR, DRATE, and PWC were significant in predicting FPT in the summer; explaining 45% of the deviation in FPT (Table 3.6). In summer, FPT was highest when dive duration was less than six minutes and during minimum and maximum descent rates (Fig. 3.6). Weddell seals generally exhibited increased FPT with increasing PWC, but a peak in FPT was observed around 20%.

During fall and winter, only 18% and 40% of the deviation in FPT was explained by PWC, respectively. In fall, FPT increased with PWC between 20 and 40% as well as for values greater than 90% (Table 3.6, Fig. 3.6). However, in winter, the highest FPT values occurred when PWC was greater than 60% (Fig. 3.6). Finally, in spring, DRATE, DDUR, and PWC explained 63% of the variation in FPT (Table 3.2). FPT was highest when descent rate was less than 0.7 ms^{-1} and when dive duration was < 12 or > 24 minutes (Fig. 3.6). In general, FPT increased with PWC depth in spring.

DISCUSSION

In the summer, after leaving the breeding colony, Weddell seals utilized open water habitat to transit to foraging grounds located within the ice environment. The western and central Ross Sea is characterized by three polynyas located (1) east of Ross Island and adjacent to the Ross Ice shelf, (2) immediately north of the Drygalski ice tongue, and (3) in McMurdo Sound (Martin et al., 2007). These three polynyas

cause a delay in ice formation and may provide a convenient pathway for Weddell seals to access foraging areas located near or within the pack-ice. The high concentrations of birds and cetaceans observed along the marginal ice zone highlights the importance of the ice edge environment for Antarctic species (Karnovsky et al., 2007).

Across seasons, Weddell seals preferentially exploited the diverse topography of the Ross Sea which is composed of a series of shallow banks (< 400 m) separated by deeper troughs (> 500 m) (Smith Jr et al., 2012). In the summer, seals preferred either troughs or the transitional areas between banks and troughs where the MCDW index was highest. However, the predominance of foraging in shallow waters with moderate MCDW index values suggest that Weddell seals may be targeting prey species on or proximate to banks while using areas over troughs for resting or transiting.

The topography of the Ross Sea strongly influences the flow of MCDW onto the shelf (Dinniman et al., 2003; Orsi and Wiederwohl, 2009) and provides a mechanism for bioaccumulation of phytoplankton by supplying iron to iron-limited waters in the summer (Peloquin and Smith, 2007). The cyclonic circulation of MCDW around banks and the anti-cyclonic circulation around troughs, or depressions (Dinniman et al., 2003), causes a higher abundance of krill along the edges of banks but not on the banks themselves (Sala et al., 2002). Although Weddell seals in the WRS are not known to ingest a large proportion of invertebrates, the

presence of krill attracts fish species, many of which are thought to be the preferred prey items of these animals.

Overall, our model results for the summer season agree with Hindell et al.'s (2002) study in which the density of Weddell seals was highest over regions of steep topography. The authors suggested that their finding was due to the topography acting as a mechanism to enhance productivity in areas where depressions were present, thereby increasing prey density. While this study only examined short foraging trips during the summer breeding season, our study found similar results over a broader temporal scale – once seals had left the breeding colony.

A small proportion of seals tagged in our study remained near Ross Island year-round while the majority of animals traveled hundreds of kilometers towards the continental shelf break. These individual preferences are likely the reason that seasonal foraging models predicted foraging areas close to and far from both the coast and shelf break. In other words, some seals continued to forage near Ross Island while most traveled to areas beyond the breeding colony, foraging along the way. Hindell et al. (2002) suggested that the limited foraging range of Weddell seals during the breeding season could lead to prey depletion around colonies. This finding is supported by our observations of a large proportion of seals traveling to foraging grounds away from Ross Island.

From summer through winter, foraging behavior was higher when seals were either less than 30% to the bottom (pelagic) or were near or at the bottom (benthopelagic). This result is in agreement with previous studies that suggest Weddell seals

exploit both pelagic and benthic-pelagic prey such as *P. antarcticum* and *D. Mawsoni* which can occur in both environments (Dearborn, 1965; Casaux et al., 1997; Burns et al., 1998; Plötz et al., 2001; Hindell et al., 2002; Davis et al., 2013). Increased foraging was associated with faster descent rates and shorter dive durations which may be related to the locomotive behavior employed by *P. antarcticum*, reaching estimated speeds of 4.9 body lengths per second when pursued by a seal (La Mesa et al., 2004).

As ice formation progressed throughout the fall and winter, Weddell seals preferentially occupied areas with open water access. However, foraging behavior was higher in dense pack-ice and far from open-water pockets, a pattern similar to summer observations. This suggests that the under-ice and ice-edge environments play an important role in foraging. Seals may prefer areas farther from land due to the preclusion of crack formation in land-fast ice, which would effectively displace them from coastal areas as ice continues to form throughout the fall (Lake et al., 2005).

The preferred depth range (400-600 m) and higher use of shallower slopes in the fall indicate that the margins separating banks from troughs play an important role for both Weddell seal presence and foraging. Unlike in summer, seals preferred to occupy flatter areas in fall, found either on the top of banks or the bottom of troughs. However, increased occupancy in areas with higher MCDW index values suggests that seals preferred areas over troughs for resting or transiting while increased foraging behavior over intermediate MCDW index values suggest that animals forage along the periphery of banks and troughs. From late fall to early spring, cold air

temperatures drive ice formation, thus causing the removal of fresh water and the sinking of dense, salty water (Smith et al., 2007; Petty et al., 2014). Increased foraging behavior with increasing MLD suggests that seals are feeding at or near the bottom of the homogenized mixed layer along the transition zone between banks and troughs.

In winter, sea-ice is at its farthest extent (Jacobs and Comiso, 1989), and the magnitude of the extent is positively correlated with higher Weddell seal recruitment to breeding colonies the following spring (Hadley et al., 2007). Weddell seals preferentially occupied areas with low to intermediate ice concentrations and, like fall, Weddell seal foraging during the winter was highest when the ice concentration was at or near 100%. Increased foraging in the dense pack-ice is likely driven by the abundance of ice algae that utilize the under-ice environment, thus attracting cryopelagic predators such as the fish species, *Pagothenia borchgrevinki*, a known prey item of Weddell seals in the WRS (Eastman and DeVries, 1985; Davis et al., 1999). Krill abundance is also positively correlated with sea-ice extent (Loeb et al., 1997) and krill is the primary prey item of *P. antarcticum*, an important dietary item of Weddell seals (Burns et al., 1998; Davis et al., 1999; Fuiman et al., 2002; Zhao et al., 2004). Based on movement and diving behavior, we found that Weddell seals are both pelagic and benthic-pelagic foragers.

In spring, when returning to breeding colonies, Weddell seals preferred areas on or peripheral to banks or land for both habitat and foraging grounds. Unlike other seasons, ice concentration did not predict preferred habitat or foraging in the spring

during ice break-up. However, Weddell seals did show a preference for open-water areas which is likely related to the rapid opening of polynyas in the spring as a response to increased air and ocean temperature (Jacobs and Comiso, 1989). The opening of the Ross Sea polynya releases iron into the water which facilitates the largest increase in primary production in the Southern Ocean (Smith and Gordon, 1997; Arrigo and Thomas, 2004). The diatom-dominated food web of the Ross Sea polynya during spring may explain the absence of predators, including Weddell seals (Karnovsky et al., 2007). During the four month period Weddell seals are on the fast-ice reproducing and molting, zooplankton such as copepods and krill graze on the phytoplankton, which, in turn, provide food for many fish species that are known prey items for Weddell seals (Smith et al., 2007). By the time seals leave the breeding colonies in late summer, the marginal ice zone around the Ross Sea polynya is highly productive and this productivity has transferred up enough trophic levels to support a large predator, such as the Weddell seal.

Conclusion

This study presents the first quantitative analysis of Weddell seal habitat preference and foraging behavior across seasons. We successfully modeled and predicted habitat preference and foraging behavior using environmental variables, as well as modeled foraging behavior using dive parameters. We observed that foraging by Weddell seals is relatively low in the summer compared to the rest of the year, which may be attributed to reproduction and molting. Weddell seals are considered capital breeders and rely largely on stored body reserves during this time, losing up to

40% of their body mass during lactation alone (Wheatley et al., 2006). Once pups are weaned, females are no longer tied to the breeding colonies and can travel farther, making the fall, winter, and spring the most important seasons for Weddell seal foraging. Our results are supported by Shero et al.'s (2015) study which found that the overwinter foraging period was important for female Weddell seals to gain mass and body condition. However, the inability of seals to gain substantial amounts of mass during this time means that they must continue to forage throughout the breeding and molting periods to sustain energetic demands.

The Ross Sea ecosystem shows strong cyclical patterns in sea-ice extent and productivity. This region is more productive than any other place in Antarctica and reaches farther south than any other marine system on Earth (Smith Jr et al., 2012). Due to its vast shelf, productive polynyas, and diverse habitats, the Ross Sea is considered a biodiversity hotspot. Weddell seals are one of the top predators in the Ross Sea but previous to this study, little was known about their seasonal habitat and foraging behavior. In this study, predictive habitat and foraging models showed the importance of the seasonal sea-ice extent, open water polynyas, and the diverse topography in the movement and foraging behavior of Weddell seals in the WRS.

Knowing how Weddell seals respond to predictable seasonal changes in environmental conditions can provide insight into how Weddell seal habitat or foraging behavior will change due to unpredictable natural and anthropogenic climate variation. Although the Ross Sea ecosystem remains relatively intact, changes in oceanography and sea ice extent have already been documented as a result of climate

change (Smith Jr et al., 2012). While there is a great deal of uncertainty on how climate change will impact the Weddell seal population here, evidence suggests that the region is cooling and sea ice is expanding, in contrast to other places in Antarctica (Smith et al., 2007). As a result, it is possible that Weddell seals will not be impacted in this region.

Studies suggest that *P. antarcticum* is the primary diet of Weddell seals in the summer (Burns et al., 1998; Fuiman et al., 2002); however, there is no evidence that the summer diet is indicative of year round foraging habits. Given the highly dynamic nature of the Ross Sea ecosystem throughout the year, it is likely that Weddell seals adapt to changes in local abundance of prey species by altering their diet. In fact, results from seals in the Weddell Sea indicate that while *P. Antarcticum* is also the primary summer diet for those animals (Plötz et al., 1991), in spring, *P. Antarcticum* was no longer present in the diet of Weddell seals; instead prey items consisted of many other notothenioid fish including *Trematomus* species (Plötz et al., 1991; Plötz et al., 2001). The Ross Sea population of Weddell seals may also alter their diet in response to a temporally changing environment.

TABLES

Table 3.1: Covariates utilized in the general additive models examining Weddell seal occurrence and foraging behavior in the western Ross Sea, Antarctica.

Dive Covariate	Unit	Abbreviation
Maximum dive depth	m	MAXDEP
Dive duration	min	DDUR
Time spent in bottom phase of dive	min	BOTDUR
Descent rate	m/s	DRATE
Percent of water column depth	%	PWC
Environmental Covariate	Unit	Abbreviation
Ice concentration	%	ICECON
Distance from 10% ice concentration	km	DICE10
Bathymetric depth	m	BATH
Bathymetric slope	degree	SLOPE
Distance to coast	km	DCOAST
Distance to shelf break	km	DSHELF
Modified circumpolar deep water at 150 m	index	MCDW
Mixed layer depth	m	MLD

Table 3.2: Mean and standard deviation of eight environmental variables: ice concentration (ICECON, %), distance from the 10% ice concentration contour (DICE10, km), bathymetric depth (BATH, m), bathymetric slope (SLOPE, degree), modified circumpolar deep water index at 150 m (MCDW), mixed layer depth (MLD, m), distance from the coast (DCOAST, km), and distance to the continental shelf, or 1000 m isobath (DSHELF, km). Results are shown for both Weddell seal (present) and Correlated Random Walk (CRW, absent) locations. Data were analyzed separately for each season and mean values represent population means obtained by averaging individual means. Asterisks indicate a significant difference between present and absent values at the $p \leq 0.05$ level for a given environmental value, within a season, obtained from Wilcoxon signed rank tests.

	Summer		Fall		Winter		Spring	
	Present	Absent	Present	Absent	Present	Absent	Present	Absent
# Loc	12,788	128,714	50,034	295,324	38,486	217,241	11,702	64,887
# Ind	52	52	58	58	48	48	30	30
ICECON	57.7 ± 17.1*	40.1 ± 14.3	89.8 ± 10.1*	81.5 ± 9.0	93.1 ± 9.3	92.6 ± 4.7	90.2 ± 10.6*	86.9 ± 8.1
DICE10	44.4 ± 32.6*	27.2 ± 7.7	427.2 ± 292.1	426.1 ± 307.7	595.7 ± 297.2*	633.5 ± 325.3	416.8 ± 285.7	419.9 ± 310.0
BATH	401.3 ± 135.2*	459.7 ± 110.8	514.0 ± 110.2	523.4 ± 97.4	534.6 ± 117.5	534.4 ± 79.2	568.4 ± 138.5	546.3 ± 73.0
SLOPE	1.3 ± 0.7*	1.0 ± 0.2	0.8 ± 0.7*	0.9 ± 0.2	0.7 ± 0.6	0.8 ± 0.2	0.8 ± 0.6	0.8 ± 0.2
MCDW	17.7 ± 12.4*	15. ± 12.3	23.6 ± 13.2*	19.9 ± 12.5	23.6 ± 13.5*	19.4 ± 11.5	21.3 ± 11.7*	18.9 ± 11.2
MLD	32.3 ± 13.6*	24.5 ± 6.9	117.1 ± 39.9*	127.8 ± 37.9	159.6 ± 77.4*	129.2 ± 59.2	111.5 ± 72.4	94.8 ± 48.5
DCOAST	23.3 ± 22.4	16.9 ± 9.7	51.5 ± 43.0*	24.5 ± 12.6	47.4 ± 40.2*	29.1 ± 13.1	38.7 ± 25.2*	26.7 ± 12.2
DSHELF	494.6 ± 79.7*	537.7 ± 24.1	437.9 ± 92.5*	523.2 ± 36.3	440.2 ± 99.8*	517.1 ± 36.9	475.7 ± 65.2*	517.5 ± 34.9

Table 3.3: Wilcoxon signed rank test results comparing seasonal values for eight environmental variables: ice concentration (ICECON, %), distance from the 10% ice concentration contour (DICE10, km), bathymetric depth (BATH, m), bathymetric slope (SLOPE, degree), modified circumpolar deep water index at 150 m (MCDW), mixed layer depth (MLD, m), distance from the coast (DCOAST, km), and distance to the continental shelf, or 1000 m isobath (DSHELF, km). Only Weddell seals with associated environmental data for all four seasons were included in this statistical analysis (n=25). Bolded *p*-values are significant at the *p* = 0.05 level.

	SUM-FALL		SUM-WIN		SUM-SPR		FALL-WIN		FALL-SPR		SPR-WIN	
	z	p	z	p	z	p	z	p	z	p	z	p
ICECON	4.35	1.19E-07	-4.37	5.96E-08	4.10	2.56E-06	-1.44	1.56E-01	-0.34	7.51E-01	-2.09	3.67E-02
DICE10	4.37	5.96E-08	-4.37	5.96E-08	4.37	5.96E-08	-2.49	1.15E-02	-0.74	4.74E-01	-0.26	8.12E-01
BATH	-3.51	1.62E-04	3.30	4.90E-04	-3.19	8.08E-04	1.82	7.10E-02	2.38	1.60E-02	-0.71	4.91E-01
SLOPE	-2.81	3.78E-03	3.65	7.50E-05	-3.54	1.40E-04	1.44	1.56E-01	2.03	4.22E-02	-0.36	7.31E-01
CDW	3.19	8.08E-04	-1.68	9.57E-02	2.09	3.67E-02	1.04	3.12E-01	0.17	8.74E-01	1.87	6.26E-02
MLD	4.37	5.96E-08	-4.32	1.79E-07	3.67	6.37E-05	-2.03	4.22E-02	0.50	6.34E-01	-2.87	3.09E-03
DCOAST	2.97	2.03E-03	-2.87	3.09E-03	2.81	3.78E-03	1.04	3.12E-01	-0.61	5.60E-01	0.98	3.39E-01
DSHELF	-2.11	3.42E-02	1.71	9.03E-02	-1.60	1.14E-01	-1.33	1.91E-01	-0.26	8.12E-01	-0.01	1.00E+00

Table 3.4: Mean and standard deviation of five Weddell seal dive metrics: dive duration (DDUR, min), bottom duration (BDUR, min), descent rate (DRATE, ms⁻¹), maximum dive depth (m), and percent water column depth (PWC, %). Data were analyzed separately for each season and mean values represent population means obtained by averaging individual means.

	Summer	Fall	Winter	Spring
# Dives	91,261	101,423	21,533	3,013
# Ind	59	57	48	30
DDUR	8.6 ± 2.2	8.2 ± 2.0	10.0 ± 2.7	12.3 ± 3.9
BOTDUR	3.8 ± 1.1	3.7 ± 1.2	4.4 ± 1.5	5.9 ± 2.1
DRATE	1.2 ± 0.2	1.2 ± 0.2	1.1 ± 0.2	1.2 ± 0.2
MXDEP	114.5 ± 36.7	128. ± 37.6	140.1 ± 51.7	223.5 ± 99.4
PWC	39.3 ± 11.6	28.4 ± 10.9	28.7 ± 11.8	39.3 ± 19.9

Table 3.5: Wilcoxon signed rank test results comparing seasonal values for five dive metrics: dive duration (DDUR, min), bottomtime (BOTDUR, min), descent rate (DRATE, ms⁻¹), maximum dive depth (MXDEP, m), and percent water column depth (PWC, %). Only Weddell seals with associated dive data for all four seasons were included in this statistical analysis (n=30). Bolded *p*-values are significant at the *p* = 0.05 level.

	SUM-FALL		SUM-WIN		SUM-SPR		FALL-WIN		FALL-SPR		WIN-SPR	
	<i>z</i>	<i>p</i>	<i>z</i>	<i>p</i>	<i>z</i>	<i>p</i>	<i>z</i>	<i>p</i>	<i>z</i>	<i>p</i>	<i>z</i>	<i>p</i>
DDUR	2.90	2.81E-03	1.75	8.12E-02	-3.57	1.48E-04	3.81	4.02E-05	4.64	3.35E-08	-2.20	2.66E-02
BOTDUR	-0.17	8.71E-01	-3.38	3.80E-04	3.36	4.18E-04	-3.61	1.23E-04	-3.61	1.23E-04	2.60	8.14E-03
DRATE	2.25	2.34E-02	2.52	1.06E-02	1.51	1.35E-01	4.28	1.42E-06	0.07	9.52E-01	2.36	1.75E-01
MXDEP	2.85	3.48E-03	-3.88	2.69E-05	4.25	1.99E-06	-2.75	5.01E-03	-3.85	2.69E-05	3.36	4.18E-04
PWC	-3.77	4.97E-05	3.55	1.70E-04	-0.22	8.39E-01	0.03	9.84E-01	-2.87	3.22E-03	2.48	1.21E-02

Table 3.6: Covariates included in the final habitat preference and foraging behavior models by season. Models preceded by ‘H’ indicate habitat preference models and those preceded by ‘F’ indicate foraging behavior models. The percent deviance explained, R² adjusted value, number of locations, number of individuals, estimated degrees of freedom, and AIC values for each model are also provided.

Model	Variables included in the model	% Dev	R ² Adj	n	# IND	EDF	AIC
H_ENV_SUM	ICECON, DICE10, BATH, SLOPE, MCDW, MLD, DCOAST, DSHELF	42	0.47	6537	50	97	4528
H_ENV_FAL	DICE10, BATH, SLOPE, MCDW, MLD, DCOAST, DSHELF	48	0.54	11728	57	104	7485
H_ENV_WIN	ICECON, DICE10, BATH, SLOPE, MCDW, MLD, DCOAST, DSHELF	41	0.44	5936	46	105	3343
H_ENV_SPR	BATH, MCDW, DCOAST, DSHELF	32	0.36	1767	28	50	1303
F_ENV_SUM	ICECON, DICE10, BATH, DCOAST, DSHELF, MCDW, MLD	47	0.44	1515	52	90	3208
F_ENV_FAL	ICECON, DICE10, BATH, DCOAST, DSHELF, MCDW, MLD	23	0.21	3250	58	95	7699
F_ENV_WIN	ICECON, BATH, SLOPE, DSHELF	44	0.41	834	46	57	2002
F_ENV_SPR	DICE10, BATH, SLOPE, DSHELF, MCDW	69	0.63	306	27	53	688
F_DIVE_SUM	DIVEDUR, DRATE, PWC	45	0.42	1309	52	67	3492
F_DIVE_FAL	PWC	18	0.15	2137	50	51	5858
F_DIVE_WIN	PWC	40	0.34	447	42	43	1290
F_DIVE_SPR	DIVEDUR, DRATE, PWC	63	0.50	126	22	33	348

FIGURES

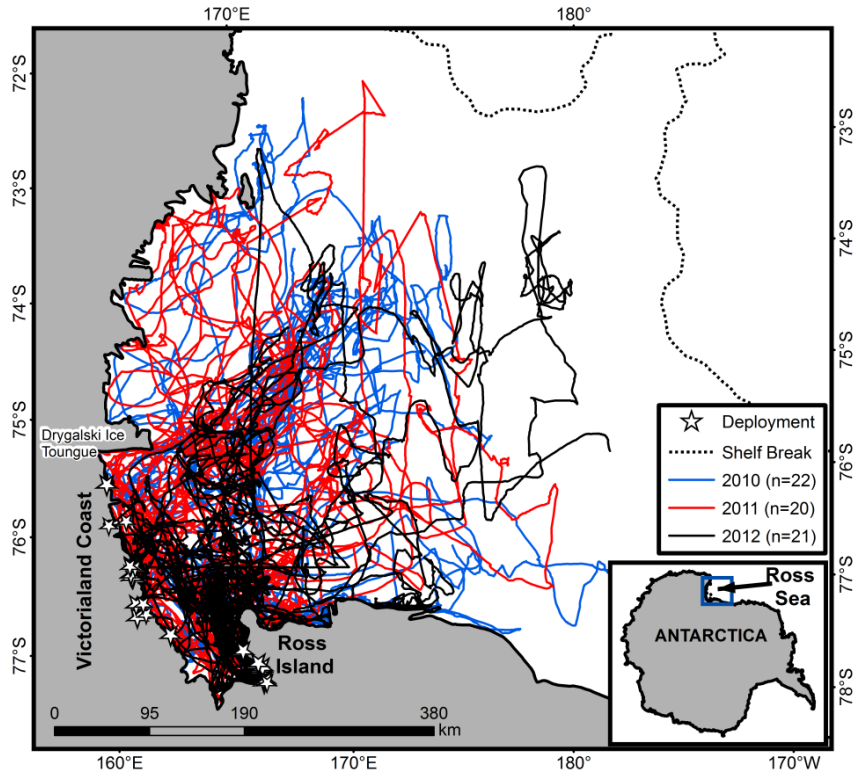


Figure 3.1: Weddell seal tracklines in the western Ross Sea during 2010 (blue), 2011 (red), and 2012 (black). Animals were tagged around Ross Island (n=22) and along the Victoria Land coast (n=41) with deployment locations denoted by stars. The dotted line represents the shelf break, or 1000 m bathymetric contour.

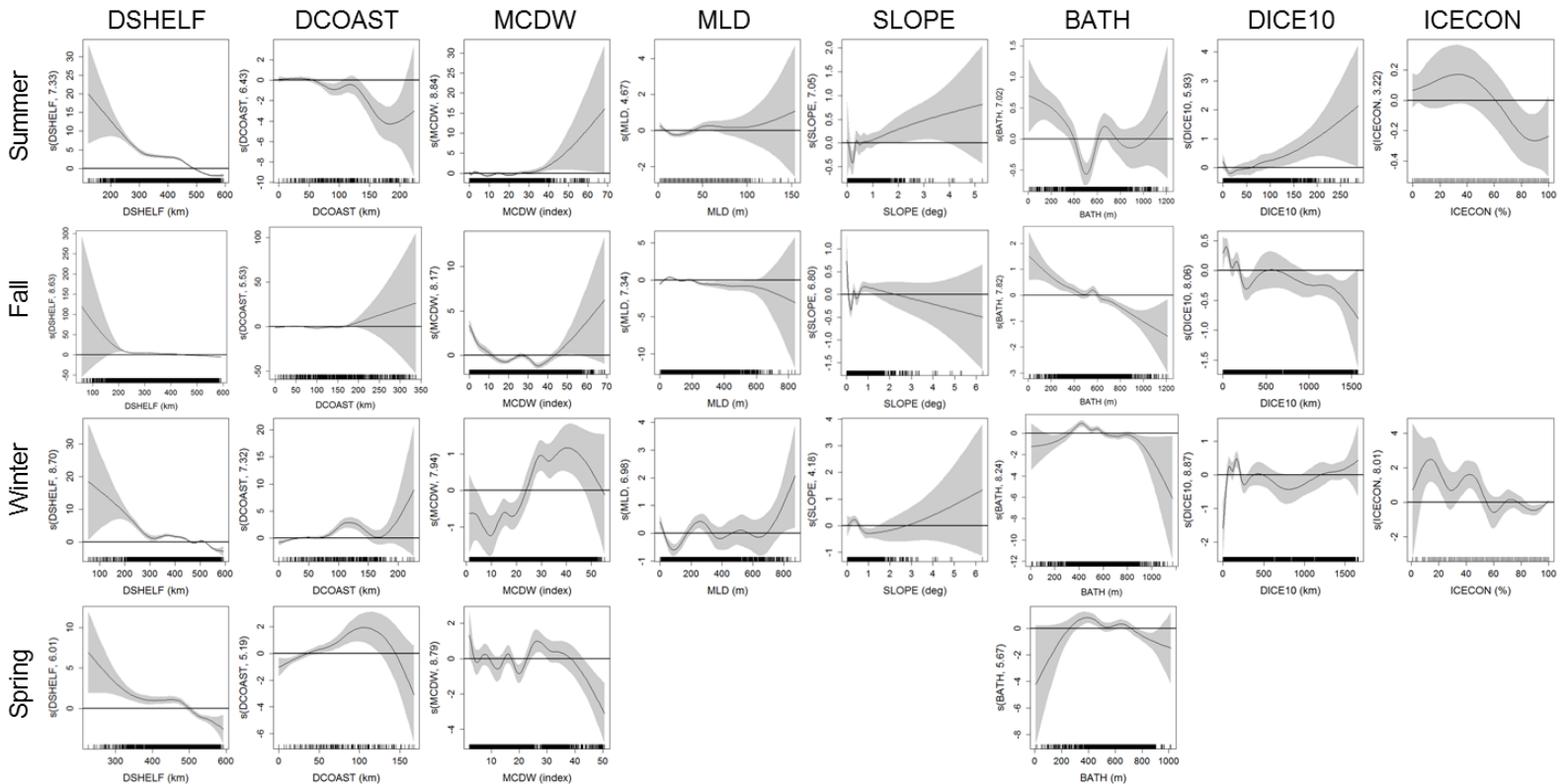


Figure 3.2: Results from the final predictive generalized additive model for each season. Plots show the relationship between Weddell seal occurrence in the western Ross Sea and eight environmental variables: ice concentration (ICECON, %), distance from the 10% ice concentration contour (ICEDIST10, km), bathymetric depth (BATH, m), bathymetric slope (SLOPE, degree), modified circumpolar deep water index (MCDW), mixed layer depth (MLD, m), distance from the coast (DCOAST, km), and distance to the continental shelf, or 1000 m isobath (DSHELF, km). The shaded areas represent the 95% confidence interval. The effect of the explanatory variable on the response is on the logit scale where zero (solid black line) or negative numbers show no effect.

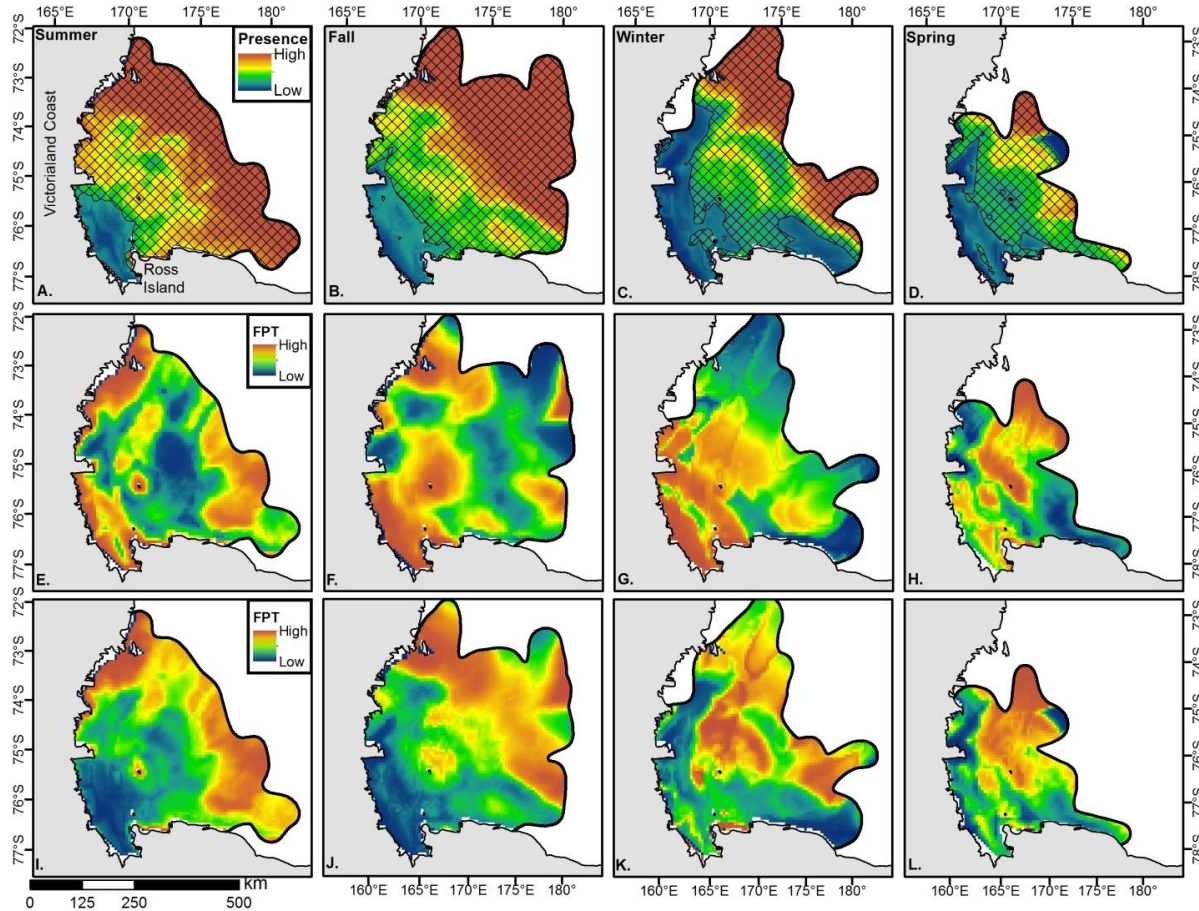


Figure 3.3: Panels A-D show the probability of Weddell seal presence in the western Ross Sea by season with warmer colors indicating a higher probability of seal occurrence and hatched areas representing preferred habitat. Predicted Weddell seal foraging, as measured by First Passage Time (FPT), is shown on panels E-H and predicted Weddell seal foraging within preferred habitat is shown on panels I-L. The analysis area was determined by the extent of tracking data for each season.

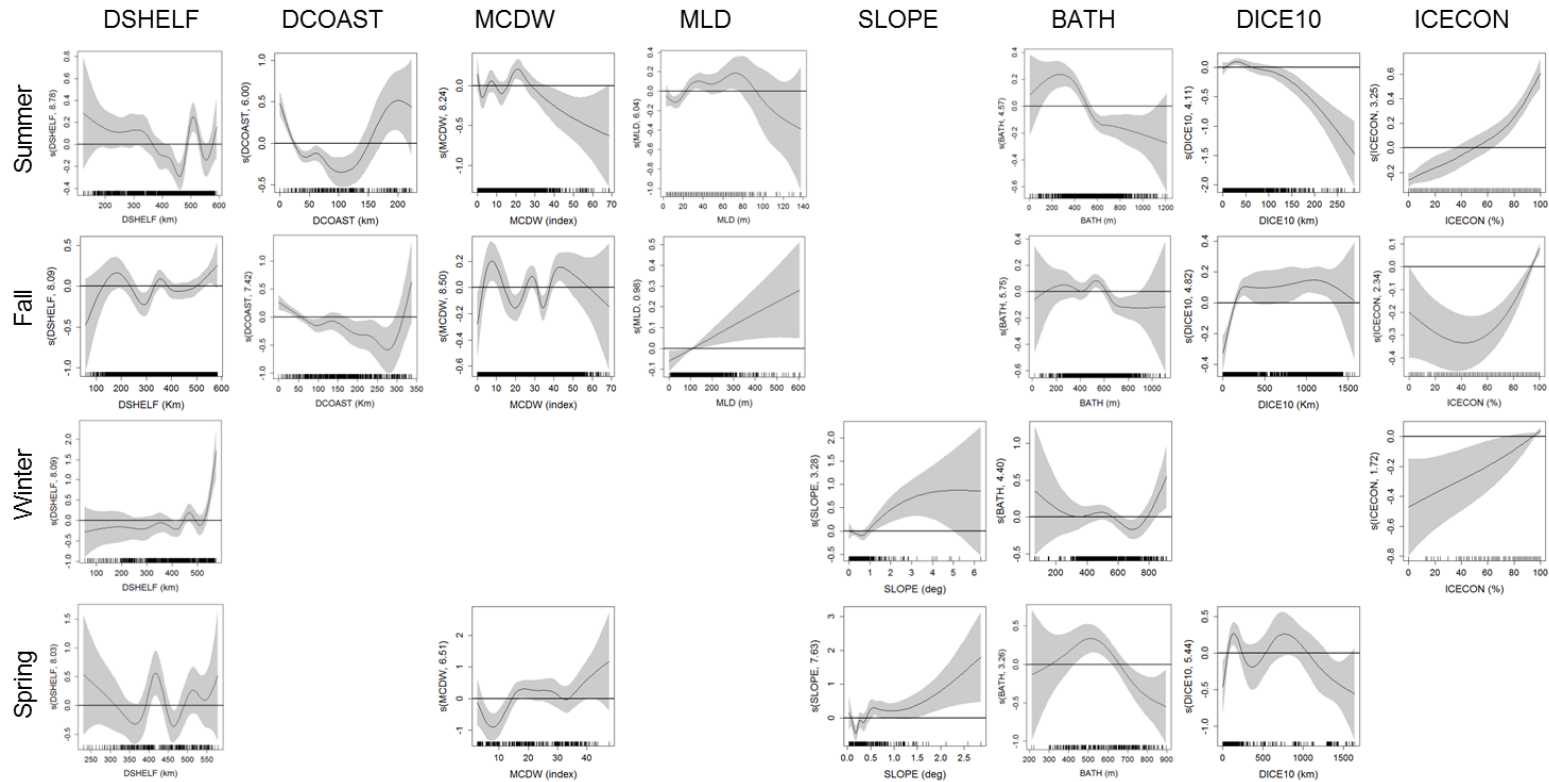


Figure 3.4: Results from the final generalized additive model for each season. Plots show the relationship between First Passage Time (FPT) for Weddell seals in the western Ross Sea and eight environmental variables: ice concentration (ICECON, %), distance from the 10% ice concentration contour (ICEDIST10, km), bathymetric depth (BATH, m), bathymetric slope (SLOPE, degree), modified circumpolar deep water index (MCDW), mixed layer depth (MLD, m), distance from the coast (DCOAST, km), and distance to the continental shelf, or 1000 m isobath (DSHELF, km). The shaded areas represent the 95% confidence interval. The effect of the explanatory variable on the response is on the log scale where zero (solid black line) or negative numbers show no effect.

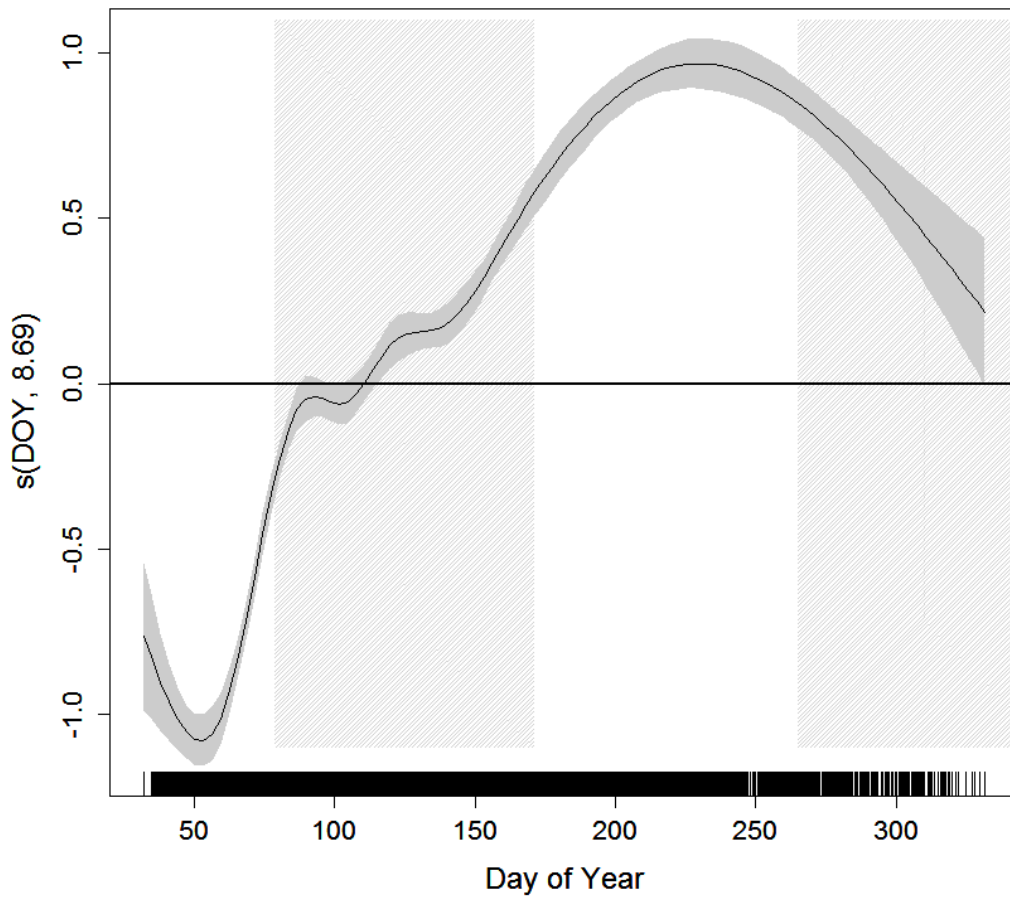


Figure 3.5: Smoothed function for day of year (DOY) in predicting log First Passage Time (FPT), shaded and non-shaded areas represent seasons, from summer to spring, respectively. The shaded areas represent the 95% confidence interval. The effect of the explanatory variable on the response is on the log scale where zero (solid black line) or negative numbers show no effect.

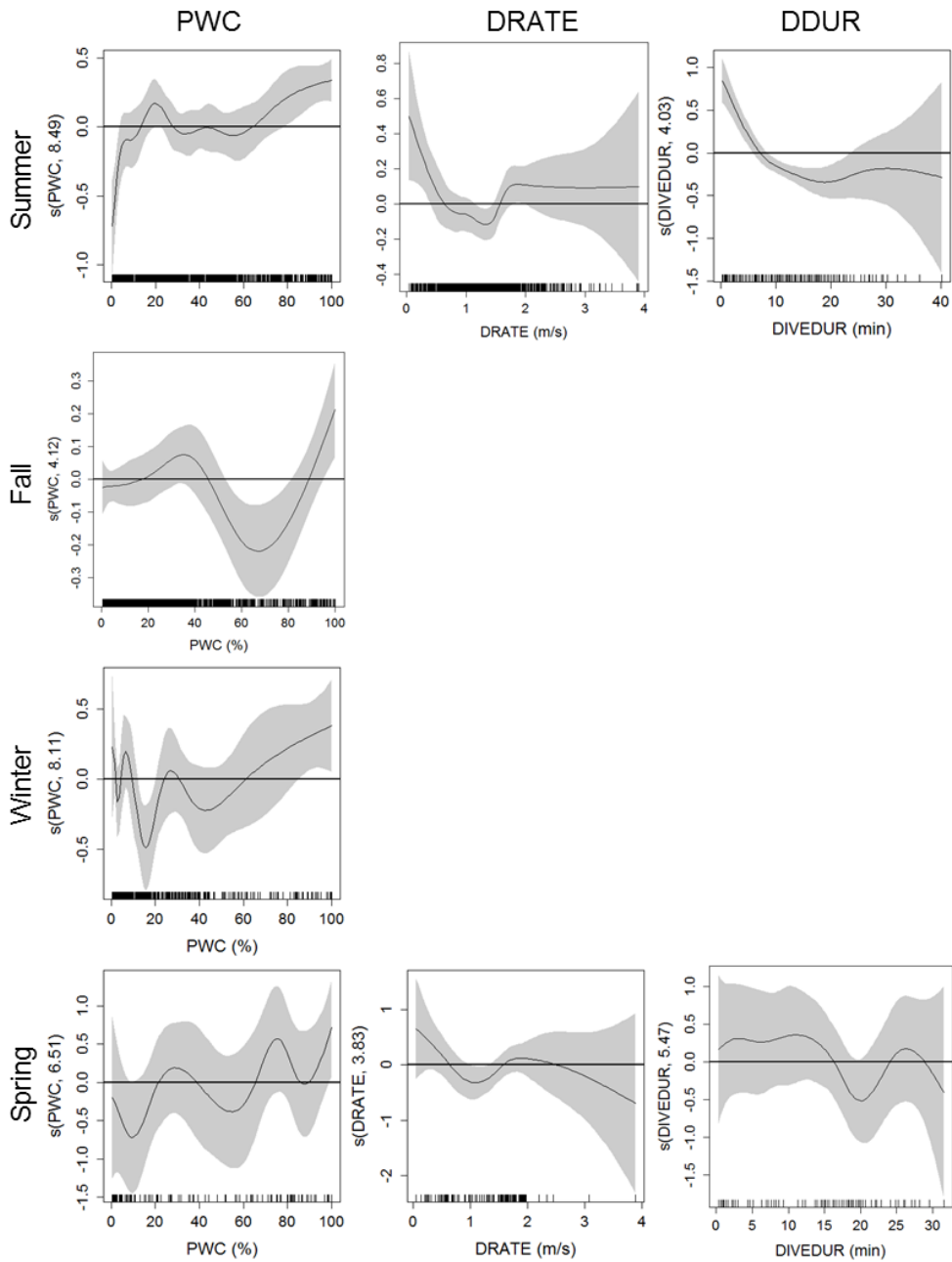


Figure 3.6: Results from the final generalized additive model used to predict First Passage Time (FPT) for each season. Plots show the relationship between FPT for Weddell seals in the western Ross Sea and three dive metrics: dive duration (DDUR, min), percent water column depth (PWC, %), and descent rate (DRATE m s^{-1}). The shaded areas represent the 95% confidence interval. The effect of the explanatory variable on the response is on the log scale where zero (solid black line) or negative numbers show no effect.

CHAPTER 4

Using stable isotopes and tracking data to reveal the foraging ecology of Weddell seals in the western Ross Sea, Antarctica

ABSTRACT

Weddell seals (*Leptonychotes weddellii*) serve an important role as one of Antarctica's top predators, yet surprisingly little is known about their diet and foraging ecology. Previous studies used scat and stomach content analyses to examine Weddell seal diet, however, these methods are biased towards prey with indigestible hard parts. Stable isotope analysis provides a more complete picture of digestible and indigestible prey items. We analyzed the stable isotope composition ($\delta^{13}\text{C}$ and $\delta^{15}\text{N}$) of Weddell seal red blood cells (RBC) and vibrissae, reflecting different time scales in the foraging history of individuals. Our objectives were to 1) examine isotopic variation in relation to Weddell seal mass, sex, season, location, percent lipid, and age, 2) quantify the contribution of prey items to overall diet, and 3) link diet to animal distribution and foraging patterns. We collected tissue samples from 96 Weddell seals near Ross Island and along the Victoria Land coast (2010-2012). Mass was a significant predictor of $\delta^{13}\text{C}$ and $\delta^{15}\text{N}$ for both tissues, though the strength and direction of the relationship varied by year. In addition, older individuals (> 10 years) had significantly enriched RBC $\delta^{13}\text{C}$ and $\delta^{15}\text{N}$, suggesting they were feeding at a higher trophic level than younger seals during the previous six weeks. Using Bayesian mixing models to estimate diet, the prey group consisting of Antarctic

silverfish (*Pleurogramma antarcticum* and *Trematomus newnesi*) was found to be an important prey item, but its proportional contribution to Weddell seal diet varied among tissue types and individuals [median RBC (range): 48.7% (39.0-57.1%); median of mean vibrissae (range): 53.3% (36.6-65.6%)]. The Antarctic icefish (*Neopagetopsis ionah*) contributed 48.7% (39.0-57.1%) of Weddell seal diet over a period of weeks, while *Pagothenia borchgrevinki*, *T. nicolai*, *T. pennellii* and *T. bernacchii* combined, contributed 43.1% (range: 30.3-58.8%) over a period of months. On average, the median Antarctic toothfish (*Dissostichus mawsoni*) contribution to the overall diet was < 10%. However, given its high energetic density, toothfish may be a relatively more important prey item for Weddell seals, especially during the post-molt recuperation period when animals are at their leanest. Differences in diet among tissue types suggest that the prey species consumed differs throughout the year. Year-round tracking data revealed that foraging patterns were associated with different diets. Overall, this study provides new information on the isotopic variation and diet of Weddell seals and provides critical insight into the feeding ecology of this important top predator of the Ross Sea ecosystem.

INTRODUCTION

Within the Southern Ocean, the Ross Sea ecosystem is particularly unique due to its vast shallow regions, significant polynyas, diverse topography, and extensive ice shelf (Smith et al., 2007). Although the Ross Sea is the most productive region in Antarctica, the biodiversity of fish fauna in this region is relatively low compared to the Southern Ocean, composed of 95 species from 16 families, and is dominated by a single taxonomic group. The family Nototheniidae comprises 77% of all fish species, and 91% of total fish biomass in the Ross Sea ecosystem (Eastman and Hubold, 1999; Lenky et al., 2012; Smith Jr et al., 2012). Despite the relative simplicity of the fish community and the extensive ecological studies that have been conducted in this region, trophic linkages between top predators and their prey are not well understood.

Weddell seals (*Leptonychotes weddellii*) are one of Antarctica's top predators and have the southernmost distribution of any mammal. While only about 32,000-50,000 of the estimated 730,000 Weddell seals in Antarctic waters inhabit the Ross Sea, they serve an important role in the trophic ecology of this unique ecosystem (Laws, 1977; Ainley, 1985). Moreover, Weddell seals are an ideal marine predator for monitoring ecosystem health and resilience given that they return to predictable breeding colonies in early austral spring (October-November) and remain there through the summer (January-February).

Previous studies used scat and stomach content analyses to examine the diet of Weddell seals in the Ross Sea and found nototheniid fish to be the most important dietary item for Weddell seals in McMurdo Sound (Dearborn, 1965; Burns et al.,

1998). While these studies provided valuable insight into the foraging ecology of Weddell seals, analyses were limited to recently consumed prey that had not been assimilated. In cases where hard parts are either not consumed or do not persist after the digestion process, prey items cannot be detected in stomach and scat contents. For example, Weddell seals have been observed feeding on large Antarctic toothfish (*Dissostichus mawsoni*) (Davis et al., 2004; Kim et al., 2005; Ponganis and Stockard, 2007; Ainley and Siniff, 2009; Kooyman, 2013); however, due to the relatively large size of these fish, seals only consume the flesh, preventing the detection of hard parts in scat and stomach contents.

Stable isotope analysis is a powerful tool for studying the foraging ecology of animals and, unlike scat and stomach content analysis, it does not over-represent indigestible material or under-represent items that leave little visual trace (Bodey et al., 2011). By providing information on food that has been incorporated into the consumer's tissue (as opposed to only ingested), stable isotope analysis can be linked to an animal's physiological condition and, therefore, its ability to adjust to environmental perturbations that may impact reproduction and survival (Jakob et al., 1996). The predictable enrichment in $\delta^{15}\text{N}$ (1.3-5.3‰) from one trophic level to the next makes it a useful indicator of a consumer's trophic position relative to its prey (DeNiro and Epstein, 1978, 1981; Rau et al., 1983; Minagawa and Wada, 1984; Peterson and Fry, 1987; Hammill et al., 2005). However, the relatively small enrichment in $\delta^{13}\text{C}$ between trophic levels (0-1‰ in marine systems) makes it a better indicator of carbon sources than trophic position, distinguishing benthic from

pelagic and nearshore from offshore environments (McConnaughey and McRoy, 1979; Zhao et al., 2004).

Although previous studies have examined $\delta^{13}\text{C}$ and $\delta^{15}\text{N}$ isotopes in Weddell seals, these studies were limited to inter-individual differences and only examined blood serum or plasma samples, which reflect diet consumed over a period of days to weeks (Burns et al., 1998; Zhao et al., 2004). By using two different tissues we were able to examine isotopic variation and diet across two different time periods. Also, a subset of seals was sampled in two different seasons, allowing us to examine both inter- and intra-individual differences in isotopes and thus diet. As tissue samples collected when tags are deployed provide diet data prior to the collection of tracking data, very few studies have examined stable isotope data concurrently with movement data (Votier et al., 2010; González-Solís et al., 2011; Zbinden et al., 2011; Seminoff et al., 2012). However, we were able to recapture and collect tissue samples from 13 Weddell seals that had carried tags during the previous 10 months, providing a unique opportunity to link foraging behavior with isotopic signatures. Mixing models capable of handling large numbers of potential prey items have recently been developed and allow diet to be quantified from isotopic values. However, these models have never been used to estimate the proportional contribution of prey items to the diet of Weddell seals.

This study presents carbon and nitrogen stable isotope data from two tissues (red blood cells, or RBC, and vibrissae) that were collected from Weddell seals in the western Ross Sea (WRS) over a three year period (2010-2012). Samples from the two

tissues allowed us to examine the trophic ecology of Weddell seals over a period of six weeks (RBC) in addition to a longer period spanning months to a year (vibrissae) relative to multiple variables (sex, location, mass, seal percent lipid, year, and age) that may influence energy requirements and, therefore, diet. This is the first study to quantify Weddell seal diet by comparing $\delta^{13}\text{C}$ and $\delta^{15}\text{N}$ isotopes from RBC and vibrissae to those from a suite of potential prey items and to examine diet relative to foraging patterns. Overall, our objectives were to: 1) examine isotopic variation in relation to mass, sex, year, season, location, percent lipid as a measure of seal body condition, and age 2) quantify the contribution of prey items to overall diet, and 3) link foraging strategies based on movement and diving behavior to differences in diet. Results from these analyses provide important information on the foraging behavior of Weddell seals, and offer context on their role as a top predators in the Ross Sea ecosystem.

METHODS

Animal capture and sample collection

All Weddell seal handling and sample collection were conducted under the National Fisheries Service permit number 87-1851-04, the Antarctic Conservation Act (ACA), and approved by the Animal Care and Use Committee (IACUC) at the University of California, Santa Cruz (UCSC).

Between 2010 and 2012, 96 Weddell seals were captured near Ross Island and along the Victoria Land coast of the Ross Sea (Fig. 4.1). Twenty of these animals were recaptured in a second season. Seals were chemically immobilized with an

initial dose of a telatamine HCL/zolazepamHCL mixture (Telazol 0.5 mg/kg) administered intramuscularly. Approximately 12 minutes post-injection, animals were captured using a hoop net. Subsequent intravenous injections of a 2:1 mixture of ketamine hydrochloride (100 mg/ml Ketaset) and diazepam (5 mg/ml) were administered, when necessary, to maintain immobilization. While sedated, seals were weighed in a canvas sling suspended from a tripod using a Dyna-Link scale (1000 ± 1 kg). The longest vibrissa on the muzzle of each animal was clipped as close as possible to the skin and blood samples were collected from the extradural vein in heparinized blood tubes. In addition, 60 seals were instrumented with Conductivity, Temperature, and Depth – Satellite Relay Data Loggers (CTD-SRDL) during the January-February breeding season.

Data were obtained from each tag and ARGOS position estimates were filtered using a threshold speed of 15 kmh^{-1} , and new positions were interpolated every two hours using a forward looking particle filtering model (Tremblay et al., 2009), that accounts for the errors associated with each ARGOS location class. Dive locations were determined by linking dive time with time along the track, and linearly interpolated to the nearest minute.

Stable isotope analysis

Following the methods of Hückstädt *et al.* (2012), all vibrissae were subjected to a two-step lipid-removal process: 1) lightly scrubbed using distilled water and detergent, and allowed to dry in an oven for a minimum of 30 minutes; 2) submerged in petroleum ether and rinsed in an ultrasonic bath for 15-20 minutes. Vibrissae were

then measured and cut into 0.5 cm segments. Samples with masses of 0.5 ± 0.05 mg were cut from the proximal end of each segment. Whole blood samples were centrifuged to extract RBCs and stored in a -20°C freezer. RBC samples were subsequently freeze-dried and subsamples with masses of 0.5 ± 0.05 mg were obtained.

Seal lipid mass (as % total body mass) was determined for each animal using the labelled water dilution technique as described in Shero et al. (2014; 2015), as it provides an indicator of body condition. Briefly, a pre-injection blood sample was taken, followed by injection of 1-1.5 mCi of tritiated water into the extradural vein. Post-equilibration blood samples were collected ≥ 90 minutes after injection and serum was distilled following Ortiz et al. (1978) to calculate lipid mass (Reilly and Fedak, 1990; Bowen and Iverson, 1998).

In order to reconstruct the diet of a consumer using stable isotopes, it is necessary to have a library of isotopic data for potential prey. Thus, prey species samples were collected in collaboration with concurrently funded projects to study Ross Sea fish (2010-2012) and stored in a -80°C freezer. In preparation for stable isotope analysis, fish were thawed at room temperature and lightly rinsed in deionized (DI) water. Standard length and weight measurements were taken before homogenizing individual whole fish. All equipment was washed repeatedly with soap and water between samples to prevent cross-contamination. Subsamples of the homogenates from each fish were freeze-dried for 48 hours, mixed into a fine powder, and a mass of 0.5 ± 0.05 mg was obtained for isotopic analysis.

Because many Antarctic fish species are rich in lipids (Clarke et al., 1984; Lenky et al., 2012), we lipid-extracted each sample in order to avoid variation in $\delta^{13}\text{C}$ caused by carbon-depleted lipids (Pinnegar and Polunin, 1999; Sweeting et al., 2006; Post et al., 2007). Lipid extraction was performed by combining 0.1 g of homogenate with 5 ml of 2:1 chloroform:methanol and submerging the container in an ultrasonic bath for 30 minutes. This process was repeated 3 to 4 times, decanting the supernatant between rinses, until the liquid appeared clear. Finally, each sample was rinsed with 2 ml of DI water and freeze-dried for an additional 48 hours. The dried homogenate was mixed into a fine powder and subsamples of 0.5 ± 0.05 mg were obtained.

Fish (original and lipid-extracted), vibrissae, and RBC subsamples were placed into tin capsules and analyzed at the Stable Isotope Laboratory at UCSC using an Elemental Analyzer interfaced with a Finnigan Delta Plus XP mass spectrometer in order to obtain $\delta^{13}\text{C}$ and $\delta^{15}\text{N}$ values. Standards of Pugel and Acetanilide were used to check for instrument drift and calibration throughout the sampling period.

Isotopic composition was expressed in δ (delta) notation, using the following equation:

$$\delta^h\text{X} = \frac{R_{\text{sample}} - R_{\text{standard}}}{R_{\text{standard}}} \times 1000$$

where h is the atomic mass of the heavy isotope, X is C or N, R_{sample} is the ratio of $^{13}\text{C}/^{12}\text{C}$ or $^{15}\text{N}/^{14}\text{N}$, and R_{standard} is Vienna PeeDee Belemnite (VPDB) limestone for $\delta^{13}\text{C}$ and atmospheric nitrogen (N_2) for $\delta^{15}\text{N}$. Units are expressed as parts per

thousand differences from the standard or per mil (‰). Replicate measurements of laboratory standards showed measurement errors of $\pm 0.2\text{‰}$ and $\pm 0.1\text{‰}$ for stable carbon and nitrogen isotope measurements, respectively.

For all dietary analyses, $\delta^{13}\text{C}$ from lipid extracted fish samples, and $\delta^{15}\text{N}$ from untreated samples were used. This was necessary as $\delta^{15}\text{N}$ becomes significantly enriched during the lipid extraction process, which may be related to the composition of essential and non-essential amino acids (Pinnegar and Polunin, 1999; Sweeting et al., 2006; Logan et al., 2008).

Statistical analysis

Isotopic variation

We evaluated the relationship between $\delta^{13}\text{C}$ and $\delta^{15}\text{N}$ and the following variables: sex, year, season, tagging location, mass, and seal percent lipid. Mass and seal percent lipid were continuous variables while sex, year, season and tagging location were factor variables (Table 4.1). Tagging location was categorized as south (around Ross Island) or North (Victoria Land Coast). Because mass was not always measured, the data set was reduced to 86 animals for RBCs and 36 for vibrissae for all linear models. Using the statistical software R (R Development Core Team, 2013) we ran generalized linear mixed models (GLMM) with an identity link on a global model (including interaction terms) for both $\delta^{13}\text{C}$ and $\delta^{15}\text{N}$ as a response variable. Separate models were run for RBC and vibrissae data and AIC scores were used for model selection. To account for animals that were sampled twice, we included

individual as a random effect. Models were validated by examining residuals for normality and homoscedasticity.

As a result of a long-term population study on Weddell seals in the McMurdo region, age was known for a subset of the animals (RBCs: n=38, vibrissae: n=21). These data subsets were examined separately from the GLMMs. Because age was approximate for several animals, we categorized seals into two categories, young adult (3-10 years) and old adult (> 10 years), and assessed whether $\delta^{13}\text{C}$ and $\delta^{15}\text{N}$ varied with age using t-tests.

Finally, we compared RBCs and vibrissae $\delta^{13}\text{C}$ and $\delta^{15}\text{N}$ values both within and between individual Weddell seals. Isotopic values for $\delta^{13}\text{C}$ and $\delta^{15}\text{N}$ along the length of individual vibrissae were plotted and compared to the overall population mean. We used GLM models with an identity link to test for individual differences in RBC and mean vibrissae $\delta^{13}\text{C}$ and $\delta^{15}\text{N}$ values between seasons for animals that were sampled in both January and October.

Diet and foraging ecology

We used a Bayesian isotope mixing model to determine the percent contribution of each prey species to the diet of Weddell seals in the WRS, as a population and individually. Because this population of seals is thought to be primarily piscivorous we limited our analysis to fish species that have been previously documented as prey items through (1) scat and stomach content analyses: *P. antarcticum*, *Trematomus bernacchii* and other *Trematomus* spp, and (2) observations: *D. mawsoni*, *P. borchgrevinki* and *N. ionah*. Although amphipods,

mysids, and polychaetes have been found in scat and stomach contents, they are thought to be a result of secondary ingestion by fish known to forage on these items (Dearborn, 1965; Eastman, 1985; Eastman and DeVries, 1985; Burns et al., 1998). Similarly, euphausiids do not appear to compose a large proportion of the Weddell seal diet in the Ross Sea likely due to their absence in large numbers from the ecosystem (Eastman, 1985)

The “siar” package in R was used to fit the mixing models, using a Bayesian framework based upon a Gaussian likelihood (Parnell, 2013). We calculated mean and standard deviation of $\delta^{13}\text{C}$ and $\delta^{15}\text{N}$ for six potential prey species, and used a student’s t-test assuming unequal variance to determine if species were isotopically distinct at the $p = 0.05$ significance level. Unless otherwise stated, the percent contribution of prey items to Weddell seal diet is presented as median (range).

We examined the diet of Weddell seals on two time scales, through the use of both RBC and vibrissa isotope values. RBCs allowed us to examine diet over the most recent weeks to more than a month (Hilderbrand et al., 1996), whereas vibrissae offered insight into diet on the time scale of months to a year depending on vibrissae growth rate. We used a trophic enrichment factor (TEF) of $1.7 \pm 0.3\text{‰}$ and $2.8 \pm 0.3\text{‰}$ for blood and vibrissae $\delta^{15}\text{N}$ values (Hobson et al., 1996) and $0.0 \pm 0.3\text{‰}$ for both blood and vibrissae $\delta^{13}\text{C}$ values. Mixing model results were plotted with violin plots which are similar to boxplots but also provide kernel density plots of the data on each side.

Complete track and dive records were recorded for 13 Weddell seals, allowing us to assess foraging patterns and determine how they might be related to diet as inferred from stable isotopes. Using the “FactoMineR” package in R (Husson et al., 2013), we performed a Principle Component Analysis (PCA) on eight variables thought to be important to Weddell seal foraging ecology: mean maximum dive depth (m), mean dive duration (min), mean time spent within 80% of maximum dive depth (min), mean decent rate (ms^{-1}), proportion of dives over 100 m, proportion of dives over 20 minutes, the calculated aerobic dive limit (Kooyman et al., 1980b), mean percent of the water column used (100% = bottom), and mean distance from the coast (km). The number of dimensions to retain in the PCA was determined by eigenvalues greater than one.

Using components from the PCA, we performed a hierarchical clustering analysis to group seals based on foraging behavior. We then analyzed the vibrissae data of seals within each cluster in a mixing model to determine if discrete foraging patterns were related to differences in diet. Once clusters were determined using dive metrics, we examined difference in $\delta^{13}\text{C}$ and $\delta^{15}\text{N}$ between the clusters using a one-way analysis of variance (ANOVA) test.

RESULTS

Isotopic variation

We measured $\delta^{13}\text{C}$ and $\delta^{15}\text{N}$ values for 96 RBC and 45 vibrissae samples from individual Weddell seals (Table 4.1). An additional 20 RBC and vibrissae samples were obtained from a second handling of seals previously sampled, and were thus

used to assess intra-individual differences over time. There was considerably less population-level variation in $\delta^{13}\text{C}$ and $\delta^{15}\text{N}$ for RBCs than vibrissae (Fig. 4.2).

Overall, $\delta^{13}\text{C}_{\text{RBC}}$ and $\delta^{15}\text{N}_{\text{RBC}}$ values ranged from -25.8 to -24.4 (mean \pm SD: $-25.2 \pm 0.0\text{‰}$) and 11.4-13.1 ($12.0 \pm 0.3\text{‰}$), respectively. Mean $\delta^{13}\text{C}_{\text{vibrissa}}$ values ranged from -24.3 to -22.5 ($-23.4 \pm 0.4\text{‰}$) and mean $\delta^{15}\text{N}_{\text{vibrissa}}$ values spanned from 12.2 to 13.8 ($13.0 \pm 0.4\text{‰}$). There was considerably less variation in $\delta^{13}\text{C}$ and $\delta^{15}\text{N}$ for RBCs than vibrissae segments (Fig. 4.2). Using resampling to ensure equal sample size between RBC and vibrissa segments, we found that the variation in $\text{C}_{\text{vibrissa}}$ (0.20) was double the variation of $\delta^{13}\text{C}_{\text{RBC}}$ (0.10) and that the variation in $\delta^{15}\text{N}_{\text{vibrissa}}$ (0.27) was nearly triple the variation of $\delta^{15}\text{N}_{\text{RBC}}$ (0.10).

Mass, location, and year were the variables that best explained the variability in $\delta^{13}\text{C}_{\text{RBC}}$ values (Table 4.2). Values for $\delta^{13}\text{C}_{\text{RBC}}$ increased with mass, though the intercept varied by year; $\delta^{13}\text{C}$ in 2010 was 0.2‰ higher than 2011 and 2012. For a given mass and year, Weddell seals tagged along the Victoria Land coast were 0.3‰ higher in $\delta^{13}\text{C}$ than seals tagged near Ross Island. For a given tagging location and year, an increase in mass of 100 kg is associated with a 0.2‰ increase in $\delta^{13}\text{C}$. In contrast, mass was the only significant predictor of $\delta^{13}\text{C}_{\text{vibrissa}}$ with a 0.1‰ increase in $\delta^{13}\text{C}$ for every 100 kg increase in mass.

For both RBCs and vibrissae, mass, and year best explained the variation in $\delta^{15}\text{N}$. However, the relationship between $\delta^{15}\text{N}$ and mass varied among years. In 2010 and 2011, $\delta^{15}\text{N}_{\text{RBC}}$ increased 0.2‰ and 0.1‰, respectively, for every 100 kg increase in mass but, in 2012, $\delta^{15}\text{N}_{\text{RBC}}$ decreased $<0.1\text{‰}$ for every 100 kg increase in seal

mass. We observed a different relationship between $\delta^{15}\text{N}_{\text{vibrissa}}$ among years than for $\delta^{15}\text{N}_{\text{RBC}}$. In both 2010 and 2012, $\delta^{15}\text{N}_{\text{vibrissa}}$ increased $\sim 0.1\text{‰}$ for every 100 kg increase in mass. However, in 2011 $\delta^{15}\text{N}_{\text{vibrissa}}$ decreased by 0.2‰ for every 100 kg increase in mass.

Both $\delta^{13}\text{C}_{\text{RBC}}$ and $\delta^{15}\text{N}_{\text{RBC}}$ were significantly higher in older adult Weddell seals ($\delta^{13}\text{C}$: $-25.1 \pm 0.4\text{‰}$; $\delta^{15}\text{N}$: $12.2 \pm 0.4\text{‰}$) than younger adults ($\delta^{13}\text{C}$: $-25.4 \pm 0.2\text{‰}$; $\delta^{15}\text{N}$: 11.9 ± 0.3) ($\delta^{13}\text{C}$: $t_{23} = 3.03$, $p = 0.01$; $\delta^{15}\text{N}$: $t_{23} = 2.32$, $p = 0.03$).

Vibrissae $\delta^{13}\text{C}$ and $\delta^{15}\text{N}$ were not significantly different between age categories.

Isotopic values varied along the length of each vibrissa, indicating both inter- and intra- individual variation. In some cases a similar trend in $\delta^{13}\text{C}$ and $\delta^{15}\text{N}$ along the vibrissa was observed (Fig. 4.3a-c) while in others, nearly an opposite trend in $\delta^{13}\text{C}$ and $\delta^{15}\text{N}$ was detected (Fig. 4.3d-f). Results from GLM models showed no significant intra-individual differences in $\delta^{15}\text{N}_{\text{RBC}}$ between January and October ($p > 0.05$). However, $\delta^{13}\text{C}_{\text{RBC}}$ from samples collected in October were significantly higher than samples collected from the same individuals in January ($p = 0.01$). There was no significant difference in either mean $\delta^{13}\text{C}_{\text{vibrissa}}$ or mean $\delta^{15}\text{N}_{\text{vibrissa}}$ for individuals sampled in January and October.

Diet and foraging ecology

One of the limitations of using stable isotopes to reconstruct diet is that this method does not allow for prey identification and, therefore, prey items considered must be isotopically distinguishable. Because several species in our study were isotopically indistinguishable, we had to combine six different species into two

groups (Table 4.3). Figure 4.4 shows the mean \pm standard deviation of $\delta^{13}\text{C}$ and $\delta^{15}\text{N}$ values for the five fish species and species groups along with mean RBC and vibrissae isotopic values for Weddell seals in the WRS.

Mixing model results from RBC isotopic values showed that over 90% of Weddell seal diet consisted of two species/species groups: group *d* (47.9% (36.1 – 56.8%)) and *N. ionah* (*e*: 48.7% (39.0 – 57.1%)) (Fig. 4.5A; Table 4.3). Similarly, mixing model estimates from isotopic vibrissae values showed that prey group *d* (53.3% (36.6 - 65.6%)) contributed the most to the diet of seals. In contrast, however, prey group *c* (43.1% (30.3 – 58.8%)) was the second greatest contributor to their diet (Fig. 4.5B).

Examining vibrissae $\delta^{13}\text{C}$ and $\delta^{15}\text{N}$, we found evidence of individual variation in the proportional contribution of prey items to the diet of Weddell seals (Fig. 4.6). *D. mawsoni* had a higher proportional contribution to the diet of seal WS12-07 while prey group *d*, consisting of *P. antarcticum* and *T. newnesi*, had a higher contribution to the diet of WS12-16 than the other three animals. Finally, prey group *c* (a combination of *P. borchgrevinki*, *T. Nicolai*, *T. bernachii*, and *T. pennellii*) contributed over 35% to the diet of three of the four individuals (Fig. 4.6). Mixing model results for all individuals are presented in Appendix A.1.

The PCA analysis identified three components, accounting for 92% of the variation, that were retained in the hierarchical cluster analysis which resulted in four clusters based on dive behavior (Table 4.4, Fig. 4.6). Clusters one and four each consisted of only one individual, which were the only two animals to remain near

Ross Island over the entire 10 month period that they were tracked. The individual in cluster one had a smaller proportion of dives > 100 m (0.25) and a shallower mean maximum dive depth (72.3 m) than the mean for all 13 animals combined (0.40 ± 0.07 and 114.2 ± 17.2 m) (Table 4.4). However, the individual in cluster four was distinguished by its significantly longer dive duration (13.56 min) and its proximate location to the bottom (0.53), though still not benthic, than the other 13 seals (9.25 ± 1.94 min and 0.33 ± 0.07) (Table 4.4).

Clusters two and three were comprised of six and five Weddell seals, respectively. Seals in cluster two had faster descent rates (1.19 ms^{-1}) and shorter dive durations (7.82 mins) than the overall mean for the 13 seals ($1.11 \pm 0.11 \text{ ms}^{-1}$ and 9.25 ± 1.94 min) (Table 4.4). In addition, the six animals in cluster two also had lower mean bottom durations (3.37 min) and a lower proportion of dives over 20 minutes (0.05) than the overall mean for both these variables (4.19 ± 1.17 min and 0.12 ± 0.08). Finally, the five animals in cluster three were distinguished by their higher-than-average (0.18 compared to 0.12 ± 0.08) proportion of dives over 20 minutes, the calculated aerobic dive limit (Table 4.4).

Mixing model results showed that the overall diet for Weddell seals was different among clusters (Fig. 4.7). Prey groups *c* and *d* contributed over 80% to the diet of seals that stayed in the vicinity of Ross Island year-round (clusters one and three). However, the individual in cluster one appeared to be consuming a larger proportion of *D. mawsoni* and *N. iohan* than the individual in cluster three. Prey groups *c* and *d* also contributed the highest proportion (>90%) to the diet of Weddell

seals in cluster two, with < 1% contribution from each of the other prey species/groups. Finally, individuals in cluster four appeared to be consuming more generally, with all prey species and prey groups represented in the diet (Fig. 4.7). Both $\delta^{13}\text{C}_{\text{vibrissae}}$ ($F_{3,209} = 10.07$, $p < 0.001$) and $\delta^{15}\text{N}_{\text{vibrissae}}$ ($F_{3,209} = 18.15$, $p < 0.001$) were significantly different between clusters.

DISCUSSION

Isotopic variation

This is the first study to quantify isotopic variation in $\delta^{13}\text{C}$ and $\delta^{15}\text{N}$ for two different tissues (RBCs and vibrissae), allowing us to determine the diet of Weddell seals over two time scales. The increase in $\delta^{13}\text{C}_{\text{RBC}}$ with mass suggests that heavier animals were diving more benthic or staying closer to the coast than smaller animals during the six weeks before blood samples were collected (France, 1995). However, the relationship between $\delta^{13}\text{C}_{\text{RBC}}$ and mass depended on year and sampling location; $\delta^{13}\text{C}$ was 0.2‰ lower in both 2011 and 2012 compared to 2010 and, after accounting for mass and year; animals along the Victoria Land coast were more $\delta^{13}\text{C}$ enriched than seals closer to Ross Island. In contrast, neither year nor location were significant predictors of $\delta^{13}\text{C}_{\text{vibrissa}}$, which is likely due to the integration of $\delta^{13}\text{C}$ values over the longer period of vibrissa growth (months to a year).

Differences in the relationship between $\delta^{13}\text{C}_{\text{RBC}}$ and Weddell seal mass among years may be related to the annual variability of ice conditions in the Ross Sea. During the three years of this study, Antarctica exhibited the lowest sea ice extent on record (Przyborski, no date). The presence of sea ice alters the plankton distribution

and composition at the base of the food web (Smith Jr et al., 2012). While the exact changes in biota related to fluctuations in sea ice concentration and extent are difficult to predict, they will undoubtedly cause a shift in the prey base, propagating up to the consumer (Lorrain et al., 2009). The observed differences in $\delta^{13}\text{C}$ over a short time period (RBCs) appear to reflect differences in these dynamic ice conditions, whereas evidence suggests that $\delta^{13}\text{C}$ values integrated over a much longer time period (vibrissae) do not reflect the highly dynamic nature of sea ice.

RBC $\delta^{15}\text{N}$ and $\delta^{15}\text{N}_{\text{vibrissa}}$ changed with mass, but the direction of the relationship varied by year and was not consistent between tissue types. Because $\delta^{15}\text{N}$ is strongly associated with trophic position, these results suggest that diet varies as a function of a seal's mass over a period of weeks as well as over a longer time period. However, the inter-annual difference in $\delta^{15}\text{N}$ in relation to mass suggests that seals shift their diet between years and is likely the result of changing environmental conditions that influence prey availability. The differences in $\delta^{15}\text{N}$ between the two tissues are likely the result of life history characteristics in which Weddell seals have a limited foraging range while tied to the breeding colonies (October-January). Wheatley et al. (2008) found that larger females fed more during the lactation period in October-November than smaller females and suggests that larger animals are able to exploit different prey resources due to their physiological capacity to dive longer. Our results support this finding and further suggest that larger animals forage on higher trophic-level prey than smaller animals.

Significantly higher $\delta^{15}\text{N}_{\text{RBC}}$ in older seals (> 10 years) suggests they feed at a higher trophic level than younger seals (< 10 years), indicating differentiation in diet or habitat use between younger and older animals. In addition, $\delta^{13}\text{C}_{\text{RBC}}$ results suggest that either the two age groups foraged in different locations or that older animals consumed a higher proportion of benthic/demersal items than younger animals. Zhao et al. (2004) found that adults had higher $\delta^{13}\text{C}$ and $\delta^{15}\text{N}$ values than subadults, suggesting that adults were feeding at a higher trophic level and were possibly engaged in more benthic foraging than subadults. However, Zhao et al. (2004) did not distinguish between adult age classes, precluding a direct comparison. Marcoux et al. (2012) found this same relationship between age and isotope values in beluga whales (*Delphinapterus leucas*) and suggested that the differences in $\delta^{13}\text{C}$ and $\delta^{15}\text{N}$ values between age groups may be explained by physiological states associated with reproduction and body condition. Although $\delta^{15}\text{N}_{\text{vibrissa}}$ was also higher in older than younger animals, the difference was not significant, likely due to the integration of diet over many months.

The variation in $\delta^{13}\text{C}$ along an individual vibrissa often did not match the variation in $\delta^{15}\text{N}$, suggesting that $\delta^{13}\text{C}$ may explain pelagic/benthic and coastal/offshore behavior of Weddell seals better than diet. However, we speculate that animals showing similar $\delta^{13}\text{C}$ and $\delta^{15}\text{N}$ fluctuation along the vibrissa exhibited consistent habitat preferences throughout the year and, therefore, is a reflection of diet.

Intra-individual differences in RBC $\delta^{13}\text{C}$ are most likely a reflection of Weddell seal life history characteristics and the rate of tissue turnover. The samples from January-February were collected after the seals had spent at least two months breeding and molting on the fast ice. While at the breeding colony, Weddell seals engage in short foraging trips and the enriched $\delta^{13}\text{C}$ values are likely an indication of an individual's coastal, and possibly benthic, foraging behavior. The RBC samples from October-November were collected shortly after animals arrived at the breeding colony and $\delta^{13}\text{C}$ values were probably a reflection of the overwinter foraging trip during which many animals travel long distances towards the continental shelf break. Individual differences in mean vibrissae $\delta^{13}\text{C}$ were not observed and, as stated previously, were likely due to the integration of $\delta^{13}\text{C}$ values over a longer period of time.

The similarity in both RBC and vibrissae $\delta^{15}\text{N}$ within individuals collected at different time periods suggest that individual Weddell seals were foraging at the same trophic level during both the summer molting season and the spring breeding season. The lack of intra-individual differences in $\delta^{15}\text{N}$ for either tissue implies that individuals either have similar diets across seasons, or that they specialize on prey items in a consistent fashion in which integration of $\delta^{15}\text{N}$ over the time in which the tissue was produced would appear consistent.

Diet and foraging ecology

Supporting the findings of previous diet studies, mixing models identified *P. antarcticum* and *Trematomus species* (including *P. borchgrevinki*, previously known

as *T. borchgrevinki*) as important prey items for Weddell seals in the WRS (Dearborn, 1965; Burns et al., 1998; Davis et al., 1999; Fuiman et al., 2002; Zhao et al., 2004); however, the percent contribution of these prey items varied by tissue type. Isotopic values for RBCs indicated that *N. ionah* contributed more to Weddell seal diet than prey group *d* (*P. antarcticum* and *T. newnesi*) over the most recent weeks-month than over a longer period. While past diet studies do not identify *N. ionah* as an important prey item, in January 2012 we observed Weddell seals in a large ice hole feeding on what is most likely this species (Fig. 4.5A). *N. ionah* is a member of the family Channichthyidae. While most channichthyids are benthic, *N. ionah* has a benthopelagic lifestyle, traveling into pelagic waters at night to feed in the water column (Eastman and Hubold, 1999; La Mesa et al., 2004).

Results from mixing models using vibrissae $\delta^{13}\text{C}$ and $\delta^{15}\text{N}$ values indicate that Weddell seals were feeding on different species and in different proportions over a period lasting months to a year compared to the six week period reflected in RBCs. Species in groups *c* (*P. borchgrevinki*, *T. Nicolai*, *T. bernachii*, and *T. pennellii*) and *d* were the two dominant prey and contributed nearly equally to the diet of Weddell seals over a period of months to a year. *P. borchgrevinki* is a cryopelagic species, associated with the undersurface of the ice, while *T. nicolai* is benthic and inhabits shallow waters 30-50 meters deep, often close to anchor ice (Eastman and DeVries, 1982; Eastman and DeVries, 1985; La Mesa et al., 2004). These results agree with Burns et al. (1998) in which Weddell seals were found to feed primarily on *P. antarcticum*, *P. borchgrevinki*, and other *Trematomus* species; however, results from

Burns et al. were obtained using isotopic values from blood plasma rather than vibrissae and *N. ionah* was not considered as a potential prey item. Animal-borne cameras have also documented Weddell seals hunting *P. borchgrevinki* in the palette ice by blowing air into subice crevices (Davis et al., 1999).

Overall, this study identified the prey group consisting of *P. antarcticum* and *T. newnesi* as an important prey item in the diet of Weddell seals over a period of weeks to a year and is likely a result of the species' abundance and unique life history characteristics. *P. antarcticum* is the dominant fish in the Ross Sea, representing over 90% of both the number and biomass of all fish species (Dewitt, 1970; Hubold, 1985), and likely plays an important role in the mid-water shelf ecosystem where krill are less abundant (Hempel, 1985). Indeed, scat and stomach content analysis have confirmed the presence of *P. antarcticum* in the diet of most Weddell seals (Castellini et al., 1992; Burns et al., 1998). By attaching video cameras to Weddell seals foraging under the sea-ice, Fuiman et al. (2002) showed that seals forage on loose aggregations of *P. antarcticum* which exhibit diel vertical migration at mean depths of 252 m at night and 346 m during the day. The diel migration of both *P. antarcticum* and *N. ionah* match the diel diving pattern observed in Weddell seals, diving deeper during the day and shallower at night (Kooyman, 1975; Kooyman, 1981).

While *P. antarcticum*, *N. ionah*, and the species in prey group *c* were found to have the highest contribution to the diet of Weddell seals in the WRS, it is important to recognize that there are also individual differences in diet. *P. antarcticum* and the species in group *f* (comprised of *T. bernacchii* and *T. pennellii*) were the most

variable in their contribution while *D. mawsoni*, *Thansoni*, and the species in group *i* (*T. newnesi* and *T. eulipidotus*) was the most consistent in the degree of their contribution to the diet of individual seals. Because the hard parts of *D. mawsoni* are not consumed, and therefore are not detected in scat and stomach content analyses, there has been considerable debate regarding the importance of this species in the diet of Weddell seals (Burns et al., 1998; Davis et al., 1999; Fuiman et al., 2002; Ponganis and Stockard, 2007; Ainley and Siniff, 2009; Kim et al., 2011). Our results show that *D. mawsoni* comprised < 1% (RBC: 0.8% (0 - 6.7%); Vibrissae: 0.5% (0 - 3.4%)) of the diet of the Weddell seal population in the WRS; however, the median contribution of *D. mawsoni* ranged from 0.8 to 14.5% among individuals.

Although the contribution of *D. mawsoni* to the diet of Weddell seals was lower than most other nototheniid species analyzed in this study, it is important to consider prey quality. Results from Lenky et al. (2012) showed that *D. mawsoni* had the highest fat content (% wet mass) and energy density (kJg^{-1} wet mass) of the six nototheniid species analyzed. While the amount of *D. mawsoni* consumed by Weddell seals may be low, high lipid and energy density provided by this species may be critical for seals recovering from periods with high energetic demands (breeding, pupping, and molting).

Linking movement and diving data to diet provided further insight into the foraging behavior of Weddell seals in the Ross Sea. The four behavioral clusters resulting from our analysis corresponded to differences in diet. The individual in the first cluster dived shallower than average which corresponded to foraging primarily

on pelagic and cryopelagic notothenid species (*P. antarcticum*, *T. newnesi* and other *Trematomus* species). Seals in the second cluster were characterized by faster dive and bottom durations and higher descent rates than average. Over 60% of the diet of these animals was composed of a combination of *P. antarcticum* and *T. newnesi*. The faster descent rate is likely related to the locomotive behavior employed by *P. antarcticum* when pursued by a seal, reaching estimated speeds of 4.9 body lengths per second (La Mesa et al., 2004). The second most prevalent prey species in the diet of animals in this cluster were those from prey group *c*, composed of three *Trematomus* species and *P. borchgrevinki*. The short dive durations observed from animals in this cluster may be the results of animals foraging on *P. borchgrevinki* immediately on the underside of the ice. The individual in cluster three had a higher proportion of dives over the calculated aerobic dive limit than average. In this case, species in prey group *c* contributed the most to the diet of this animal, followed by species in group *d*. This increased frequency of dives longer than anticipated based on oxygen stores may be related to benthic foraging on *T. bernacchii* (included in prey group *c*), or perhaps foraging for longer periods of time on *P. borchgrevinki* (also in prey group *c*) on the underside of the ice. Finally, Weddell seals in the last cluster were characterized by longer, more benthic dives than average. The diet of these seals was composed of the species in prey groups *c* and *d*. As previously mentioned, the longer, more benthic dive behavior is likely related to foraging on benthic prey items such as *T. bernacchii*.

As a whole, Weddell seals appear to prefer nototheniid fish that have adapted to an epipelagic, pelagic, or cryopelagic lifestyle despite most fish in this family being benthic (La Mesa et al., 2004). By far, the largest contributors to the diet of Weddell seals were *N. ionah* (pelagic), and two species groups: (1) *T. newnesi* and *P. antarcticum* and (2) *P. borchgrevinki* (cryopelagic), *T. Nicolai* (cryopelagic and benthic in shallow waters), *T. bernacchi* (benthic) and *T. pennellii* (benthic).

Caveats of isotopic interpretation

Although we are confident in our findings, we must also acknowledge the complications associated with interpreting isotopic results. For example, there are several unknowns regarding vibrissae growth rates, retention, and shedding patterns in Weddell seals. While these traits are known for several phocid species, results are usually obtained from experiments conducted on captive animals (Hirons et al., 2001; Greaves et al., 2004; Hall-Aspland et al., 2005; Beltran et al., 2015). To date, there are no known Weddell seals in captivity, thus precluding captive growth rate experiments. Therefore, tracing the temporal changes in Weddell seal diet along a vibrissa was not possible. For this study, we assumed that the mean isotopic value for each vibrissae represented tissue metabolized during the previous months to a year, giving a broad indication of diet as suggested by Newland et al. (2011).

While mixing models are an invaluable tool for understanding food web complexities, like all models, they are only as good as the inputs. Diet, as determined by mixing models, is strongly dependent on the prey sources included in the model. Since the contribution of all dietary sources must sum to 100% of the consumer's

diet, it is critical to account for all prey items (Phillips et al., 2014). Therefore, previous knowledge on the consumer's diet is required. Finally, appropriate diet-tissue discrimination factors are essential for obtaining accurate results from dietary mixing models (Phillips et al., 2014).

In this study, we limited prey sources to fish species that were (1) confirmed in the diet of Weddell seals through stomach or scat contents, or (2) observed being predated on by Weddell seals in the WRS, Antarctica. While some studies suggest invertebrates such as octopods and cephalopods may contribute to the diet of Weddell seals, we did not include them as dietary sources. Therefore, it is important to note that if any particular invertebrate species contributed substantially to the diet of Weddell seals, they would not be reflected in our models (Burns et al., 1998). In addition, the trophic enrichment factor used in our models may have contributed some degree of error. Trophic enrichment factors have not been calculated for Weddell seals so we applied values from Hobson et al. (1996) that were calculated from three different species of captive seals. While the study did not find differences in fractionation among species, it is possible that Weddell seals have a different fractionation value.

Conclusions

The Ross Sea ecosystem is well studied, yet little is known about the role of top predators within the food-web. While previous studies identified Antarctic silverfish (*P. antarcticum*) as an important Weddell seal prey item through stomach and scat content analysis (Castellini et al., 1992; Burns et al., 1998), our study

provides the first quantitative confirmation of this finding, showing that the prey group consisting of *P. antarcticum* and *T. newnesi* comprises 36-66% of the Weddell seal diet. In addition, the cryopelagic fish, *N. ionah*, has never before been identified as an important prey item of Weddell seals; however, both visual observations and isotopic analysis confirmed the importance of *N. ionah* in the diet of Weddell seals over a period of weeks.

While there has been considerable debate about the importance of Antarctic toothfish, *D. mawsoni*, to the diet of top predators in the Ross Sea, our study showed that the median contribution of this species to the diet of Weddell seals ranged from 0.8% to 14.5% among individuals. Evidence from this work suggests that older animals may be more capable of capturing and consuming a higher trophic level fish like *D. mawsoni*, and because this fish species has the highest fat content (% wet mass) and energy density (kJg^{-1} wet mass) of the species analyzed in this study (Lenky et al., 2012), *D. mawsoni* may be critical for seals recovering from periods with high energetic demands (breeding, pupping, and molting).

Overall, our study showed that Weddell seals exhibit inter- and intra-individual differences in isotopic signatures over two time scales. In addition, we found that foraging patterns identified by dive parameters were linked to differences in $\delta^{13}\text{C}$ and $\delta^{15}\text{N}$ values and thus, different prey preferences. By providing the first quantitative estimates of isotopic variation and diet of Weddell seals, this study provides insight into the feeding ecology of this important top predator and its role within the Ross Sea ecosystem

TABLES

Table 4.1: Weddell seal tissue samples (RBC: red blood cells, and vibrissae) per variable (mass, sex, location, year, season, and age) used in generalized linear mixed models and Student's *t*-test for age.

		RBC	Vibrissae
Sex	Male	16	16
	Female	80	29
Age	<10	15	10
	>10	23	11
	Unknown	58	24
Location	North	31	14
	South	65	31
Year	2010	33	11
	2011	38	16
	2012	25	18
Season	Summer	44	25
	Spring	52	20
Mass	Known	91	40
	Unknown	5	5
Total		96	45

Table 4.2: Predictors of $\delta^{13}\text{C}$ and $\delta^{15}\text{N}$ from two Weddell seal tissues (RBC: red blood cells, and vibrissae) obtained from generalized linear mixed models.

Carbon RBCs	$\delta^{13}\text{C}$ estimate (95% CI)	SE	t-value	p
Intercept	-2.55E+01 (-2.58E+01--2.52E+01)	1.18E-01	-215.46	< 0.001
Mass	1.66E-03 (8.47E-04-2.47E-03)	4.21E-04	3.94	< 0.001
Year2011	-1.80E-01 (-3.12E-01--4.82E-02)	6.82E-02	-2.64	0.008
Year2012	-2.34E-01 (-3.85E-01--8.21E-02)	7.86E-02	-2.97	0.003
LocationSouth	-2.65E-01 (-4.01E-01--1.29E-01)	7.05E-02	-3.76	< 0.001
Carbon Vibrissae	$\delta^{13}\text{C}$ estimate (95% CI)	SE	t-value	p
Intercept	-2.37E+01 (-2.40E+01-2.33E+01)	-1.93E-01	122.94	0.000
Mass	8.51E-04 (-2.74E-04-1.98E-03)	5.69E-04	1.50	0.135
Nitrogen RBCs	$\delta^{15}\text{N}$ estimate (95% CI)	SE	t-value	p
Intercept	1.13E+01 (1.09E+01-1.16E+01)	1.71E-01	65.84	0.000
Mass	2.07E-03 (9.84E-04-3.17E-03)	5.64E-04	3.66	< 0.001
Year2011	4.50E-01 (-6.99E-02-9.69E-01)	2.70E-01	1.67	0.096
Year2012	9.24E-01 (3.38E-01-1.50E+00)	2.95E-01	3.13	0.002
Mass:Year2011	-1.18E-03 (-2.82E-03-4.66E-04)	8.54E-04	-1.38	0.168
Mass:Year2012	-2.44E-03 (-4.08E-03--7.49E-04)	8.52E-04	-2.86	0.004
Nitrogen Vibrissae	$\delta^{15}\text{N}$ estimate (95% CI)	SE	t-value	p
Intercept	1.23E+01 (1.17E+01-1.28E+01)	2.76E-01	44.52	0.000
Mass	1.55E-03 (-1.44E-04-3.36E-03)	8.88E-04	1.75	0.080
Year2011	1.30E+00 (4.27E-01-2.20E+00)	4.53E-01	2.87	0.004
Year2012	2.43E-01 (-5.60E-01-1.09E+00)	4.19E-01	0.58	0.562
Mass:Year2011	-3.28E-03 (-6.10E-03--5.53E-04)	1.41E-03	-2.33	0.020
Mass:Year2012	3.27E-05 (-2.52E-03-2.45E-03)	1.25E-03	0.03	0.979

Table 4.3: Species identification, assigned prey group, number of individuals, standard length, mass and isotopic values ($\delta^{13}\text{C}$ and $\delta^{15}\text{N}$) of Weddell seal prey species collected from the Ross Sea 2010-2012. Isotope values are presented as mean \pm standard deviation. Due to indistinguishable isotopic differences, species belonging to the same prey group were combined before using in mixing models to estimate Weddell seal diet.

Species	Prey Group	n	Length (cm)	Mass (g)	$\delta^{13}\text{C} \pm \text{SD}$	$\delta^{15}\text{N} \pm \text{SD}$
<i>Dissostichus mawsoni</i>	a	9	98.7 (67.0-123.0)	17744.4 (5500.0-37000.0)	-23.6 \pm 0.5	13.5 \pm 0.5
<i>Trematomus hansonii</i>	b	6	20.6 (16.9-27.2)	160.4 (77.4-374.4)	-24.8 \pm 0.2	12.3 \pm 0.3
<i>Pagothenia borchgrevinkii</i>	c	8	16.1 (11.4-19.3)	62.6 (20.7-97.3)	-23.3 \pm 0.5	10.4 \pm 0.3
<i>Trematomus nicolai</i>	c	11	14.8 (11.7-17.6)	74.3 (27.7-114.7)	-23.0 \pm 0.8	10.5 \pm 0.5
<i>Trematomus bernacchii</i>	c	26	17.2 (12.0-21.9)	114.5 (38.6-236.8)	-22.3 \pm 1.5	11.0 \pm 0.5
<i>Trematomus pennellii</i>	c	3	12.2 (10.8-14.6)	41.29 (22.4-76.6)	-22.7 \pm 0.4	10.7 \pm 0.9
<i>Trematomus newnesi</i>	d	11	15.5 (14.8-17.6)	73.1 (49.4-123.0)	-24.5 \pm 0.5	10.0 \pm 0.3
<i>Pleurogramma antarcticum</i>	d	3	11.5 (6.4-18.0)	15.0 (1.8-33.2)	-24.3 \pm 0.9	9.4 \pm 0.2
<i>Neopagetopsis ionah</i> *	e	2	-	-	-26.1 \pm 0.1	11.1 \pm 0.7

* Isotopic values for *Neopagetopsis ionah* are from Jo et al. (2013)

Table 4.4: Results from hierarchical cluster analysis to examine Weddell seal foraging strategies. Variables are defined as: P100M: proportion of dives > 100 m; AMAXDEP: average maximum dive depth (m); ADESCENT: average descent rate during a dive; ABOTDUR: average time spent within 80% of maximum dive depth (min); ADIVEDUR: average dive duration (min), P20MIN: proportion of dives over 20 minutes; APERDEP: average proportion of the water column used by diving Weddell seals.

Cluster	Variable	Cluster Mean	Overall Mean \pm SD	p-val
1	P100M	0.25	0.40 \pm 0.07	0.035
	AMAXDEP	72.34	114.21 \pm 17.16	0.015
2	ADESCENT	1.19	1.11 \pm 0.11	0.024
	ABOTDUR	3.37	4.19 \pm 1.17	0.024
	ADIVEDUR	7.82	9.25 \pm 1.94	0.019
	P20MIN	0.05	0.12 \pm 0.08	0.012
3	P20MIN	0.18	0.12 \pm 0.08	0.048
4	APERDEP	52.5	33.4 \pm 7.1	0.007
	ADIVEDUR	13.56	9.25 \pm 1.94	0.026

FIGURES

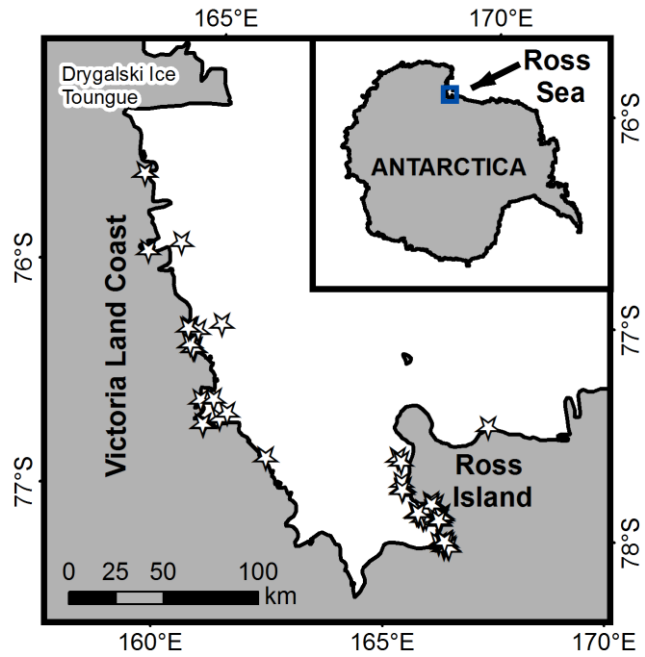


Figure 4.1: Weddell seal capture and sample (red blood cells and vibrissae) locations near Ross Island and along the Victoria Land coast.

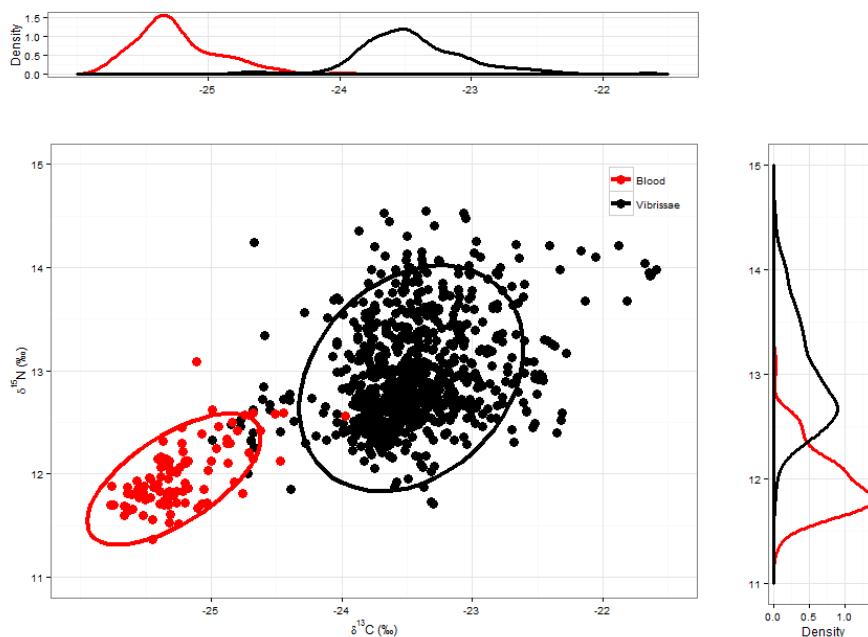


Figure 4.2: Isotopic values ($\delta^{13}\text{C}$ and $\delta^{15}\text{N}$) for red blood cells (RBC) and vibrissae segments. Ellipses indicate the 95% confidence interval and density plots show less variation in $\delta^{13}\text{C}$ and $\delta^{15}\text{N}$ values for RBC than vibrissae.

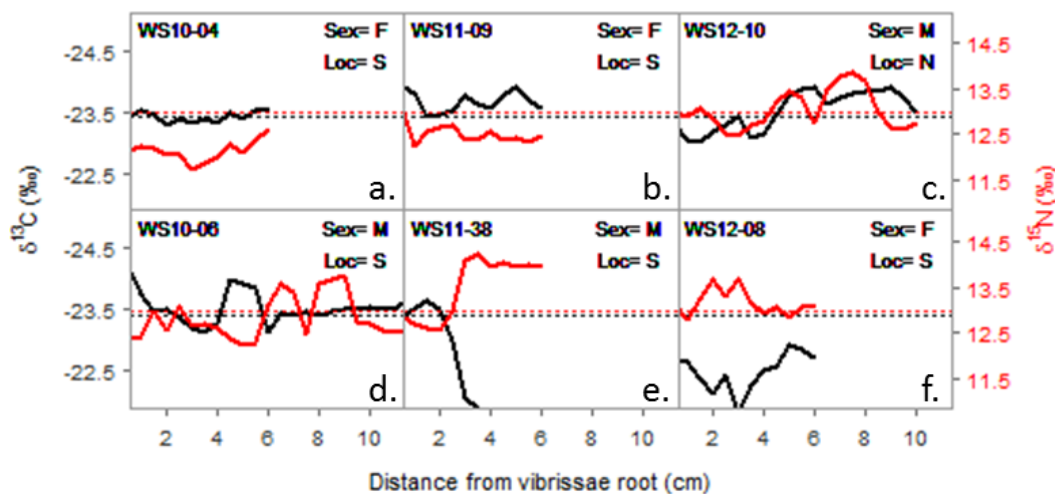


Figure 4.3: Vibrissae $\delta^{13}\text{C}$ and $\delta^{15}\text{N}$ values from the base of the vibrissa to the furthest extent for six individual Weddell seals. Values for $\delta^{13}\text{C}$ are shown on the left axis (black) and $\delta^{15}\text{N}$ values are shown on the right (red). Dotted lines represent the mean vibrissae $\delta^{13}\text{C}$ and $\delta^{15}\text{N}$ values for all Weddell seals ($n=45$).

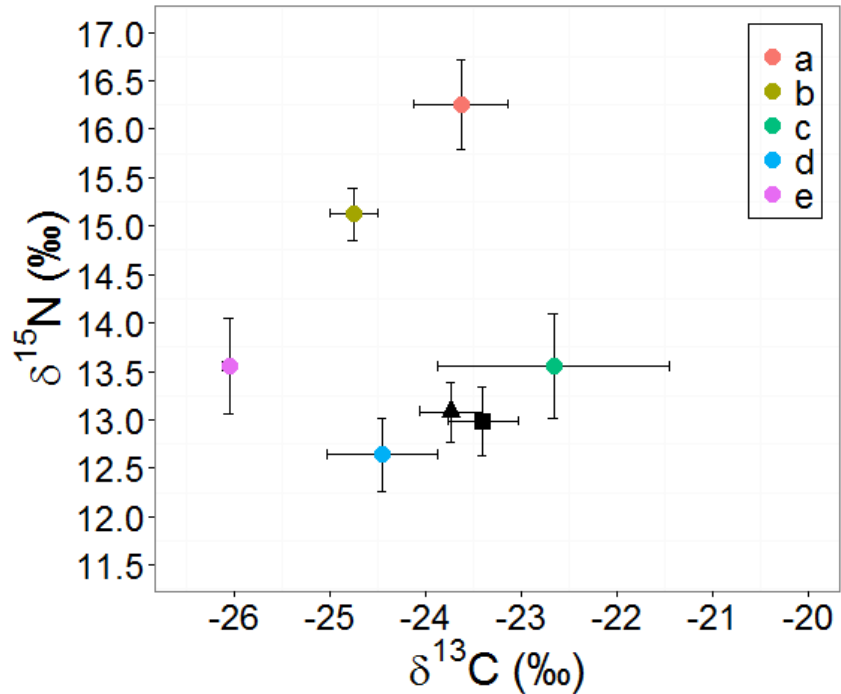


Figure 4.4: Stable isotope values ($\delta^{13}\text{C}$ and $\delta^{15}\text{N}$) for nine fish species or species groups. Points and lines represent means and standard deviations, respectively, of $\delta^{13}\text{C}$ and $\delta^{15}\text{N}$ values. Red blood cell and vibrissae isotopic values for Weddell seals are shown as a black triangle and square, respectively.

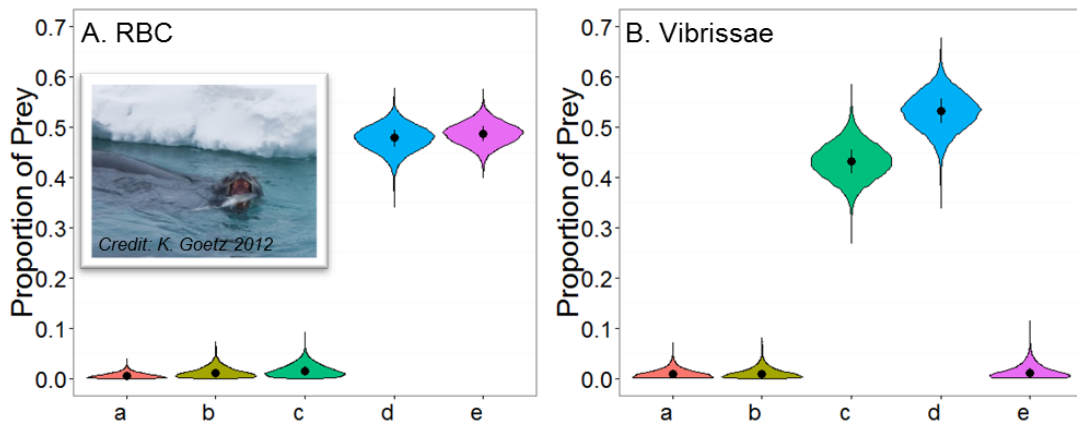


Figure 4.5: The proportional contribution of nine fish species or species groups to the diet of Weddell seals in the western Ross Sea, Antarctica, as determined by (A) red blood cells (RBC) and (B) mean vibrissae $\delta^{13}\text{C}$ and $\delta^{15}\text{N}$ values. Points and lines show median and interquartile range, respectively.

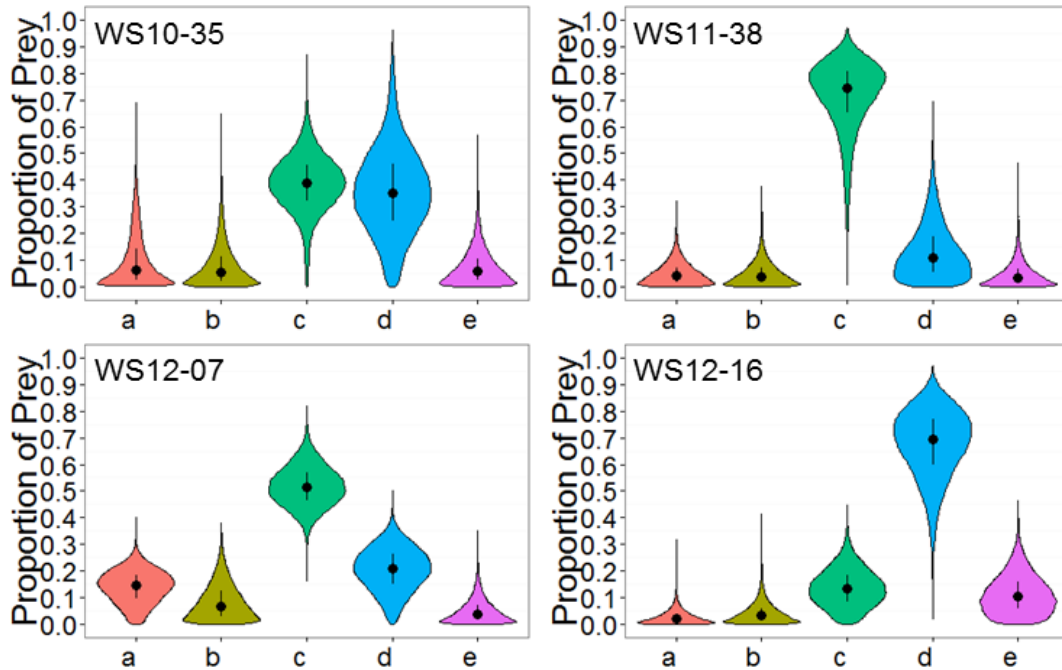


Figure 4.6: The proportional contribution of nine fish species or species groups to the diet of four individual Weddell seals, as determined by vibrissae $\delta^{13}\text{C}$ and $\delta^{15}\text{N}$ values. Points and lines show median and interquartile range, respectively.

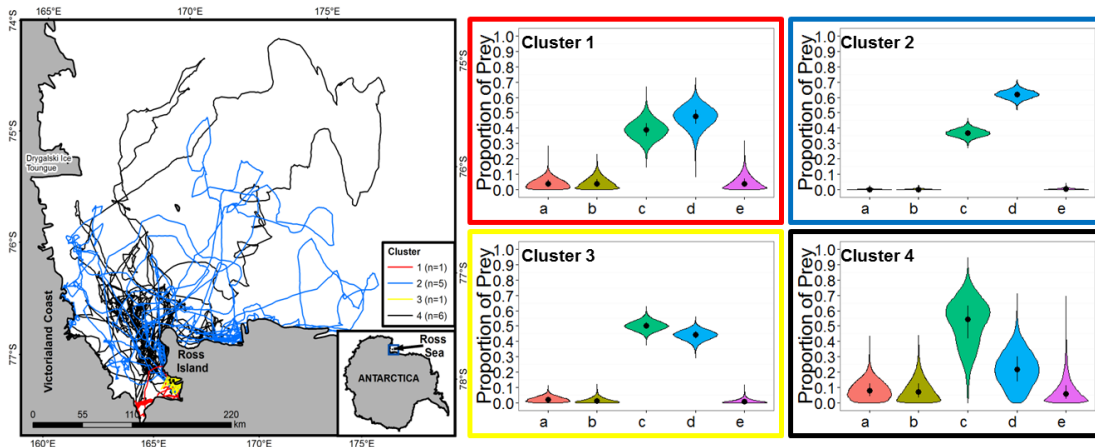


Figure 4.7: Complete tracks (January-October) for 13 Weddell seals in the western Ross Sea and the proportional contribution of nine fish species or species groups to the diet of seals clustered into four different foraging strategies, as determined by vibrissae $\delta^{13}\text{C}$ and $\delta^{15}\text{N}$. Points and lines show median and interquartile range, respectively.

CHAPTER 5

Synthesis

Recommended improvements to CTD-SRDL tags

CTD-SRDL tags deployed on marine megafauna collect oceanographic data in areas and seasons otherwise inaccessible to standard oceanographic equipment. These data can complement oceanographic data collected by other methods as long as there is an awareness of sensor accuracy. Although I found the accuracy of both temperature and conductivity values measured by CTD tag sensors to be less than the manufacturer stated accuracy, it is important to interpret this finding in the context of how the data will be used. For ecologists interested in interpreting environmental parameters at the level of animal behavior, the accuracy of CTD tags, despite being lower than the manufacturer stated accuracy, makes them fully capable of identifying water mass characteristics and seasonal changes in relation to animal movement. However, for oceanographers requiring highly accurate and precise data, especially in areas such as the Ross Sea where there is low variation in temperature and salinity, CTD data either need to be corrected or not included in such analyses. In order to improve the accuracy of oceanographic data collected by CTD tags, we recommend either performing an independent calibration of tag sensors pre-deployment, especially when environmental conditions are expected to be outside the manufacturer's calibration range, or using methods presented in Roquet et al (2014) post-deployment.

Due to the substantial loss in accuracy after deployment, we strongly recommend re-calibrating tags before re-deployment. Similarly, if CTD tags are recovered after a multi-month deployment, we advise replacing the battery (due to the power requirements of the conductivity sensor) and re-calibrating the tag sensors. Finally, researchers should be aware that under *in situ* conditions, the quality of data collected by CTD sensors may be impacted by measurement drift, sensor fouling, and interference of the magnetic field around the conductivity sensor (McCafferty et al., 1999; Hooker and Boyd, 2003; Fedak, Mike, 2004; Boehme et al., 2009; Roquet et al., 2011). In order to improve the quality of data collected by CTD tags, we recommend 1) improving the stability of the conductivity sensor when exposed to external objects, 2) calibrating the temperature sensor to *in-situ* conditions, and 3) decreasing the response time of the tag sensors.

Habitat preference, foraging behavior and diet

Previous work found that female Weddell seals lose up to 40% of their body mass during the four months they are breeding and molting on the fast-ice (Wheatley et al., 2006). However, once pups are weaned, animals are no longer tied to breeding colonies and spend the remaining eight months foraging at sea. Indeed, the overwinter period was recently found to be essential for seals to regain mass and body condition in preparation for the next breeding season (Shero et al 2015). My results on seal behavior provide additional support for these findings: foraging behavior in the winter was higher than any other season. Overall, seasonal habitat preferences and foraging behavior were linked to diverse bathymetric features and strong cyclical

patterns in the sea-ice extent and productivity of the Ross Sea. Sea-ice concentration and extent can change dramatically from year to year, resulting in annual fluctuations in primary productivity which, in turn, drives variability in the composition and abundance of higher trophic level prey that impact the diet and feeding efficiency of top predators. The stable isotope results presented in this dissertation reflected annual variability in the relationship between $\delta^{13}\text{C}$ and $\delta^{15}\text{N}$ values and seal mass, which strongly depended on year. This result suggests that there was a shift in both foraging location and prey items across years, likely related to the dynamic changes in sea-ice concentration and/or extent observed throughout the duration of this study.

While previous studies identified Antarctic silverfish (*P. antarcticum*) as an important Weddell seal prey species (Castellini et al., 1992; Burns et al., 1998), by using stable isotope analyses in conjunction with mixing models, my dissertation provides the first quantitative confirmation of this finding. In addition, the cryopelagic fish *N. ionah* has never before been identified as an important prey species of Weddell seals; however, my work confirmed the importance of *N. ionah* to their diet through both visual observations and isotopic analyses. While the proportional contribution of toothfish to the overall diet of Weddell seals was < 10%, results presented in my dissertation suggest that older animals may be more capable of capturing and consuming these higher trophic level fish than younger seals. Despite its low dietary contribution, my results suggest that the relatively high fat content (% wet mass) and energy density (kJg^{-1} wet mass) of toothfish compared to

other fish species (Lenky et al., 2012) may still be important to seals, especially those recovering from periods of high energetic demands (breeding, pupping, and molting).

My dissertation provides the first information on the *year-round* movements, behavior, and foraging ecology of Weddell seals in the Ross Sea. Indeed, over 20 years have passed since the last attempt was made to understand the overwinter behavior of these animals. Overall, the body of work presented in my dissertation provides new information on the role Weddell seals play within the Ross Sea ecosystem.

Response to anthropogenic disturbance

The Ross Sea is one of the least anthropogenically -impacted places on the planet (Halpern et al., 2008). Despite the pristine nature of this ecosystem, the population of Weddell seals in the Ross Sea is currently facing two main anthropogenic threats: climate change and overfishing. Currently, the climate around Antarctica is rapidly changing and sea-ice is predicted to decrease by 7% per decade along the western Antarctic peninsula while increasing by at least 5% per decade in the Ross Sea (Smith et al., 2007). Changes in oceanography and sea-ice extent have already been documented as a result of climate change (Smith Jr et al., 2012). While there is a great deal of uncertainty on how climate change will impact the Weddell seals in the Ross Sea, evidence suggests that the region is cooling and sea-ice is expanding, in contrast to what is occurring in other regions along the Antarctic continent (Smith et al., 2007). As a result, it is possible that Weddell seals will not be negatively impacted in this region.

Antarctic toothfish have been a target of commercial long-lining in the Southern Ocean since 1996 (Hanchet et al., 2008) and their biomass is expected to halve by 2031 (Pinkerton et al., 2007). Toothfish are consumed by many top predators, yet how industrial fishing might indirectly impact Weddell seals remains unclear. Near the low-latitude Antarctic islands, a decrease in fish-consuming penguins was correlated with over-exploitation and depletion of fish stocks (Ainley and Blight, 2009). While no obvious impacts to Weddell seals have been observed from the current levels of toothfish removal, the continued extraction of this high trophic-level fish may cause top predators such as Weddell seals to switch to consuming less energy-rich species such as silverfish. While there is little doubt that Weddell seals can adjust their diet due to changes in prey availability, the energetic consequences to the population remains unknown. The results of my dissertation emphasize the importance of overwinter foraging to Weddell seals recouping body condition lost during the breeding and molting season. The loss of high-lipid toothfish from the diet of foraging seals may lead to a smaller gain in body mass, impacting a seal's reproductive success the following breeding season and ultimately leading to population-level consequences.

Future directions

My dissertation has provided new information on the movement, habitat preference, foraging behavior, and diet of Weddell seals in the WRS, Antarctica. This body of work has shown that both habitat preference and foraging behavior were largely determined by bathymetry, seasonal ice conditions, and oceanography. While

animals tagged in the WRS preferred to inhabit and forage along the east side of shallow banks, no information exists on the overwinter movement of Weddell seals in the eastern Ross Sea, near the Bay of Whales. Based on my findings, I suspect that seals in the east utilize similar habitats to those in the western Ross Sea, particularly areas along local shallow banks, and that overlap between populations is minimal, even if exploiting similar prey resources.

While I have identified the importance of certain prey items to the diet of Weddell seals, these results reflect the present-state of the Ross Sea ecosystem. Anthropogenic changes may have already altered the trophic assemblages in this region but such changes would not have been detected in this short-term study. However, a study is currently underway to analyze samples collected from Weddell seal pelts found at several historical huts along the Ross Island coast. I plan to work collaboratively with colleagues conducting this study to compare isotopic results from historical samples with those from samples collected for my dissertation to provide insight into ecosystem changes that may have occurred over the last century. Finally, I plan to compare my isotope results to fatty acids and energetics data collected alongside my dissertation to add additional insight into the diet of Weddell seals in the western Ross Sea.

Appendix

A.1: Median and range percent contribution of prey species and prey groups to the diet of individual Weddell seals from the Ross Sea, Antarctic, as determined from stable isotopes ($\delta^{13}\text{C}$ and $\delta^{15}\text{N}$). Animals that were sampled twice are denoted by (a) or (b) following the individual ID. Prey species are defined as follows: *a: Dissostichus mawsoni*; *b: T.hansoni*; *c: Pagothernia borchgrevinki*, *Trematomus Nicolai*, *T. pennellii*, and *T. bernacchii*; *d: Pleurogramma antarcticum* and *T. newnesi*; *e: Neopagetopsis ionah*

ID	a	b	c	d	e
WS10-01a	1.2 (0.0 - 23.2)	1.3 (0.0 - 20.9)	42.3 (0.3 - 81.5)	52.0 (7.8 - 95.8)	1.7 (0.0 - 21.2)
WS10-01b	1.6 (0.0 - 47.4)	1.8 (0.0 - 33.4)	31.6 (0.0 - 65.9)	60.0 (3.8 - 98.0)	2.7 (0.0 - 34.2)
WS10-02a	7.3 (0.0 - 36.5)	5.1 (0.0 - 33.5)	54.8 (25.5 - 88.2)	26.5 (0.0 - 57.1)	3.6 (0.0 - 33.9)
WS10-02b	8.2 (0.0 - 49.2)	7.1 (0.0 - 45.8)	54.7 (0.2 - 92.8)	21.3 (0.0 - 67.0)	5.9 (0.0 - 55.1)
WS10-03a	1.9 (0.0 - 37.3)	2.1 (0.0 - 30.2)	43.6 (0.0 - 78.7)	47.5 (0.9 - 92.5)	2.6 (0.0 - 28.6)
WS10-03b	6.1 (0.0 - 60.0)	5.5 (0.0 - 54.2)	38.8 (0.0 - 82.4)	35.9 (0.0 - 94.5)	5.7 (0.0 - 59.6)
WS10-04	3.6 (0.0 - 58.1)	3.3 (0.0 - 46.9)	42.8 (2.4 - 79.0)	42.6 (0.0 - 93.2)	3.4 (0.0 - 35.9)
WS10-05a	1.1 (0.0 - 30.4)	1.2 (0.0 - 18.8)	41.1 (0.2 - 70.1)	53.5 (13.5 - 94.3)	1.8 (0.0 - 20.6)
WS10-05b	1.2 (0.0 - 16.0)	1.4 (0.0 - 24.8)	29.7 (4.4 - 59.7)	64.5 (14.0 - 91.0)	2.1 (0.0 - 28.8)
WS10-06	1.3 (0.0 - 13.5)	1.4 (0.0 - 15.9)	36.0 (12.2 - 58.1)	58.1 (30.4 - 79.7)	1.9 (0.0 - 18.4)
WS10-07a	0.8 (0.0 - 14.2)	0.9 (0.0 - 13.4)	34.9 (3.9 - 64.6)	61.4 (32.0 - 88.9)	1.3 (0.0 - 17.1)
WS10-07b	1.2 (0.0 - 21.4)	1.4 (0.0 - 27.6)	30.5 (0.8 - 57.0)	63.3 (24.5 - 93.5)	2.0 (0.0 - 25.1)
WS10-19	4.1 (0.0 - 53.1)	3.9 (0.0 - 48.1)	42.3 (1.7 - 84.0)	40.8 (0.1 - 91.3)	4.3 (0.0 - 39.0)
WS10-20	0.9 (0.0 - 18.9)	1.0 (0.0 - 18.1)	36.6 (3.0 - 63.6)	59.0 (24.0 - 93.2)	1.4 (0.0 - 21.6)
WS10-21a	1.3 (0.0 - 16.3)	1.6 (0.0 - 22.6)	50.4 (0.0 - 96.3)	43.2 (0.0 - 92.9)	2.4 (0.0 - 30.5)
WS10-21b	1.7 (0.0 - 32.3)	2.0 (0.0 - 25.4)	45.9 (0.0 - 98.6)	45.8 (0.0 - 96.6)	3.2 (0.0 - 46.5)

ID	a	b	c	d	e
WS10-22	2.3 (0.0 - 31.1)	2.4 (0.0 - 33.7)	42.1 (10.0 - 72.6)	48.1 (2.9 - 79.2)	3.0 (0.0 - 28.7)
WS11-03a	1.1 (0.0 - 24.8)	1.3 (0.0 - 21.3)	38.9 (9.0 - 63.8)	55.7 (19.1 - 84.4)	1.8 (0.0 - 18.7)
WS11-03b	3.7 (0.0 - 39.8)	3.7 (0.0 - 36.9)	38.0 (3.0 - 69.5)	47.9 (2.0 - 79.1)	4.1 (0.0 - 40.0)
WS11-04a	2.3 (0.0 - 21.7)	2.5 (0.0 - 26.0)	47.2 (7.9 - 82.2)	42.9 (0.5 - 78.4)	3.1 (0.0 - 33.9)
WS11-04b	4.2 (0.0 - 32.1)	3.7 (0.0 - 27.9)	42.0 (14.3 - 70.5)	44.2 (2.6 - 74.6)	3.4 (0.0 - 29.1)
WS11-05	2.5 (0.0 - 57.1)	2.7 (0.0 - 28.0)	41.4 (9.1 - 74.2)	47.8 (7.5 - 80.1)	3.2 (0.0 - 33.2)
WS11-06	13.4 (0.0 - 46.5)	10.5 (0.0 - 47.1)	32.1 (3.2 - 69.0)	34.4 (0.1 - 70.6)	6.6 (0.0 - 42.8)
WS11-08a	7.7 (0.0 - 45.9)	7.2 (0.0 - 44.1)	47.9 (0.2 - 94.5)	27.4 (0.0 - 68.5)	6.3 (0.0 - 61.8)
WS11-08b	1.1 (0.0 - 18.2)	1.2 (0.0 - 23.4)	58.0 (0.5 - 91.9)	37.0 (0.3 - 94.8)	1.7 (0.0 - 19.7)
WS11-09	2.6 (0.0 - 42.8)	3.0 (0.0 - 43.0)	32.1 (0.5 - 63.9)	55.3 (2.1 - 94.9)	4.2 (0.0 - 39.7)
WS11-12a	1.2 (0.0 - 42.4)	1.4 (0.0 - 28.7)	26.7 (0.1 - 57.5)	66.9 (9.7 - 97.9)	2.2 (0.0 - 33.7)
WS11-12b	1.0 (0.0 - 14.1)	1.2 (0.0 - 14.7)	33.1 (1.9 - 54.7)	62.0 (32.3 - 89.4)	1.7 (0.0 - 23.3)
WS11-17a	3.9 (0.0 - 42.1)	4.3 (0.0 - 39.7)	37.9 (0.8 - 72.8)	45.5 (0.3 - 82.6)	5.4 (0.0 - 43.4)
WS11-17b	1.3 (0.0 - 16.4)	1.5 (0.0 - 16.7)	37.3 (12.6 - 60.7)	56.5 (25.3 - 80.2)	2.0 (0.0 - 18.7)
WS11-18	3.6 (0.0 - 28.6)	3.9 (0.0 - 26.5)	44.0 (3.2 - 79.6)	42.2 (0.4 - 73.9)	4.1 (0.0 - 39.4)
WS11-19	1.2 (0.0 - 21.8)	1.4 (0.0 - 19.6)	39.6 (3.0 - 66.1)	54.5 (11.7 - 91.4)	1.9 (0.0 - 23.4)
WS11-21a	1.0 (0.0 - 18.8)	1.2 (0.0 - 21.8)	24.1 (0.0 - 47.2)	70.3 (26.6 - 98.6)	2.0 (0.0 - 25.6)
WS11-21b	1.8 (0.0 - 17.4)	2.3 (0.0 - 21.6)	25.8 (0.7 - 48.5)	65.0 (29.3 - 91.2)	3.7 (0.0 - 25.6)
WS11-37	2.1 (0.0 - 45.1)	2.3 (0.0 - 33.5)	42.7 (1.2 - 79.8)	47.6 (0.5 - 88.1)	3.0 (0.0 - 31.8)
WS11-38	4.2 (0.0 - 33.9)	3.9 (0.0 - 50.9)	73.9 (0.1 - 97.6)	11.3 (0.0 - 69.3)	3.8 (0.0 - 48.9)
WS11-39	1.1 (0.0 - 20.4)	1.3 (0.0 - 21.3)	31.7 (5.5 - 59.1)	62.8 (13.8 - 89.1)	1.9 (0.0 - 28.7)
WS11-40	1.9 (0.0 - 16.9)	2.2 (0.0 - 20.0)	32.4 (2.1 - 67.1)	58.6 (20.1 - 86.1)	3.3 (0.0 - 27.2)
WS11-41	1.3 (0.0 - 13.6)	1.4 (0.0 - 18.5)	47.8 (26.0 - 70.5)	46.4 (17.8 - 69.4)	1.8 (0.0 - 20.9)

ID	a	b	c	d	e
WS12-01a	1.3 (0.0 - 34.6)	1.5 (0.0 - 34.9)	31.5 (0.1 - 64.1)	61.9 (9.8 - 94.3)	2.2 (0.0 - 23.3)
WS12-01b	1.0 (0.0 - 19.7)	1.2 (0.0 - 17.3)	34.1 (5.4 - 68.5)	60.8 (13.7 - 89.8)	1.7 (0.0 - 19.4)
WS12-02a	1.4 (0.0 - 22.9)	1.7 (0.0 - 22.0)	26.7 (0.1 - 52.6)	66.2 (28.6 - 93.3)	2.7 (0.0 - 26.9)
WS12-02b	1.4 (0.0 - 13.8)	1.6 (0.0 - 14.0)	35.2 (11.8 - 59.1)	58.1 (27.7 - 78.0)	2.3 (0.0 - 21.3)
WS12-04a	0.8 (0.0 - 10.9)	1.0 (0.0 - 11.5)	41.0 (8.4 - 69.4)	54.9 (23.7 - 84.2)	1.4 (0.0 - 21.1)
WS12-04b	4.0 (0.0 - 22.2)	3.9 (0.0 - 27.6)	38.7 (12.1 - 67.6)	47.6 (9.8 - 74.5)	3.9 (0.0 - 32.4)
WS12-05	6.5 (0.0 - 49.7)	5.3 (0.0 - 38.2)	53.5 (3.3 - 87.8)	27.6 (0.1 - 62.6)	4.1 (0.0 - 37.5)
WS12-06	2.2 (0.0 - 29.9)	2.3 (0.0 - 22.0)	50.9 (11.3 - 88.4)	39.8 (2.2 - 77.2)	2.9 (0.0 - 26.3)
WS12-07	14.5 (0.0 - 37.7)	6.9 (0.0 - 38.1)	51.5 (19.0 - 82.3)	21.1 (0.0 - 52.3)	3.8 (0.0 - 29.0)
WS12-08	2.0 (0.0 - 19.4)	2.2 (0.0 - 24.5)	64.6 (0.2 - 96.1)	26.9 (0.0 - 88.6)	2.8 (0.0 - 39.2)
WS12-09a	3.9 (0.0 - 28.6)	3.9 (0.0 - 30.3)	55.7 (4.4 - 90.0)	30.0 (0.1 - 68.1)	4.0 (0.0 - 31.6)
WS12-09b	5.9 (0.0 - 26.4)	3.6 (0.0 - 23.6)	62.3 (39.7 - 88.3)	23.8 (0.1 - 45.3)	2.4 (0.0 - 23.3)
WS12-10	1.9 (0.0 - 16.6)	2.0 (0.0 - 17.8)	40.2 (18.2 - 64.6)	51.7 (20.0 - 72.6)	2.5 (0.0 - 25.2)
WS12-11	1.2 (0.0 - 14.0)	1.4 (0.0 - 17.2)	49.3 (15.0 - 77.4)	45.0 (12.3 - 75.3)	1.8 (0.0 - 24.3)
WS12-12a	0.9 (0.0 - 11.7)	1.0 (0.0 - 20.0)	38.4 (5.8 - 62.8)	57.5 (22.7 - 89.6)	1.4 (0.0 - 17.7)
WS12-12b	1.6 (0.0 - 20.9)	1.9 (0.0 - 19.5)	36.3 (7.6 - 65.4)	56.1 (22.7 - 84.3)	2.5 (0.0 - 25.0)
WS12-13a	8.8 (0.0 - 44.7)	8.4 (0.0 - 44.8)	30.7 (2.6 - 62.4)	41.6 (0.8 - 81.0)	7.3 (0.0 - 42.2)
WS12-13b	7.6 (0.0 - 34.7)	6.5 (0.0 - 38.1)	57.0 (12.4 - 90.6)	21.4 (0.0 - 61.7)	4.9 (0.0 - 42.0)
WS12-14	6.0 (0.0 - 38.7)	4.6 (0.0 - 36.0)	47.0 (19.7 - 84.0)	35.6 (0.2 - 65.4)	3.6 (0.0 - 34.1)
WS12-15	2.0 (0.0 - 27.0)	2.2 (0.0 - 25.9)	35.0 (3.8 - 63.3)	55.9 (17.4 - 86.8)	2.9 (0.0 - 24.9)
WS12-16	2.1 (0.0 - 24.1)	3.3 (0.0 - 43.3)	13.5 (0.0 - 46.6)	69.1 (6.5 - 98.1)	10.6 (0.0 - 45.3)
WS12-17a	1.3 (0.0 - 17.0)	1.6 (0.0 - 24.9)	33.2 (4.0 - 62.5)	60.3 (24.2 - 87.2)	2.3 (0.0 - 23.3)
WS12-17b	2.5 (0.0 - 13.5)	2.7 (0.0 - 15.8)	36.2 (17.0 - 56.8)	54.2 (28.6 - 75.0)	3.0 (0.0 - 21.3)

ID	a	b	c	d	e
WS12-19a	1.1 (0.0 - 14.4)	1.2 (0.0 - 14.0)	35.7 (14.4 - 59.0)	59.0 (30.5 - 82.3)	1.7 (0.0 - 18.7)
WS12-19b	3.1 (0.0 - 18.7)	3.1 (0.0 - 21.2)	45.1 (21.0 - 70.1)	43.9 (13.3 - 66.7)	3.1 (0.0 - 26.4)
WS12-20	1.2 (0.0 - 12.0)	1.5 (0.0 - 14.8)	21.6 (0.0 - 44.1)	71.5 (38.1 - 96.3)	2.9 (0.0 - 24.0)

Bibliography

- Aarts, G., MacKenzie, M., McConnell, B., Fedak, M. and Matthiopoulos, J.** (2008). Estimating space-use and habitat preference from wildlife telemetry data. *Eco geography* **31**, 140-160.
- Ainley, D.** (1985). Biomass of birds and mammals in the Ross Sea. In *Antarctic nutrient cycles and food webs*, pp. 498-515: Springer.
- Ainley, D. G. and Siniff, D. B.** (2009). The importance of Antarctic toothfish as prey of Weddell seals in the Ross Sea. *Antarctic Science* **21**, 317-327.
- Ainley, D. G. and Blight, L. K.** (2009). Ecological repercussions of historical fish extraction from the Southern Ocean. *Fish and Fisheries* **10**, 13-38.
- Amante, C. and Eakins, B.** (2009). ETOPO1 1 Arc-Minute Global Relief Model: Procedures, Data Sources and Analysis, pp. 19: NOAA Technical Memorandum NESDIS NGDC-24.
- Arrigo, K. R. and Thomas, D. N.** (2004). Large scale importance of sea ice biology in the Southern Ocean. *Antarctic Science* **16**, 471-486.
- Arrigo, K. R., Worthen, D., Schnell, A. and Lizotte, M. P.** (1998). Primary production in Southern Ocean waters. *Journal of Geophysical Research-Oceans* **103**, 15587-15600.
- Atkinson, B. and Mahoney, D.** (2004). S-Plus ROC functions, vol. 2009. Rochester, MN: Mayo Foundation for Medical Education and Research.
- Bailleul, F., Charrassin, J. B., Monestiez, P., Roquet, F., Biuw, M. and Guinet, C.** (2007). Successful foraging zones of southern elephant seals from the Kerguelen Islands in relation to oceanographic conditions. *Philos. Trans. R. Soc. B-Biol. Sci.* **362**, 2169-2181.

Beltran, R. S., Sadou, M. C., Condit, R., Peterson, S. H., Reichmuth, C. and Costa, D. P. (2015). Fine-scale whisker growth measurements can reveal temporal foraging patterns from stable isotope signatures. *Mar Ecol Prog Ser* **523**, 243-253.

Beyer, H. (2004). Hawth's Analysis Tools for ArcGIS. Available at <http://www.spatial ecology.com/htools>.

Biuw, M., Boehme, L., Guinet, C., Hindell, M., Costa, D., Charrassin, J. B., Roquet, F., Bailleul, F., Meredith, M., Thorpe, S. et al. (2007). Variations in behavior and condition of a Southern Ocean top predator in relation to in situ oceanographic conditions. *Proceedings of the National Academy of Sciences of the United States of America* **104**, 13705-13710.

Block, B. A., Costa, D. P., Boehlert, G. W. and Kochevar, R. E. (2002). Revealing pelagic habitat use: the tagging of Pacific pelagics program. *Oceanologica Acta* **25**, 255-266.

Bluhm, B. A., Coyle, K. O., Konar, B. and Highsmith, R. (2007). High gray whale relative abundances associated with an oceanographic front in the south-central Chukchi Sea. *Deep-Sea Research Part II-Topical Studies in Oceanography* **54**, 2919-2933.

Bodey, T., Bearhop, S. and McDonald, R. (2011). Invasions and stable isotope analysis—informing ecology and management. In *Island invasives: eradication and management. Proceedings of the international conference on island invasives*, eds. C. Veitch M. Clout and D. Towns), pp. 148-151. Gland, Switzerland: IUCN and Auckland, New Zealand.

Boehme, L., Meredith, M. P., Thorpe, S. E., Biuw, M. and Fedak, M. (2008). Antarctic Circumpolar Current frontal system in the South Atlantic: Monitoring using merged Argo and animal-borne sensor data. *Journal of Geophysical Research-Oceans* **113**.

Boehme, L., Lovell, P., Biuw, M., Roquet, F., Nicholson, J., Thorpe, S. E., Meredith, M. P. and Fedak, M. (2009). Technical Note: Animal-borne CTD-Satellite Relay Data Loggers for real-time oceanographic data collection. *Ocean Science* **5**, 685-695.

- Bograd, S. J., Block, B. A., Costa, D. P. and Godley, B. J.** (2010). Biologging technologies: new tools for conservation. Introduction. *Endangered Species Research* **10**, 1-7.
- Bornemann, H., Mohr, E., Plötz, J. and Krause, G.** (1998). The tide as zeitgeber for Weddell seals. *Polar Biology* **20**, 396-403.
- Bowen, W. and Iverson, S.** (1998). Estimation of total body water in pinnipeds using hydrogen-isotope dilution. *Physiological Zoology* **71**, 329-332.
- Burns, J. M. and Castellini, M. A.** (1998). Dive data from satellite tags and time-depth recorders: A comparison in Weddell seal pups. *Marine Mammal Science* **14**, 750-764.
- Burns, J. M., Castellini, M. A. and Schreer, J. F.** (1997). Physiological effects on dive patterns and foraging strategies in yearling Weddell seals (*Leptonychotes weddellii*). *Canadian Journal of Zoology* **75**, 1796-1810.
- Burns, J. M., Castellini, M. A. and Testa, J. W.** (1999). Movements and diving behavior of weaned Weddell seal (*Leptonychotes weddellii*) pups. *Polar Biology* **21**, 23-36.
- Burns, J. M., Trumble, S. J., Castellini, M. A. and Testa, J. W.** (1998). The diet of Weddell seals in McMurdo Sound, Antarctica as determined from scat collections and stable isotope analysis. *Polar Biology* **19**, 272-282.
- Cameron, M. F., Siniff, D. B., Proffitt, K. M. and Garrott, R. A.** (2007). Site fidelity of Weddell seals: the effects of sex and age. *Antarctic Science* **19**, 149-155.
- Campagna, C., Rivas, A. L. and Marin, R.** (2000). Temperature and depth profiles recorded during dives of elephant seals reflect distinct ocean environments.
- Casaux, R., Baroni, A. and Carlini, A.** (1997). The diet of the Weddell seal *Leptonychotes weddellii* at Harmony Point, South Shetland Islands. *Polar Biology* **18**, 371-375.

- Castellini, M. A., Davis, R. W. and Kooyman, G. L.** (1992). Annual cycles of diving behavior and ecology of the Weddell seal.
- Chapman, E. W., Ribic, C. A. and Fraser, W. R.** (2004). The distribution of seabirds and pinnipeds in Marguerite Bay and their relationship to physical features during austral winter 2001. *Deep-Sea Research Part II-Topical Studies in Oceanography* **51**, 2261-2278.
- Charrassin, J. B. and Bost, C. A.** (2001). Utilisation of the oceanic habitat by king penguins over the annual cycle. *Marine Ecology Progress Series* **221**, 285-297.
- Charrassin, J. B., Hindell, M., Rintoul, S. R., Roquet, F., Sokolov, S., Biuw, M., Costa, D., Boehme, L., Lovell, P., Coleman, R. et al.** (2008). Southern Ocean frontal structure and sea-ice formation rates revealed by elephant seals. *Proceedings of the National Academy of Sciences of the United States of America* **105**, 11634-11639.
- Clarke, A., Doherty, N., DeVries, A. L. and Eastman, J. T.** (1984). Lipid content and composition of three species of Antarctic fish in relation to buoyancy. *Polar Biology* **3**, 77-83.
- Costa, D. P.** (1993). The secret life of marine mammals: Novel tools for studying their behavior and biology at sea. In *Oceanography*, vol. 6, pp. 120-128.
- Costa, D. P. and Crocker, D. E.** (1996). Marine Mammals of the Southern Ocean. In *Foundations for Ecological Research West of the Antarctic Peninsula*, pp. 287-301: American Geophysical Union.
- Costa, D. P., Breed, G. A. and Robinson, P. W.** (2012). New Insights into Pelagic Migrations: Implications for Ecology and Conservation. *Annual Review of Ecology, Evolution, and Systematics* **43**, 73-96.
- Costa, D. P., Klinck, J. M., Hofmann, E. E., Dinniman, M. S. and Burns, J. M.** (2008). Upper ocean variability in west Antarctic Peninsula continental shelf waters as measured using instrumented seals. *Deep-Sea Research Part II-Topical Studies in Oceanography* **55**, 323-337.

- Costa, D. P., Huckstadt, L. A., Crocker, D. E., McDonald, B. I., Goebel, M. E. and Fedak, M. A.** (2010). Approaches to studying climatic change and its role on the habitat selection of Antarctic pinnipeds. *Integrative and Comparative Biology*, icq054.
- Crocker, D. E., Costa, D. P., Le Boeuf, B. J., Webb, P. M. and Houser, D. S.** (2006). Impact of El Nino on the foraging behavior of female northern elephant seals. *Marine Ecology Progress Series* **309**, 1-10.
- Davis, R. W., Hagey, W. and Horning, M.** (2004). Monitoring the behavior and multi-dimensional movements of Weddell seals using an animal-borne video and data recorder. *Memoirs of the National Institute of Polar Research* **58**, 150-156.
- Davis, R. W., Fuiman, L. A., Madden, K. M. and Williams, T. M.** (2013). Classification and behavior of free-ranging Weddell seal dives based on three-dimensional movements and video-recorded observations. *Deep-Sea Research Part II-Topical Studies in Oceanography* **88-89**, 65-77.
- Davis, R. W., Fuiman, L. A., Williams, T. M., Collier, S. O., Hagey, W. P., Kanatous, S. B., Kohin, S. and Horning, M.** (1999). Hunting behavior of a marine mammal beneath the Antarctic fast ice. *Science* **283**, 993-996.
- Dearborn, J. H.** (1965). Food of Weddell seals at McMurdo Sound, Antarctica. *Journal of Mammalogy* **46**, 37-43.
- DeNiro, M. J. and Epstein, S.** (1978). Influence of diet on the distribution of carbon isotopes in animals. *Geochimica et cosmochimica acta* **42**, 495-506.
- DeNiro, M. J. and Epstein, S.** (1981). Influence of diet on the distribution of nitrogen isotopes in animals. *Geochimica et cosmochimica acta* **45**, 341-351.
- DeVries, A. L. and Wohlschlag, D. E.** (1964). Diving Depths of the Weddell Seal. *Science* **145**, 292.

- Dewitt, H.** (1970). The character of the midwater fish fauna of the Ross Sea, Antarctica. In *Antarctic ecology*, vol. 1 (ed. M. Holdgate), pp. 305-314. London: Academic Press.
- Diggle, P. and Ribeiro Jr, P.** (2007). Model based geostatistics. New York: Springer.
- Dinniman, M. S., Klinck, J. M. and Smith Jr, W. O.** (2003). Cross-shelf exchange in a model of the Ross Sea circulation and biogeochemistry. *Deep Sea Research Part II: Topical Studies in Oceanography* **50**, 3103-3120.
- Dinniman, M. S., Klinck, J. M. and Smith, W. O.** (2007). Influence of sea ice cover and icebergs on circulation and water mass formation in a numerical circulation model of the Ross Sea, Antarctica. *Journal of Geophysical Research-Oceans* **112**.
- Durussel, C., Feudel, U. and Morre, S.** (2009). Characteristics of Humpback Whale Habitat in the Scotia Sea and the Antarctic Peninsula.
- Eastman, J.** (1985). *Pleuragramma antarcticum* (Pisces, Nototheniidae) as food for other fishes in McMurdo Sound, Antarctica. *Polar Biology* **4**, 155-160.
- Eastman, J. T. and DeVries, A. L.** (1982). Buoyancy studies of notothenioid fishes in McMurdo Sound, Antarctica. *Copeia* **1982**, 385-393.
- Eastman, J. T. and DeVries, A. L.** (1985). Adaptations for cryopelagic life in the antarctic notothenioid fish *Pagothenia borchgrevinki*. *Polar Biology* **4**, 45-52.
- Eastman, J. T. and Hubold, G.** (1999). The fish fauna of the Ross Sea, Antarctica. *Antarctic Science* **11**, 293-304.
- Etnoyer, P., Canny, D., Mate, B. R., Morgan, L. E., Ortega-Ortiz, J. G. and Nichols, W. J.** (2006). Sea-surface temperature gradients across blue whale and sea turtle foraging trajectories off the Baja California Peninsula, Mexico. *Deep-Sea Research Part II-Topical Studies in Oceanography* **53**, 340-358.

- Fauchald, P. and Tveraa, T.** (2003). Using first-passage time in the analysis of area-restricted search and habitat selection. *Ecology* **84**, 282-288.
- Fedak, M.** (2004). Marine animals as platforms for oceanographic sampling: a "win/win" situation for biology and operational oceanography. *Memoirs of National Institute of Polar Research. Special issue* **58**, 133-147.
- Fedak, M.** (2004). Marine animals as platforms for oceanographic sampling: a "win/win" situation for biology and operational oceanography. *Mem Natl Inst Polar Res* **58**, 133-147.
- Fofonoff, N. P.** (1983). Algorithms for Computation of Fundamental Properties of Seawater. Endorsed by Unesco [microform] : SCOR/ICES/IAPSO Joint Panel on Oceanographic Tables and Standards and SCOR Working Group 51. Unesco Technical Papers in Marine Science, No. 44/ N. P. Fofonoff and R. C. Millard, Jr. [Washington, D.C.]: Distributed by ERIC Clearinghouse.
- France, R.** (1995). Carbon-13 enrichment in benthic compared to planktonic algae: foodweb implications. *Marine Ecology Progress Series* **124**, 307-312.
- Fuiman, L., Davis, R. and Williams, T.** (2002). Behavior of midwater fishes under the Antarctic ice: observations by a predator. *Marine Biology* **140**, 815-822.
- Goetz, K. T., Rugh, D. J., Read, A. J. and Hobbs, R. C.** (2007). Habitat use in a marine ecosystem: beluga whales *Delphinapterus leucas* in Cook Inlet, Alaska. *Marine Ecology Progress Series* **330**, 247-256.
- Goetz, K. T., Rugh, D. J., Vate Brattstrom, L. and Mocklin, J. A.** (2011). Aerial surveys of bowhead whales near Barrow in late summer 2010. In: Bowhead Whale Feeding Ecology Study (BOWFEST) annual report for 2010. Seattle, WA: National Marine Mammal Lab, NOAA Fisheries Service.
- González-Solís, J., Smyrli, M., Militão, T., Gremillet, D., Tveraa, T., Phillips, R. A. and Boulinier, T.** (2011). Combining stable isotope analyses and geolocation to reveal kittiwake migration. *Marine Ecology Progress Series* **435**, 251-261.

- Greaves, D. K., Hammill, M. O., Eddington, J. D., Pettipas, D. and Schreer, J. F.** (2004). Growth rate and shedding of vibrissae in the gray seal, *Halichoerus grypus*: a cautionary note for stable isotope diet analysis. *Marine Mammal Science* **20**, 296-304.
- Grist, J. P., Josey, S. A., Boehme, L., Meredith, M. P., Davidson, F. J. M., Stenson, G. B. and Hammill, M. O.** (2011). Temperature signature of high latitude Atlantic boundary currents revealed by marine mammal-borne sensor and Argo data. *Geophysical Research Letters* **38**.
- Guisan, A. and Zimmermann, N. E.** (2000). Predictive habitat distribution models in ecology. *Ecological Modelling* **135**, 147-186.
- Hadley, G., Rotella, J. and Garrott, R.** (2007). Influence of maternal characteristics and oceanographic conditions on survival and recruitment probabilities of Weddell seals. *Oikos* **116**, 601-613.
- Hall-Aspland, S. A., Rogers, T. L. and Canfield, R. B.** (2005). Stable carbon and nitrogen isotope analysis reveals seasonal variation in the diet of leopard seals. *Marine Ecology Progress Series* **305**, 249-259.
- Halpern, B. S., Walbridge, S., Selkoe, K. A., Kappel, C. V., Micheli, F., D'Agrosa, C., Bruno, J. F., Casey, K. S., Ebert, C., Fox, H. E. et al.** (2008). A Global Map of Human Impact on Marine Ecosystems. *Science* **319**, 948-952.
- Hamazaki, T.** (2002). Spatiotemporal prediction models of cetacean habitats in the mid-western north Atlantic Ocean (from Cape Hatteras, North Carolina, U.S.A. to Nova Scotia, Canada) *Marine Mammal Science* **18**, 920-939.
- Hammill, M., Lesage, V. and Carter, P.** (2005). What do harp seals eat? Comparing diet composition from different compartments of the digestive tract with diets estimated from stable-isotope ratios. *Canadian Journal of Zoology* **83**, 1365-1372.
- Hanchet, S., Rickard, G., Fenaughty, J., Dunn, A. and Williams, M.** (2008). A hypothetical life cycle for Antarctic toothfish (*Disostichus mawsoni*) in the Ross Sea region. *CCAMLR Science* **15**, 35-53.

- Harcourt, R. G., Hindell, M. A., Bell, D. G. and Waas, J. R.** (2000). Three-dimensional dive profiles of free-ranging Weddell seals. *Polar Biology* **23**, 479-487.
- Heerah, K., Andrews-Goff, V., Williams, G., Sultan, E., Hindell, M., Patterson, T. and Charrassin, J.-B.** (2013). Ecology of Weddell seals during winter: Influence of environmental parameters on their foraging behaviour. *Deep Sea Research Part II: Topical Studies in Oceanography* **88-89**, 23-33.
- Hempel, G.** (1985). Antarctic marine food webs. In *Antarctic nutrient cycles and food webs*, eds. R. Siegfried P. Condy and R. Laws), pp. 266-270: Springer.
- Hilderbrand, G. V., Farley, S. D., Robbins, C. T., Hanley, T. A., Titus, K. and Servheen, C.** (1996). Use of stable isotopes to determine diets of living and extinct bears. *Canadian Journal of Zoology* **74**, 2080-2088.
- Hindell, M., Harcourt, R., Waas, J. and Thompson, D.** (2002). Fine-scale three-dimensional spatial use by diving, lactating female Weddell seals *Leptonychotes weddellii*. *Marine Ecology Progress Series* **242**, 275-284.
- Hindle, A. G. and Horning, M.** (2010). Energetics of breath-hold hunting: Modeling the effects of aging on foraging success in the Weddell seal. *Journal of Theoretical Biology* **264**, 673-682.
- Hindle, A. G., Horning, M., Mellish, J.-A. E. and Lawler, J. M.** (2009). Diving into old age: muscular senescence in a large-bodied, long-lived mammal, the Weddell seal (*Leptonychotes weddellii*). *Journal of Experimental Biology* **212**, 790-796.
- Hirons, A. C., Schell, D. M. and St. Aubin, D. J.** (2001). Growth rates of vibrissae of harbor seals (*Phoca vitulina*) and Steller sea lions (*Eumetopias jubatus*). *Canadian Journal of Zoology* **79**, 1053-1061.
- Hobson, K. A., Schell, D. M., Renouf, D. and Noseworthy, E.** (1996). Stable carbon and nitrogen isotopic fractionation between diet and tissues of captive seals: Implications for dietary reconstructions involving marine mammals. *Canadian Journal of Fisheries and Aquatic Sciences* **53**, 528-533.

- Hooker, S. K. and Boyd, I. L.** (2003). Salinity sensors on seals: use of marine predators to carry CTD data loggers. *Deep-Sea Research Part I-Oceanographic Research Papers* **50**, 927-939.
- Hooker, S. K., Whitehead, H. and Shannon, G.** (1999). Marine Protected Area Design and the Spatial and Temporal Distribution of Cetaceans in a Submarine Canyon. *Conservation Biology* **13**, 592-602.
- Hubold, G.** (1985). The early life-history of the high-Antarctic silverfish, *Pleuragramma antarcticum*. In *Antarctic Nutrient Cycles and Food Webs*, eds. W. Siegfried P. Condy and R. Laws), pp. 445-451: Springer Berlin Heidelberg.
- Husson, F., Josse, J., Le, S. and Mazet, J.** (2013). FactoMineR: Multivariate exploratory data analysis and data mining with R. R package version 1.25. <http://CRAN.R-project.org/package=FactoMineR>.
- Hyrenbach, K. D., Veit, R. R., Weimerskirch, H., Metzl, N. and Hunt, G. L.** (2007). Community structure across a large-scale ocean productivity gradient: Marine bird assemblages of the Southern Indian Ocean. *Deep-Sea Research Part I-Oceanographic Research Papers* **54**, 1129-1145.
- Jacobs, S. S. and Comiso, J. C.** (1989). Sea ice and oceanic processes on the Ross Sea continental shelf. *Journal of Geophysical Research: Oceans* **94**, 18195-18211.
- Jakob, E. M., Marshall, S. D. and Uetz, G. W.** (1996). Estimating fitness: A comparison of body condition indices. *Oikos* **77**, 61-67.
- Jo, H.-S., Yeon, I., Lim, C., Hanchet, S., D-W, L. and Kang, C.-K.** (2013). Fatty acid and stable isotope analyses to infer diet of Antarctic toothfish caught in the southern Ross Sea. *CCAMLR Science* **20**, 21-36.
- Joiris, C. R.** (1991). Spring distribution and ecological role of seabirds and marine mammals in the Weddell Sea, Antarctica *Polar Biology* **11**, 415-424.
- Karnovsky, N., Ainley, D. G. and Lee, P.** (2007). The impact and importance of production in polynyas to top-trophic predators: three case histories. In *Elsevier*

Oceanography Series, vol. Volume 74 eds. W. O. Smith and D. G. Barber), pp. 391-410: Elsevier.

Keiper, C. A., Ainley, D. G., Allen, S. G. and Harvey, J. T. (2005). Marine mammal occurrence and ocean climate off central California, 1986 to 1994 and 1997 to 1999. *Marine Ecology-Progress Series* **289**, 285-306.

Kim, S. L., Conlan, K., Malone, D. P. and Lewis, C. V. (2005). Possible food caching and defence in the Weddell seal: observations from McMurdo Sound, Antarctica. *Antarctic Science* **17**, 71-72.

Kim, S. Z., Ainley, D. G., Pennycook, J. and Eastman, J. T. (2011). Antarctic toothfish heads found along tide cracks of the McMurdo Ice Shelf. *Antarctic Science* **23**, 469-470.

Knox, G. A. (2007). *Biology of the Southern Ocean* Boca Raton, Fla: CRC Press/Taylor & Francis.

Kooyman, G. (1981). *Weddell seal: consummate diver*: Cambridge University Press New York.

Kooyman, G. L. (1966). Maximum Diving Capacities of the Weddell Seal, *Leptonychotes weddelli*. *Science* **151**, 1553-1554.

Kooyman, G. L. (1975). A Comparison between Day and Night Diving in the Weddell Seal. *Journal of Mammalogy* **56**, 563-574.

Kooyman, G. L. (2013). An analysis of some behavioral and physiological characteristics related to diving in the Weddell Seal. In *Biology of the Antarctic Seas III*, pp. 227-261: American Geophysical Union.

Kooyman, G. L., Wahrenbrock, E. A., Castellini, M. A., Davis, R. W. and Sinnett, E. E. (1980a). Aerobic and anaerobic metabolism during voluntary diving in Weddell seals: Evidence of preferred pathways from blood chemistry and behavior. *J Comp Physiol B* **138**, 335-346.

- Kooyman, G. L., Wahrenbrock, E. A., Castellini, M. A., Davis, R. W. and Sinnett, E. E.** (1980b). Aerobic and anaerobic metabolism during voluntary diving in Weddell seals - evidence of preferred pathways from blood chemistry and behavior *J Comp Physiol B* **138**, 335-346.
- La Mesa, M., Eastman, J. and Vacchi, M.** (2004). The role of notothenioid fish in the food web of the Ross Sea shelf waters: a review. *Polar Biology* **27**, 321-338.
- Lake, S., Burton, H. and Van den Hoff, J.** (2003). Regional, temporal and fine-scale spatial variation in Weddell seal diet at four coastal locations in east Antarctica. *Marine Ecology Progress Series* **254**, 293-305.
- Lake, S., Wotherspoon, S. and Burton, H.** (2005). Spatial utilisation of fast-ice by Weddell seals *Leptonychotes weddellii* during winter. *Ecography* **28**, 295-306.
- Lake, S., Burton, H. and Wotherspoon, S.** (2006). Movements of adult female Weddell seals during the winter months. *Polar Biology* **29**, 270-279.
- Lake, S. E., Burton, H. R. and Hindell, M. A.** (1997). Influence of time of day and month on Weddell seal haul-out patterns at the Vestfold Hills, Antarctica. *Polar Biology* **18**, 319-324.
- LaRue, M., Rotella, J., Garrott, R., Siniff, D., Ainley, D., Stauffer, G., Porter, C. and Morin, P.** (2011). Satellite imagery can be used to detect variation in abundance of Weddell seals (*Leptonychotes weddellii*) in Erebus Bay, Antarctica. *Polar Biology* **34**, 1727-1737.
- Laws, R. M.** (1977). Seals and Whales of the Southern Ocean. *Philosophical Transactions of the Royal Society of London* **279**, 81-96.
- Legendre, P. and Legendre, L.** (2012). Numerical ecology: Elsevier.
- Lenky, C., Eisert, R., Oftedal, O. T. and Metcalf, V.** (2012). Proximate composition and energy density of nototheniid and myctophid fish in McMurdo Sound and the Ross Sea, Antarctica. *Polar Biology* **35**, 717-724.

- Loeb, V., Siegel, V., Holm-Hansen, O., Hewitt, R., Fraser, W., Trivelpiece, W. and Trivelpiece, S.** (1997). Effects of sea-ice extent and krill or salp dominance on the Antarctic food web. *Nature* **387**, 897-900.
- Logan, J. M., Jardine, T. D., Miller, T. J., Bunn, S. E., Cunjak, R. A. and Lutcavage, M. E.** (2008). Lipid corrections in carbon and nitrogen stable isotope analyses: comparison of chemical extraction and modelling methods. *Journal of Animal Ecology* **77**, 838-846.
- Lorrain, A., Graham, B., Ménard, F., Popp, B., Bouillon, S., Van Breugel, P. and Cherel, Y.** (2009). Nitrogen and carbon isotope values of individual amino acids: a tool to study foraging ecology of penguins in the Southern Ocean. *Marine Ecology Progress Series* **391**, 293-306.
- Lydersen, C., Nost, O. A., Lovell, P., McConnell, B. J., Gammelsrod, T., Hunter, C., Fedak, M. A. and Kovacs, K. M.** (2002). Salinity and temperature structure of a freezing Arctic fjord - monitored by white whales (*Delphinapterus leucas*). *Geophysical Research Letters* **29**, 34-31-34.
- Marcoux, M., McMeans, B. C., Fisk, A. T. and Ferguson, S. H.** (2012). Composition and temporal variation in the diet of beluga whales, derived from stable isotopes. *Marine ecology. Progress series* **471**, 283-291.
- Martin, S., Drucker, R. S. and Kwok, R.** (2007). The areas and ice production of the western and central Ross Sea polynyas, 1992–2002, and their relation to the B-15 and C-19 iceberg events of 2000 and 2002. *Journal of Marine Systems* **68**, 201-214.
- McCafferty, D. J., Boyd, I. L., Walker, T. R. and Taylor, R. I.** (1999). Can marine mammals be used to monitor oceanographic conditions? *Marine Biology* **134**, 387-395.
- McConnaughey, T. and McRoy, C.** (1979). Food-web structure and the fractionation of carbon isotopes in the Bering Sea. *Marine Biology* **53**, 257-262.
- McIntyre, T., Stansfield, L. J., Bornemann, H., Plötz, J. and Bester, M. N.** (2013). Hydrographic influences on the summer dive behaviour of Weddell seals (*Leptonychotes weddellii*) in Atka Bay, Antarctica. *Polar Biology* **36**, 1693-1700.

- Millero, F. J., Chen, C.-T., Bradshaw, A. and Schleicher, K.** (1980). A new high pressure equation of state for seawater. *Deep Sea Research Part A. Oceanographic Research Papers* **27**, 255-264.
- Minagawa, M. and Wada, E.** (1984). Stepwise enrichment of ^{15}N along food chains: further evidence and the relation between $\delta^{15}\text{N}$ and animal age. *Geochimica et cosmochimica acta* **48**, 1135-1140.
- Mitani, Y., Sato, K., Ito, S., Cameron, M., Siniff, D. and Naito, Y.** (2003). A method for reconstructing three-dimensional dive profiles of marine mammals using geomagnetic intensity data: results from two lactating Weddell seals. *Polar Biology* **26**, 311-317.
- Naito, Y.** (2004). New steps in bio-logging science. *Mem Natl Inst Polar Res Spec*, 50-57.
- Newland, C., Field, I. C., Cherel, Y., Guinet, C., Bradshaw, C. J., McMahon, C. R. and Hindell, M. A.** (2011). Diet of juvenile southern elephant seals reappraised by stable isotopes in whiskers. *Mar Ecol Prog Ser* **424**, 247-258.
- Nordstrom, C. A., Benoit-Bird, K. J., Battaile, B. C. and Trites, A. W.** (2013). Northern fur seals augment ship-derived ocean temperatures with higher temporal and spatial resolution data in the eastern Bering Sea. *Deep Sea Research Part II: Topical Studies in Oceanography* **94**, 257-273.
- Orsi, A. H. and Wiederwohl, C. L.** (2009). A recount of Ross Sea waters. *Deep Sea Research Part II: Topical Studies in Oceanography* **56**, 778-795.
- Ortiz, C. L., Costa, D. and Boeuf, B. J. L.** (1978). Water and energy flux in elephant seal pups fasting under natural conditions. *Physiological Zoology* **51**, 166-178.
- Padman, L., Costa, D. P., Bolmer, S. T., Goebel, M. E., Huckstadt, L. A., Jenkins, A., McDonald, B. I. and Shoosmith, D. R.** (2010). Seals map bathymetry of the Antarctic continental shelf. *Geophysical Research Letters* **37**.

- Parnell, A.** (2013). siar: Stable Isotope Analysis in R. R package version 4.2.
<http://CRAN.R-project.org/package=siar>.
- Pearce, J. and Ferrier, S.** (2000). An evaluation of alternative algorithms for fitting species distribution models using logistic regression. *Ecological Modelling* **128**, 127-147.
- Peloquin, J. A. and Smith, W. O.** (2007). Phytoplankton blooms in the Ross Sea, Antarctica: Interannual variability in magnitude, temporal patterns, and composition. *Journal of Geophysical Research: Oceans* **112**, C08013.
- Peterson, B. J. and Fry, B.** (1987). Stable isotopes in ecosystem studies. *Annual review of ecology and systematics*, 293-320.
- Petty, A., Holland, P. and Feltham, D.** (2014). Sea ice and the ocean mixed layer over the Antarctic shelf seas. *The Cryosphere* **8**, 761-783.
- Phillips, D. L., Inger, R., Bearhop, S., Jackson, A. L., Moore, J. W., Parnell, A. C., Semmens, B. X. and Ward, E. J.** (2014). Best practices for use of stable isotope mixing models in food-web studies. *Canadian Journal of Zoology* **92**, 823-835.
- Pinkerton, M., Hanchet, S. and Bradford-Grieve, J.** (2007). Finding the role of the Antarctic toothfish in the Ross Sea ecosystem. *Water and Atmosphere* **15**, 20-21.
- Pinnegar, J. K. and Polunin, N. V. C.** (1999). Differential fractionation of delta C-13 and delta N-15 among fish tissues: implications for the study of trophic interactions. *Functional Ecology* **13**, 225-231.
- Plötz, J., Ekau, W. and Reijnders, P. J. H.** (1991). Diet of Weddell seals *Leptonychotes weddellii* at Vestkapp, Eastern Weddell Sea (Antarctica), in relation to local food supply *Marine Mammal Science* **7**, 136-144.
- Plötz, J., Bornemann, H., Knust, R., Schröder, A. and Bester, M.** (2001). Foraging behaviour of Weddell seals, and its ecological implications. *Polar Biology* **24**, 901-909.

- Ponganis, P. J. and Stockard, T. K.** (2007). Short Note: The Antarctic toothfish: how common a prey for Weddell seals? *Antarctic Science* **19**, 441-442.
- Post, D. M., Layman, C. A., Arrington, D. A., Takimoto, G., Quattrochi, J. and Montana, C. G.** (2007). Getting to the fat of the matter: models, methods and assumptions for dealing with lipids in stable isotope analyses. *Oecologia* **152**, 179-189.
- Przyborski, P.** (no date). World of change: Antarctic sea ice., vol. 2015. NASA Goddard Space Flight Center: NASA Earth Observatory.
- R Development Core Team.** (2013). R: A language and environment for statistical computing. Vienna, Austria: R Foundation for Statistical Computing.
- Rau, G., Mearns, A., Young, D., Olson, R., Schafer, H. and Kaplan, I.** (1983). Animal C/C correlates with trophic level in pelagic food webs. *Ecology*, 1314-1318.
- Redfern, J. V., Ferguson, M. C., Becker, E. A., Hyrenbach, K. D., Good, C., Barlow, J., Kaschner, K., Baumgartner, M. F., Forney, K. A., Ballance, L. T. et al.** (2006). Techniques for cetacean-habitat modeling. *Marine Ecology Progress Series* **310**, 271-295.
- Reilly, J. J. and Fedak, M. A.** (1990). Measurement of the body composition of living gray seals by hydrogen isotope dilution. *Journal of Applied Physiology* **69**, 885-891.
- Ribeiro Jr, P. and Diggle, P.** (2001). geoR: a package for geostatistical analysis. *R-NEWS* **1**, 15-18.
- Ribic, C. A., Ainley, D. G. and Fraser, W. R.** (1991). Habitat selection by marine mammals in the marginal ice zone *Antarctic Science* **3**, 181-186.
- Roberts, J. J., Best, B. D., Dunn, D. C., Treml, E. A. and Halpin, P. N.** (2010). Marine Geospatial Ecology Tools: An integrated framework for ecological geoprocessing with ArcGIS, Python, R, MATLAB, and C++. *Environmental Modelling & Software* **25**, 1197-1207.

- Robinson, P. W., Tremblay, Y., Crocker, D. E., Kappes, M. A., Kuhn, C. E., Shaffer, S. A., Simmons, S. E. and Costa, D. P.** (2007). A comparison of indirect measures of feeding behaviour based on ARGOS tracking data. *Deep Sea Research Part II: Topical Studies in Oceanography* **54**, 356-368.
- Robinson, P. W., Costa, D. P., Crocker, D. E., Pablo Gallo-Reynoso, J., Champagne, C. D., Fowler, M. A., Goetsch, C., Goetz, K. T., Hassrick, J. L., Hueckstaedt, L. A. et al.** (2012). Foraging Behavior and Success of a Mesopelagic Predator in the Northeast Pacific Ocean: Insights from a Data-Rich Species, the Northern Elephant Seal. *Plos One* **7**.
- Ropert-Coudert, Y. and Wilson, R. P.** (2005). Trends and perspectives in animal-attached remote sensing. *Frontiers in Ecology and the Environment* **3**, 437-444.
- Ropert-Coudert, Y., Beaulieu, M., Hanuise, N. and Kato, A.** (2009). Diving into the world of biologging. *Endangered Species Research* **10**, 21-27.
- Roquet, F., Park, Y.-H., Guinet, C., Bailleul, F. and Charrassin, J.-B.** (2009). Observations of the Fawn Trough Current over the Kerguelen Plateau from instrumented elephant seals. *Journal of Marine Systems* **78**, 377-393.
- Roquet, F., Charrassin, J.-B., Marchand, S., Boehme, L., Fedak, M., Reverdin, G. and Guinet, C.** (2011). Delayed-Mode Calibration of Hydrographic Data Obtained from Animal-Borne Satellite Relay Data Loggers. *Journal of Atmospheric and Oceanic Technology* **28**, 787-801.
- Roquet, F., Williams, G., Hindell, M. A., Harcourt, R., McMahon, C., Guinet, C., Charrassin, J.-B., Reverdin, G., Boehme, L., Lovell, P. et al.** (2014). A Southern Indian Ocean database of hydrographic profiles obtained with instrumented elephant seals. *Scientific Data* **1**.
- Rotella, J. J., Link, W. A., Chambert, T., Stauffer, G. E. and Garrott, R. A.** (2012). Evaluating the demographic buffering hypothesis with vital rates estimated for Weddell seals from 30 years of mark-recapture data. *Journal of Animal Ecology* **81**, 162-173.

- Rutz, C. and Hays, G. C.** (2009). New frontiers in biologging science. *Biology Letters* **5**, 289-292.
- Sala, A., Azzali, M. and Russo, A.** (2002). Krill of the Ross Sea: distribution, abundance and demography of *Euphausia superba* and *Euphausia crystallorophias* during the Italian Antarctic Expedition (January-February 2000). *Scientia Marina* **66**, 123-133.
- Seminoff, J. A., Benson, S. R., Arthur, K. E., Eguchi, T., Dutton, P. H., Tapilatu, R. F. and Popp, B. N.** (2012). Stable Isotope Tracking of Endangered Sea Turtles: Validation with Satellite Telemetry and $\delta^{15}\text{N}$ Analysis of Amino Acids. *Plos One* **7**, e37403.
- Shero, M. R., Pearson, L. E., Costa, D. P. and Burns, J. M.** (2014). Improving the precision of our ecosystem calipers: A modified morphometric technique for estimating marine mammal mass and body composition. *Plos One* **9**, e91233.
- Shero, M. R., Krotz, R. T., Costa, D. P., Avery, J. P. and Burns, J. M.** (2015). How do overwinter changes in body condition and hormone profiles influence Weddell seal reproductive success? *Functional Ecology*, n/a-n/a.
- Simmons, S. E., Tremblay, Y. and Costa, D. P.** (2006). Sampling ocean temperature using elephant seals as platforms: Behavior and sampling frequency effects on data quality. *Integrative and Comparative Biology* **46**, E250-E250.
- Simmons, S. E., Tremblay, Y. and Costa, D. P.** (2009). Pinnipeds as ocean-temperature samplers: calibrations, validations, and data quality. *Limnology and Oceanography- Methods* **7**, 648-656.
- Simmons, S. E., Crocker, D. E., Kudela, R. M. and Costa, D. P.** (2007). Linking foraging behaviour of the northern elephant seal with oceanography and bathymetry at mesoscales. *Marine Ecology-Progress Series* **346**, 265-275.
- Smith Jr, W. O., Marra, J., Hiscock, M. R. and Barber, R. T.** (2000). The seasonal cycle of phytoplankton biomass and primary productivity in the Ross Sea, Antarctica. *Deep Sea Research Part II: Topical Studies in Oceanography* **47**, 3119-3140.

- Smith Jr, W. O., Sedwick, P. N., Arrigo, K. R., Ainley, D. G. and Orsi, A. H.** (2012). The Ross Sea in a sea of change. *Oceanography*.
- Smith, W. O. and Gordon, L. I.** (1997). Hyperproductivity of the Ross Sea (Antarctica) polynya during austral spring. *Geophysical Research Letters* **24**, 233-236.
- Smith, W. O., Ainley, D. G. and Cattaneo-Vietti, R.** (2007). Trophic interactions within the Ross Sea continental shelf ecosystem. *Philos. Trans. R. Soc. B-Biol. Sci.* **362**, 95-111.
- Stirling, I.** (1968). Population studies on the Weddell seal. *Tautara* **15**, 131-141.
- Stirling, I.** (1969). Ecology of the Weddell Seal in McMurdo Sound, Antarctica. *Ecology* **50**, 573-586.
- Sweeting, C. J., Polunin, N. V. C. and Jennings, S.** (2006). Effects of chemical lipid extraction and arithmetic lipid correction on stable isotope ratios of fish tissues. *Rapid Communications in Mass Spectrometry* **20**, 595-601.
- Sy, A. and Wright, D.** (2000). XBT/XCTD Standard test procedures for reliability and performance tests of expendable probes at sea. In *JCOMMOPS*. La Jolla.
- Testa, J. W.** (1994). Over winter movements and diving behavior of female Weddell seals (*Leptonychotes weddellii*) in the southwestern Ross Sea, Antarctica *Canadian Journal of Zoology-Revue Canadienne De Zoologie* **72**, 1700-1710.
- Thuiller, W., Araújo, M. B., Lavorel, S. and Kenkel, N.** (2009). Generalized models vs. classification tree analysis: Predicting spatial distributions of plant species at different scales. *Journal of Vegetation Science* **14**, 669-680.
- Torres, L. G., Read, A. J. and Halpin, P.** (2008). Fine-scale habitat modeling of a top marine predator: Do prey data improve predictive capacity? *Ecological Applications* **18**, 1702-1717.

- Tremblay, Y., Robinson, P. W. and Costa, D. P.** (2009). A Parsimonious Approach to Modeling Animal Movement Data. *Plos One* **4**, 11.
- Tynan, C. T., Ainley, D. G., Barth, J. A., Cowles, T. J., Pierce, S. D. and Spear, L. B.** (2005). Cetacean distributions relative to ocean processes in the northern California Current System. *Deep-Sea Research Part II-Topical Studies in Oceanography* **52**, 145-167.
- Votier, S. C., Bearhop, S., Witt, M. J., Inger, R., Thompson, D. and Newton, J.** (2010). Individual responses of seabirds to commercial fisheries revealed using GPS tracking, stable isotopes and vessel monitoring systems. *Journal of Applied Ecology* **47**, 487-497.
- Wessel, P. and Smith, W. H. F.** (1996). A global, self-consistent, hierarchical, high-resolution shoreline database. *Journal of Geophysical Research: Solid Earth* **101**, 8741-8743.
- Wheatley, K., Bradshaw, C. A., Harcourt, R. and Hindell, M.** (2008). Feast or famine: evidence for mixed capital–income breeding strategies in Weddell seals. *Oecologia* **155**, 11-20.
- Wheatley, K. E., Bradshaw, C. J. A., Davis, L. S., Harcourt, R. G. and Hindell, M. A.** (2006). Influence of maternal mass and condition on energy transfer in Weddell seals. *Journal of Animal Ecology* **75**, 724-733.
- Wheatley, K. E., Nichols, P. D., Hindell, M. A., Harcourt, R. G. and Bradshaw, C. J. A.** (2007). Temporal variation in the vertical stratification of blubber fatty acids alters diet predictions for lactating Weddell seals. *Journal of Experimental Marine Biology and Ecology* **352**, 103-113.
- Wilson, E.** (1907). Mammalia (whales and seals). In *National antarctic expedition 1901-04*, vol. 4, pp. 1-66. British Museum, London: Natural History, Zoology.
- Wilson, R. P., Culik, B. M., Bannasch, R. and Lage, J.** (1994). Monitoring antarctic environmental variables using penguins. *Marine Ecology Progress Series* **106**, 199-202.

Wood, S.N. (2011). Fast stable restricted maximum likelihood and marginal likelihood estimation of semiparametric generalized linear models. *Journal of the Royal Statistical Society: Series B (Statistical Methodology)* **73**, 3-36.

Zbinden, J. A., Bearhop, S., Bradshaw, P., Gill, B., Margaritoulis, D., Newton, J. and Godley, B.J. (2011). Migratory dichotomy and associated phenotypic variation in marine turtles revealed by satellite tracking and stable isotope analysis. *Marine Ecology Progress Series* **421**, 291-302.

Zhao, L., Castellini, M., Mau, T. and Trumble, S. (2004). Trophic interactions of Antarctic seals as determined by stable isotope signatures. *Polar Biology* **27**, 368-373.